# Improved frequency control strategies for geothermal power plants

*Master of Science Thesis*

Birkir Heimisson

Department of Energy & Environment
Division Electrical Power Engineering
Chalmers University of Technology
Göteborg, Sweden 2014

# Improved frequency control strategies for geothermal power plants

BIRKIR HEIMISSON

Department of Energy and Environment
Division of Electric Power Engineering
CHALMERS UNIVERSITY OF TECHNOLOGY
Göteborg, Sweden 2014

Improved frequency control strategies for geothermal power plants
BIRKIR HEIMISSON

© BIRKIR HEIMISSON, 2014.

Department of Energy and Environment
Division of Electric Power Engineering
Chalmers University of Technology
SE–412 96 Göteborg
Sweden
Telephone +46 (0)31–772 1000

Cover: Krafla Geothermal Power Plant ©Óli Þór Jónsson

Chalmers Bibliotek, Reproservice
Göteborg, Sweden 2014

Improved frequency control strategies for geothermal power plants
BIRKIR HEIMISSON
Department of Energy and Environment
Division of Electric Power Engineering
Chalmers University of Technology

## Abstract

The Icelandic transmission system has one of the highest ratios of installed capacity of geothermal power plants in the world, as it covers 25% of the total capacity. The current frequency controls of the geothermal power plants are outdated and needs to be revised in order to improve the frequency regulation of the industry-intensive power system. Consequently, the stability of the system is more vulnerable and the risk of island operation and load shedding is increased. In this thesis the frequency controls of the geothermal power plants has been analysed with both simulations and real-time measurements. The Icelandic PSS/E model was used for dynamic simulations of the system. As a result, several improvements of the governor model responses were suggested. Revised frequency control strategies based on wide area monitoring and control systems has been investigated. The results suggested that customized control strategies should be used for each of the geothermal power plants, in order to improve their active power support capability during dynamic events and to secure the system stability. Some system scenarios require more frequency regulation from the geothermal power plants while for other conditions a blocking of the regulation participation is more favourable. Finally, the results suggest that the real-time implementation of the wide-area control schemes, i.e. measurements, data processing and control outputs, should be based on a single application platform, in order to guarantee reliability and uniformity in the operation.

**Index Terms:** Power System Stability, Geothermal Power Plants, Primary Frequency Control, Load Frequency Control, Phasor Measurement Units (PMU), Wide Area Control.

## Acknowledgements

The work presented in this thesis was carried out at Landsnet, the TSO of Iceland. First and foremost I would like to express my appreciation and thanks to my supervisors at Landsnet, dr. Ragnar Guðmannsson and dr. Magni Þór Pálsson. Their support and guidance through the course of my work has been valuable and they have given me the opportunity to work independently. I would like to thank my supervisor at Chalmers, dr. Peiyuan Chen, for his advice and great discussions throughout the project. Furthermore, I would like to thank the employees of Landsnet, Psymetrix, Landsvirkjun and Orka Náttúrunnar who supported me with informations and ideas. I would like to express my gratitude to all the organizations that funded my studies and research, i.e. Landsvirkjun Orkurannsóknarsjóður, Gothia Power Scholarship and K G Hallbys fund.

I want to thank Jóhannes Þorleiksson and Hafdís Helgadóttir for their assistance in reviewing and proofreading my thesis report. Last but not least, my family and friends deserves my deepest gratitude for their patience and encouragement throughout my studies.

Birkir Heimisson, Reykjavík 2014

# Nomenclature

| | |
|---|---|
| TSO | Transmission system operator |
| WAMS | Wide-area measurement systems |
| PMU | Phasor measurement unit |
| WADS | Wide-area defence schemes |
| PSS | Power system stabilizer |
| SCADA | Supervisory control and data acquisition |
| FACTS | Flexible ac transmission systems |
| AVR | Automatic voltage regulator |
| LFC | Load frequency control |
| AGC | Automatic generation control |
| EMF | Electromotive force |
| RoCoF | Rate of change of frequency |
| S-PDC | Substation phasor data concentrator |
| TETRA | Terrestrial trunked radio |

# Contents

# 1

# Introduction

## 1.1 Background

The Icelandic transmission system is a unique system. First, all of its electric power is produced from renewable energy sources. Secondly, it is an islanded network, therefore it has no interconnection to importing and exporting energy and the load of the system has to be met with a generation within the system itself. The third unique characteristic of the system is the high ratio of installed capacity of geothermal power plants, as it covers 25% of the total capacity of the system, which is approximately 2670 MW. The peak load of the system is about 2200 MW and the annual consumption is approximately 17 TWh [1].

Geothermal power is a great and reliable source of energy, however it has its drawbacks. One of the drawbacks is an outdated frequency control of the Icelandic geothermal power plants. The geothermal power plants do not participate in the frequency control, which is not favourable for an industry intensive country like Iceland. Power intensive industry loads consume 80% of the total load demand of the system. Occasional trips of those heavy industry loads will put immense stress on the power system and the frequency oscillation following the faults will usually result in load shedding and islanding operation [2]. This thesis will focus on investigating the frequency control of geothermal power plants and to design more suitable control schemes, in order to improve frequency regulation and stability of the Icelandic power system.

## 1.2 Problem Description

Hydro power is the most dominant energy source in the Icelandic power system. It has a very good frequency regulation characteristics, which is essential for the frequency regulation of the system. The installed hydro is 71% of the total capacity of the system and the remaining 4% is diesel generation, only needed during fault event and other outages in the system [3]. Almost all of the hydro power plants are assigned to the primary frequency control and roughly 90% of them are in the secondary frequency control. However, the geothermal power plants are operated in a load limit control mode, i.e. the output power is kept constant according to setpoint, normally at maximum power possible. For this reason the geothermal power plants do not contribute to the frequency regulation of the power system. Only during severe events when the frequency deviation exceeds a certain frequnency band (typically $\pm 1$ Hz), the geothermal plants will participate in the frequency regulation by switching to governor control. Present control scheme of the geothermal power plants are outdated so the plants do not contribute to stabilizing the system during disturbances, but rather increases the unstability. Thus, the scheme has to be revised in order to improve the operation and the frequency stability of the power system.

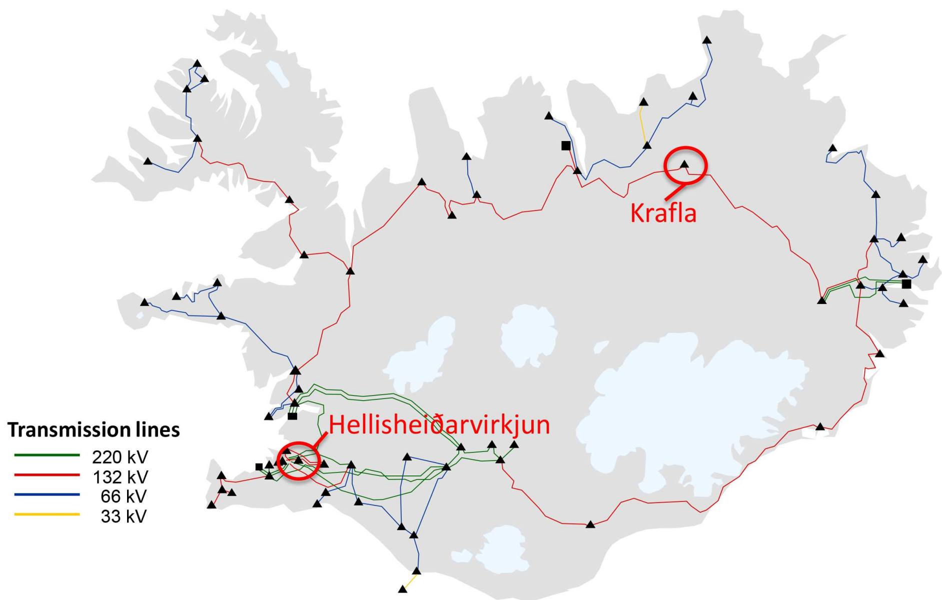


**Figure 1.1:** Map showing the Icelandic transmission system and the location of the two geothermal power plants which will be in focus in the studies [4].

Today's control strategies tend to cause stability problems during large industry faults in the system. A key aspect of ensuring a secure operation of the system is to limit the risk of getting island operation, i.e. a split between the West and East Iceland. The 132 kV ring connection, which can be seen in Figure 1.1, is a bottleneck in the system. Overloading of the ring connection triggers system protections that split the network, which can cause stability issues and load shedding. Additionally, the existing control strategy of the geothermal plants increases the stress on the hydro power plants following a fault, since the hydro power plants have to compensate for the control action of the geothermal plants. These challenges will be discussed in further details in Chapter 3.

## 1.3 Aim

The objective of this thesis work is to investigate alternative control strategies for the geothermal power plants in Iceland, which should improve the frequency regulation and increase the overall stability of the Icelandic transmission system.

## 1.4 Scope

The main scope of this master thesis is to investigate how the primary and secondary frequency control of geothermal power plants can be improved, in order to increase the frequency regulation and stability of the power system. In addition, the possibilities of using control signals from phasor measurements units (PMUs) to improve controls of geothermal plants will be studied. Krafla and Hellisheiðarvirkjun are the two geothermal plants that will be in focus in this thesis work, the locations of the plants can be seen in Figure 1.1. Krafla is located at a weak point in the system, connected with the 132 kV ring connection in the Northeast part of Iceland where the short circuit power varies between 499-722 MVA. Hellisheiðarvirkjun is located in Southwest in a strong point of the 220 kv network where the short circuit power varies between 1600-3432 MVA [4]. Studies of power system stabilizers (PSS), flexible ac transmission systems (FACTS) and power market analysis will be outside the scope of this thesis. The thesis will include theoretical evaluations, simulations and comparison with actual field measurement results. The work will be carried out in cooperation with Landsnet, Landsvirkjun and Psymetrix.

# 2

# Overview of Geothermal Power Plants and Frequency Regulation

In this chapter the fundamentals and theory of geothermal power plants will be presented. The principles of frequency control in power systems will be explained and different power plant models will be introduced.

## 2.1 Different Types of Geothermal Power Plants

Geothermal power plants utilize heat energy found below the Earth's surface to produce electricity. A classic schematic of geothermal power plant can be seen in Figure 2.1, where a hot water of 50-400°$C$ coming from a 1000-2000 m deep boreholes is pumped to the power plant. For power plants with combined heating and electricity production a ground water from nearby environment is also collected and pumped to the plant. The outputs from the plant is electricity, hot water of around 85°$C$ for district heating and wastewater which is pumped back down into the ground. The advantages of geothermal power plants are as follows [5]:

- High degree of availability ($>$ 98% of the year)
- Low land usage
- Low atmospheric pollution compared to fossil fuelled plants
- Minimum liquid pollution with re-injection of effluent liquid
- Insignificant dependence on weather conditions
- Comparatively low visual impact

When compared to hydro power plants the geothermal power plants have; higher atmospheric pollution, require less land usage (if reservoirs are considered) and have higher degree of availability because the hydro power plants are highly dependant on the weather conditions.

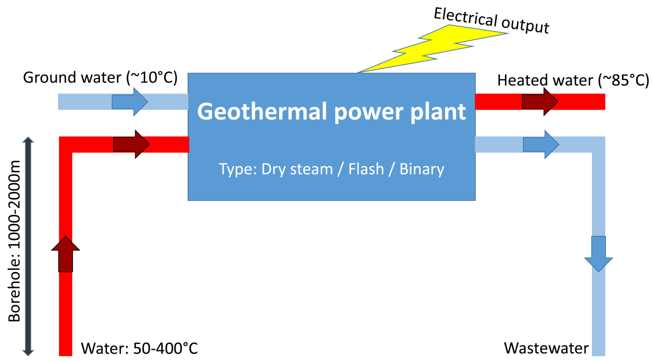


**Figure 2.1:** Basic schematic of a geothermal power plant.

There are three main technologies used to convert hydrothermal fluids into processed steam to run turbines for electricity generation, i.e. dry steam (back pressure), flash (condensing), and binary. The type of conversion used depends on the fluids temperature and the state (steam or water).

### 2.1.1 Dry Steam - Back Pressure Type

The first generation of geothermal power plants used dry steam technology. In dry steam power plants the steam has low water content and a temperature of 180-225$°C$ which is routed through the turbine. Next it flows out of the cooling towers and the steam condenses into water, this process returns very little wastewater down to the wells compared to modern plants. The performance of this type of design is really poor compared to modern power plant solutions, they have low overall thermal efficiency but this design is robust and the least expensive. A design using a back pressure system can be seen in Figure 2.2, where steam and moisture separators are used [5].

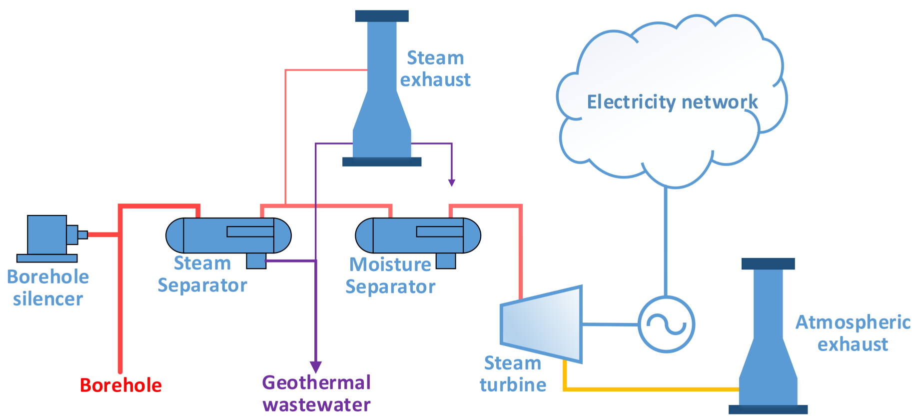


**Figure 2.2:** Typical back-pressure system[5].

### 2.1.2 Flash - Condensing Type

The most common type of geothermal power plants is the flash steam type. They are more complex than back pressure type because they require condensers and gas exhaust systems. Highly pressured hot water of minimum $200°C$ is pumped from wells into a steam separator with a lower pressure. The resulting steam, called flash is used to drive the turbines. In Figure 2.3 a typical condensing type unit can be seen. Producing both electricity and heat. This configuration improves the thermal efficiency and the flexibility of the plant compared to the back pressure type [5].

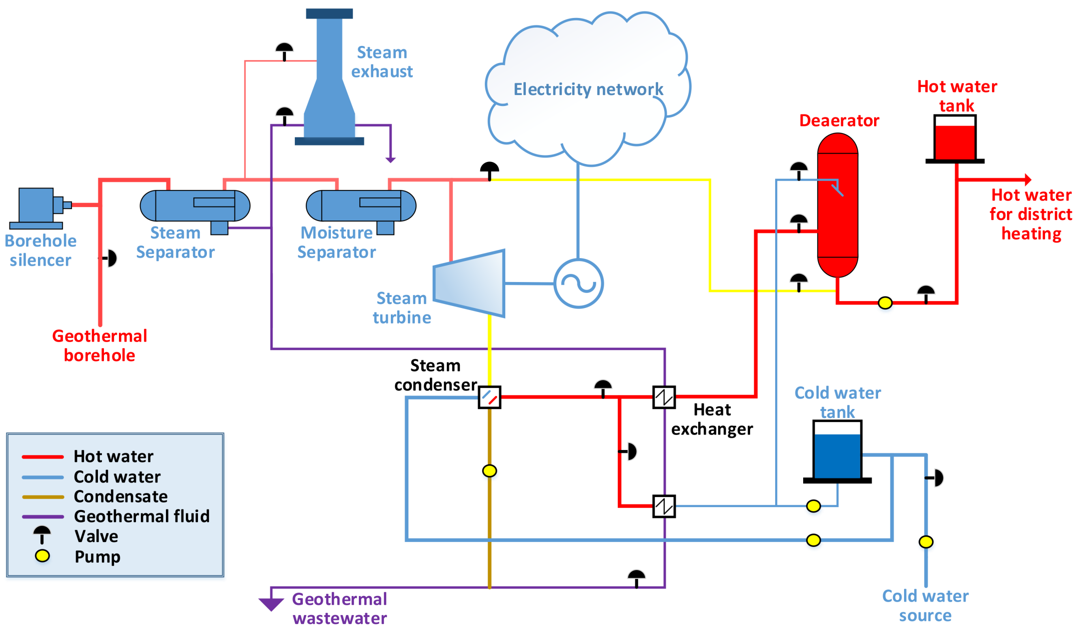


**Figure 2.3:** Typical condensing type unit in combined utilisation[5].

### 2.1.3 Binary Type

Binary cycle geothermal power plants are the most recent development. They differ from the dry steam and flash steam systems in the way that the water or steam from the geothermal reservoir never comes in contact with the turbine units. The heat from the fluid is transferred via heat exchangers to a secondary fluid with a lower boiling point. This allows the geothermal water to be of lower temperature than for conventional solutions. The secondary fluid flash vaporizes and the resulting steam drives the turbine. The advantages of the flash and binary types is that they can be utilized in a combined solution for a power plant [5].

## 2.2 Electricity Generation

Electricity production from geothermal energy follows the same principles as for any other conventional steam based production, e.g. fossil fuel power plants or nuclear power plants. The steam drives a turbine which rotates a shaft, a rotor is attached to the shaft and the generated torque spins the rotor inside the generator which generates rotating magnetic field. Currents are then induced in the stator windings of the generator and a three phase power output from the generator is connected to a transformer which steps up the voltage and electric power generated by the generator is transmitted to a load via transmission lines. A basic schematic of the process is shown in Figure 2.4.

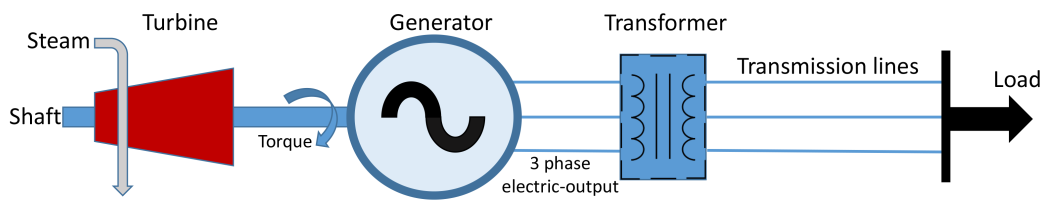


**Figure 2.4:** Simple schematic of an electrical generation of a thermal based power plant.

### 2.2.1 Turbine

Steam turbines are available in wide-variety of designs and sizes, depending on the application. Their purpose is to convert energy stored in high pressure and high temperature steam into rotating energy. Steam turbines usually consist of two or more turbine sections coupled in series. Each turbine section has a set of moving blades attached to the rotor shaft and a set of stationary vanes. The stationary vanes are referred to as a nozzle sections, form nozzles that accelerate the steam to high velocity. The kinetic energy of this high velocity steam is converted into shaft torque by the moving blades [6].

Turbines are mechanically and materially complex components, which have to be designed and manufactured carefully to provide safe and robust operation. The turbines must be well balanced to handle the high speed and to avoid vibrations. Materials have to have good temperature characteristics and be resistant against corrosion from chemicals in the steam. The most common turbine type used today is condensing type turbine. Figure 2.5 shows a diagram of a condensing turbine with two stages, a high pressure (HP) and a intermediate pressure (IP) / low pressure (LP). These turbines are advantageous when large quantities of reliable power source is available [7].

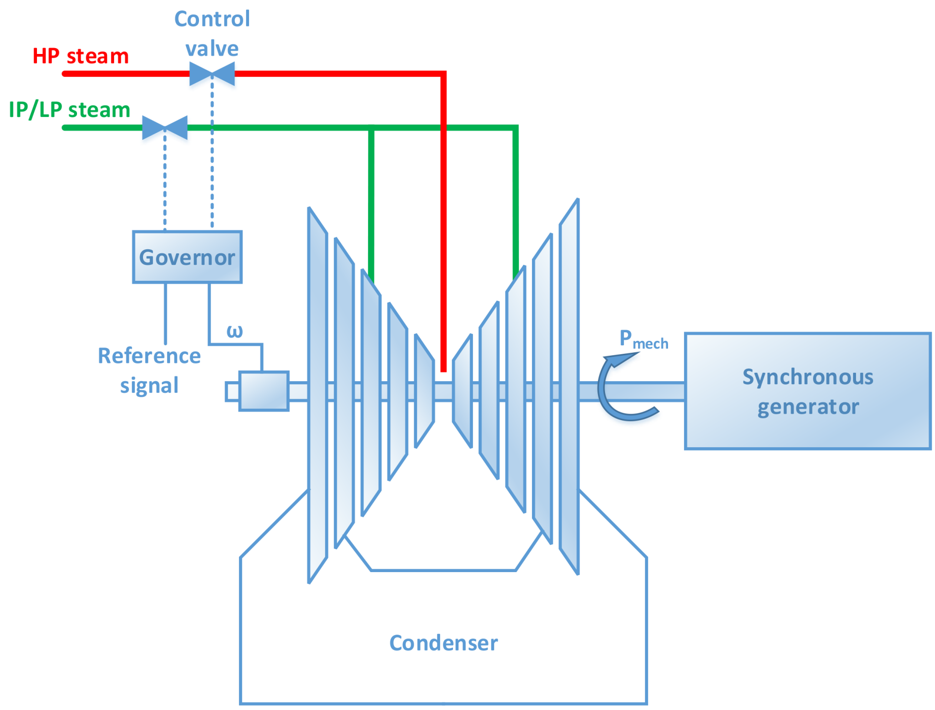


**Figure 2.5:** Compound steam turbine with HP and IP/LP steam inlets.

Inputs of the governor system are speed reference signal and the angular speed $\omega$ of the shaft. The output signals are control signals to the governor control valves, which control the flow of high and low pressure steams to the turbine. The specified values for the geothermal power plant Krafla is 7.4 bar at $180°C$ for the high pressure steam and 1.3 bar at $110°C$ for the low pressure steam.

### 2.2.2 Synchronous Generator

Three-phase synchronous generators are used in geothermal power plants like for any other steam based power plant. Turbo or high speed generators are used in steam driven applications, while low speed generators are used for water based turbines. Turbo generators have relatively low diameter but large axial length. They are mounted horizontally in order to reduce centrifugal forces at high speeds. Typically those generators are designed with one or two electrical pole pairs, resulting in synchronous speed of 3000 or 1500 rpm respectively, i.e. for power systems operated at 50 Hz. The result can be derived from following equation

$$n = \frac{60 \cdot f}{p_{pair}} \tag{2.1}$$

where n is the speed in rpm, f is the frequency in Hz and $p_{pair}$ is the number of pole pairs. The generator itself is made of two main magnetic parts, i.e. a stator and a rotor. The armature winding which carries the load current and supplies power to the system consists of three identical phase windings which are placed on the inner surface of the stator [8].

Figure 2.6 shows a block diagram of a typical generation unit, including the control systems. Three phase voltage and current measurements are taken from the output of the synchronous generator. The measured voltage and current signals are used in the automatic voltage regulator (AVR), power and frequency are determined from the voltage and current measurements and used in the governor control [8].

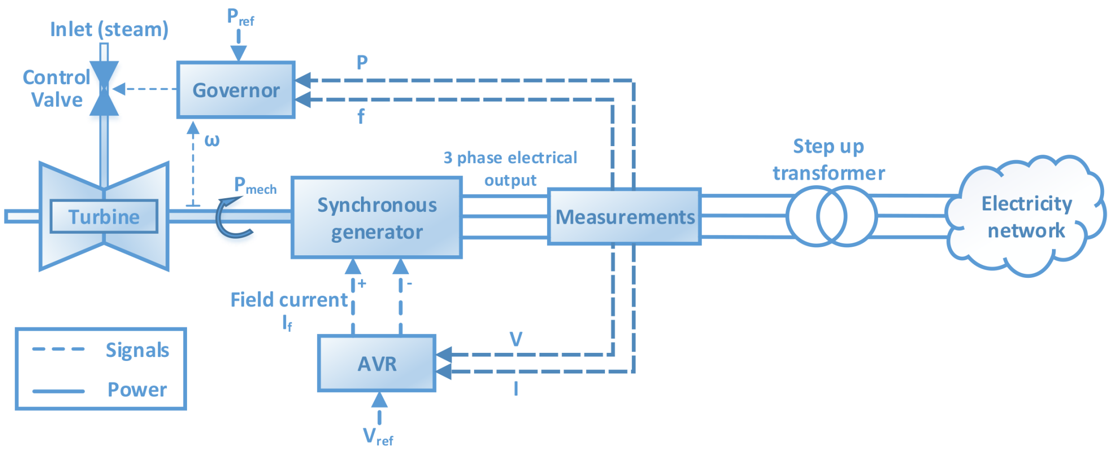


**Figure 2.6:** Block diagram of a typical generator unit, with the control systems.

### 2.2.3 Excitation System of a Generator

The rotor of the synchronous generator contains a dc excitation winding and an additional short circuited damper which damps the mechanical oscillations of the rotor. The excitation system of the generator unit consists of an exciter and an AVR, which is needed to control the dc field current. The dc current produces magnetic flux in the rotor windings which is proportional to the strength of the field current $I_f$. The flux induces an electromotive force (EMF) in each phase of the stator's armature windings, which forces ac currents to flow out to the power system. The purpose of the excitation system is to regulate the terminal voltage of the generator and control the reactive power. Power system stabilizer (PSS) is a device that can be installed to the AVR to improve the small-signal performance of the generator unit. The device uses auxiliary input signals to control the AVR in order to damp and stabilize power oscillations in the power system. [8]. For local mode power oscillation an input of active power $\Delta P$ to the PSS is usually most effective. For inter-area mode power oscillation an input of frequency $\Delta f$ or generator speed $\Delta\omega$ is preferred. Finally for complex power oscillation the PSS can have multiple inputs, usually $\Delta P + \Delta f$ [9]

Small changes in active power are mainly dependent on the system frequency, while the reactive power is more dependent on the amplitude of the voltage. Furthermore, the time constant of the excitation system is much smaller than the time constant of the prime mover of the governor system and its transient decay is much faster. Therefore the cross-coupling between the AVR and the governor can be neglected and the excitation voltage and load frequency can be analysed separately [10].

### 2.2.4 Governor System of a Generator

The function of the governor system is to control either the output power or the speed of the turbine, generally referred as load limit control mode and governor control mode, respectively. The governor uses signals of the active power P and the system frequency f, measured at the output terminals of the synchronous generator to control steam flow through the valves of the turbine. The governor also measures the rotational speed of the turbine $\omega$ for overspeed protection. The four main control functions of the governor system are

- *Run-up control*: For startup of unsynchronized generator.
- *Load/speed control*: Fundamental control during the operation of a generator, including load limit control mode and governor control mode.
- *Overspeed control*: Limits the maximum speed during disturbances and provides fast-valving protection.
- *Overspeed trip*: Independent trip function to ensure quick stop of the turbine.

More details and modelling of the governors will be discussed in Chapter 2.3.1 [8].

## 2.3 Power System Frequency Control

The system frequency represents the rotation speed of synchronised generators in an interconnected system. The balance between generated power and load demand needs to be maintained in constant equilibrium, in order to keep the frequency at the nominal value of 50 Hz. If the total demand of a system decreases the frequency/speed of generators will increase. On the other hand, if the demand increases then the frequency will decrease. Disturbances in the power balance will cause deviation of the system frequency, which will offset initially by the difference in kinetic energy of the rotating generators and the connected loads. The purpose of the governors is to regulate the frequency of the network by controlling the speed of the generators. The control of the system frequency is divided into following three parts:

- *Primary control.*
- *Secondary control.*
- *Tertiary control.*

These different controls are shown in Figure 2.7. Primary control is the first response of the governors, few seconds later the secondary control re-establishes the setpoints of the generators in order to reduce the steady state frequency deviation. Finally the tertiary control adjusts the generation according to economical dispatch, calculated from scheduled values and balancing power [11].

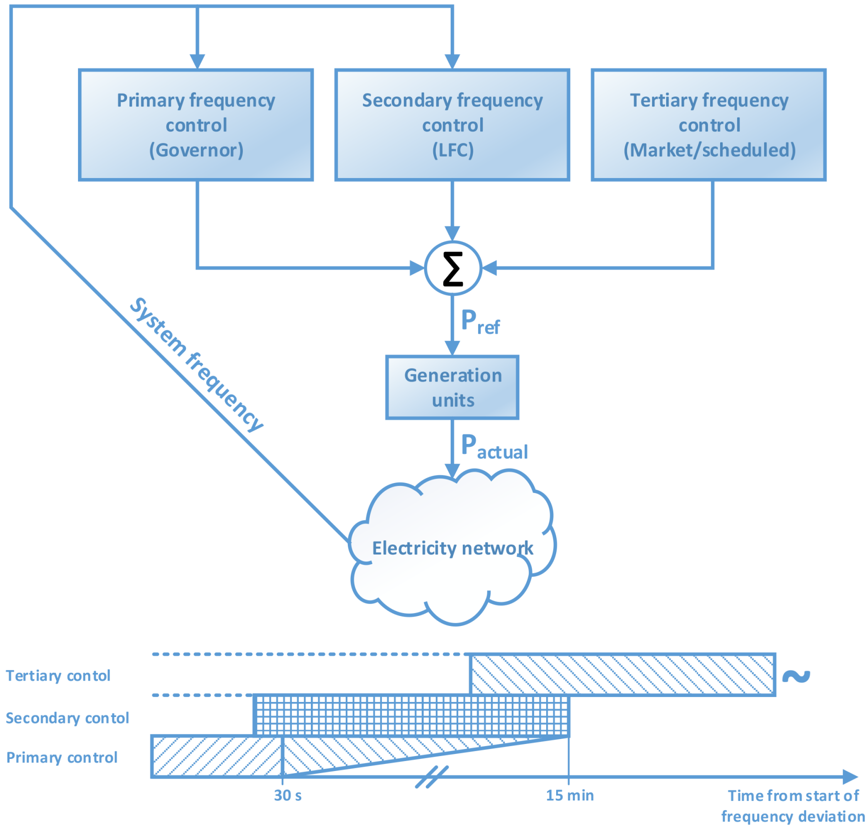


**Figure 2.7:** Overview of a frequency controls for a power system[6][11].

### 2.3.1 Primary Frequency Control

Primary frequency control is the first response to a frequency deviation. The local automatic governors of the generating units compensate for the mismatch by delivering reserve powers to oppose any change in system frequency. Regardless of location of the load change, all generator on governor control will participate in the frequency regulation [6].

Total generation should be in equilibrium with the demand at all times, i.e.

$$P_G = P_D \tag{2.2}$$

where $P_G$ is the generated power and $P_D$ is the power consumed by the loads in the system, including losses. Kinetic energy of all rotating masses (i.e. generators and motors) in the system is expressed as

$$E_{rot} = \frac{1}{2}J\omega^2 \tag{2.3}$$

where $J$ is the total moment of inertia and $\omega$ is the angular frequency. Unbalance between $P_G$ and $P_D$ causes changes in kinetic energy

$$\frac{d}{dt}(E_{rot}) = P_G - P_D \tag{2.4}$$

$$\frac{d}{dt}(\frac{1}{2}J\omega^2) = P_G - P_D. \tag{2.5}$$

By derivating with respect to t, the equation can be rearranged

$$\frac{d\omega}{dt} = \frac{P_G - P_D}{J\omega}. \tag{2.6}$$

The amount of inertia is generally quantified through the inertia constant $H$, defined as [6]

$$H = \frac{\text{Kinetic energy at rated speed}}{\text{total base power}} \tag{2.7}$$

the inertia constant H becomes

$$H = \frac{\frac{1}{2}J\omega_0^2}{S_b} \tag{2.8}$$

$$J = 2H\frac{S_b}{\omega_0^2} \tag{2.9}$$

plug (2.9) into (2.6)

$$\frac{d\omega}{dt} = \frac{P_G - P_D}{2H\frac{S_b}{\omega_0^2}\omega}. \tag{2.10}$$

For small variation in rotor speed ($\omega \simeq \omega_0$) the (2.10) can be simplified

$$\frac{d\omega}{dt} = \frac{\omega_0}{2H}\frac{P_G - P_D}{S_b}. \tag{2.11}$$

Finally, when expressed in per unit the frequency $f$ and angular frequency $\omega$ are the same , therefore (2.11) can be re-written as

$$\frac{df}{dt} = \frac{f_0}{2H}(P_{G_{pu}} - P_{D_{pu}}). \tag{2.12}$$

Equation (2.12) expresses the frequency deviation in hertz in terms of the power imbalance in a power system [12]. Equivalently (2.11) can be expressed as per unit deviation model with the mechanical power $P_M$ and electrical power $P_E$ of a generator unit instead of $P_G$ and $P_D$ respectively

$$\frac{d\Delta\omega}{dt} = \frac{1}{2H}(P_{M_{pu}} - P_{E_{pu}}) \tag{2.13}$$

where the electrical power $P_E$ represents the load characteristics

$$\Delta P_E = \Delta P_L + D\Delta\omega \tag{2.14}$$

where $\Delta P_L$ is a non-frequency sensitive load change, $D\Delta\omega$ is the frequency sensitive load and $D$ is the load damping constant expressed as percent change in load divided by percent change in frequency [10]. Figure 2.8 shows a block diagram of the simulation model of a generator unit in an isolated power system. The model includes; a governor system, a turbine model and a rotating mass and a load. Speed or frequency deviation are based on (2.13). When frequency deviation is detected the governor system will change the signal to the valves of the turbine, i.e. $\Delta Y$, in order to change the mechanical output of the generator.

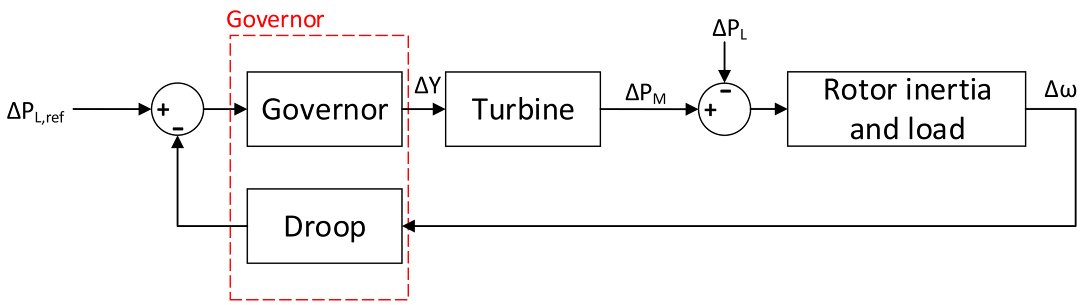


**Figure 2.8:** Block diagram of a power plant model in per unit.

The droop in the governor system makes it possible for two or more generators to share a load and have a unique frequency. Without the droop, all generator connected to the same network would fight over the control of frequency. Figure 2.9 shows the ideal steady state characteristics of a drooping governor, where the slope of the line represents the droop

$$R = \frac{\Delta f}{\Delta P}. \tag{2.15}$$

The droop is normally defined in percentage in the range of 3-6%, e.g. 3% droop means that for 3% change in frequency there will be 100% change in output [6].

Landsnet's grid code does not have any documented requirements for the response times of the primary and secondary frequency controls. Previous tunings of the governor controls have been done in full cooperation between Landsnet and the power plant owners. Standardization of frequency control requirements is one of Landsnet's future objectives.

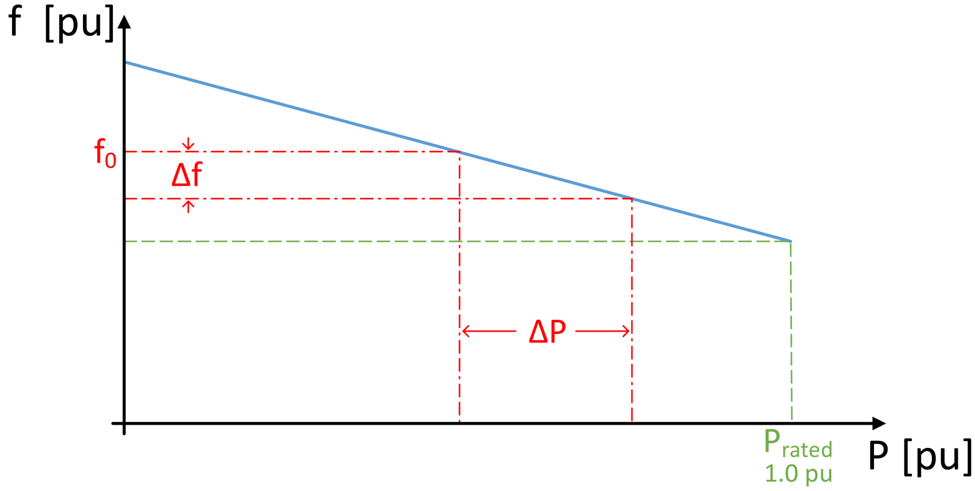


**Figure 2.9:** Steady state drooping governor characteristics[10].

### 2.3.2 Secondary Frequency Control

When unbalance between generation and demand occurs, the primary frequency control will always result in a steady-state frequency deviation, which depends on the governor droop characteristics $R$ and the frequency sensitivity $D$ of the load. The secondary frequency control is needed to adapt the load reference setpoints to the generators, for the restoration of the frequency to its nominal value. This function is generally referred to as a load frequency control (LFC) or an automatic generation control (AGC). The loads are continuously changing in real-time operation, therefore these systems have to be automatic. The AGC is usually built into the supervisory control and data acquisition (SCADA) system [6]. Functionality of AGC is illustrated in Figure 2.10. The AGC uses the system frequency and tie line power signal in order to calculate new generation setpoints, which are sent to the governor systems of the power plants participating in the secondary frequency control. Configuration of which power plants should contribute to the secondary control and the size of each plant's share can be programmed in the AGC software. For instance, the geothermal power plants in Iceland are currently not used in the AGC.

The purpose of the AGC is to restore the frequency by delivering reserve power and to bring schedules between interconnected systems to their target values. AGC also ensures that the power used in the primary frequency control will be made available again. The secondary control operates for periods of minutes, therefore it is timely dissociated with the primary control. The Icelandic network is an isolated system, therefore the purpose of the AGC is only to restore the system frequency and not to control a tie line power-flow between other interconnected networks [11].

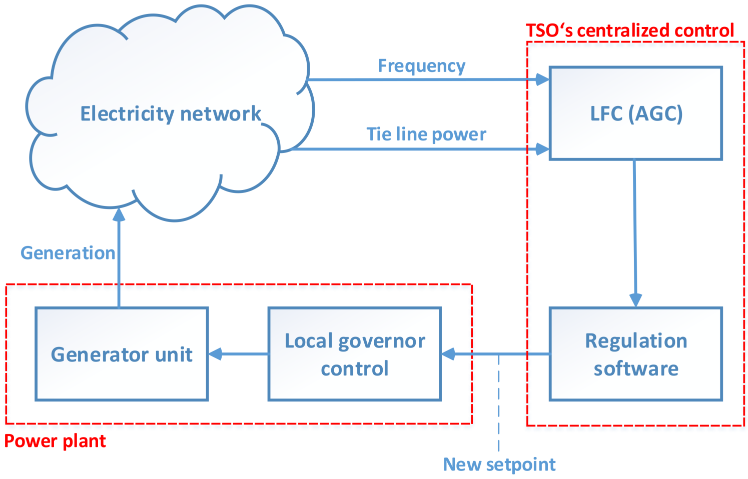


**Figure 2.10:** Block diagram of a load frequency control.

### 2.3.3 Tertiary Frequency Control

Tertiary control is much slower than the primary and secondary frequency controls. The objective of the tertiary control is to change the dispatch to restore secondary control reserves, to manage possible bottleneck issues, to bring frequency and interchange values back to target. The dispatch is commonly calculated with optimal power-flow (OPF), which minimizes the operational cost while satisfying the system constraints. Another way is to set the operating setpoints of the power plants based on an economic dispatch. It is usually executed via an energy market where power plants owners bid their prices to a centralized pool. The system operators then have to adjust the supplied bids by controlling manually or automatically the setpoints to the individual turbine governor [8]. In Iceland the economic dispatch is used, except it is not connected with centralized market pool. Power plant owners having a balance responsibility send in their bids directly to the TSO, i.e. Landsnet. A software developed by Landsnet verifies the bids and schedules before they are taken into operation. The software adjusts the setpoints to the power plants in the most economical way and dispatches them automatically via connection with the SCADA system.

## 2.4

The different models used in this study will be briefly introduced in this chapter. Both the simple models analysed in MATLAB/Simulink along with the more detailed models for the PSS/E simulations.

### 2.4.1 Simplified Models for MATLAB/Simulink Simulations

The hydro power plant, seen in Figure 2.11, is modelled with a linear turbine water column model, which only depends on a water starting time constant [13]

$$\tau_W = \left(\frac{L}{Ag}\right)\frac{q}{h} \tag{2.16}$$

where

$$\begin{aligned}
A &= \text{Penstock area } [m^2] \\
L &= \text{Penstock length } [m] \\
g &= \text{Gravitational acceleration } [m/s^2] \\
q &= \text{Flow of water through turbine } [m^3/s] \\
h &= \text{Operating head at turbine admission } [m].
\end{aligned}$$

The governor is modelled as a transfer function representing the gate valve servo motor, where $\tau_G$ is the pilot valve and servomotor time constant. The permanent droop is $R_p$ and an additional transient droop is needed due to peculiar response of the water turbine. The transfer function of the hydro turbine is non-minimum phase system due to the right half-plane zero in the numerator, resulting in peculiar response. Change in the valve position initially produces opposite change in power output. A large transient droop $R_T$ and long resetting time $\tau_R$ is required to achieve stable control performance [6].

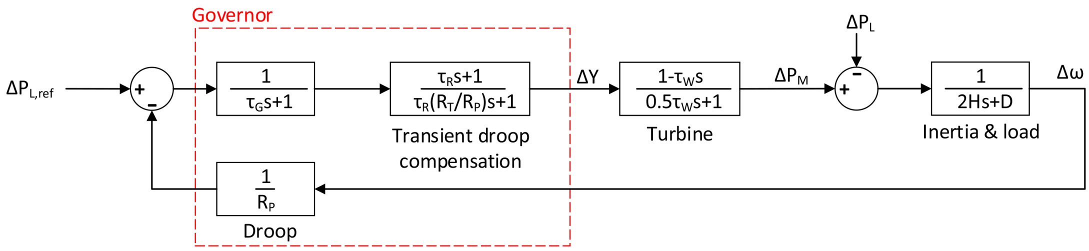


**Figure 2.11:** Block diagram of a hydro power plant model.

For the model of the geothermal power plant it is assumed that it behaves similar to a conventional non-reheat thermal plant. For there is no boiler for reheating purposes of the steam in geothermal power plants. Only turbine intakes of HP and LP steam, as seen in Figure 2.5. A block diagram of the geothermal power plant model is presented in Figure 2.12. The turbine is modelled as a simple transfer function, only dependent on the time constant of main inlet volumes and steam chest $\tau_{CH}$. The governor for the steam turbine does not require transient droop compensation, otherwise the modelling is the same as for the hydro power plant.

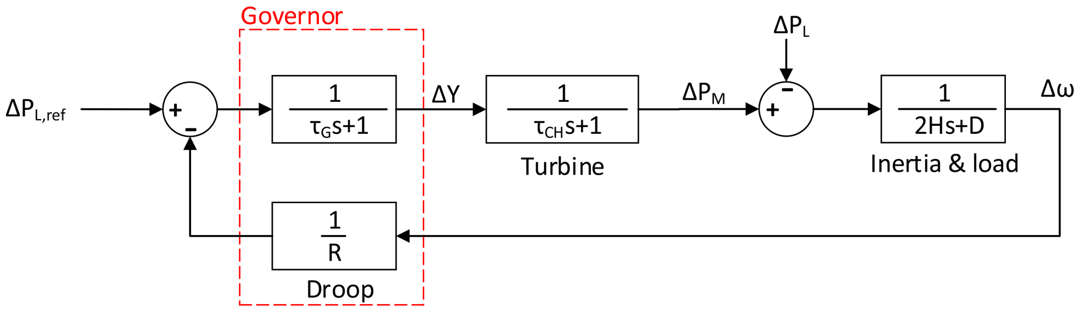


**Figure 2.12:** Block diagram of a geothermal power plant model[6].

Figure 2.13 shows the responses of valve position, mechanical power and speed/frequency of both hydro and geothermal models when the load, i.e. $\Delta P_L$, is subjected to a 0.1 pu increase.

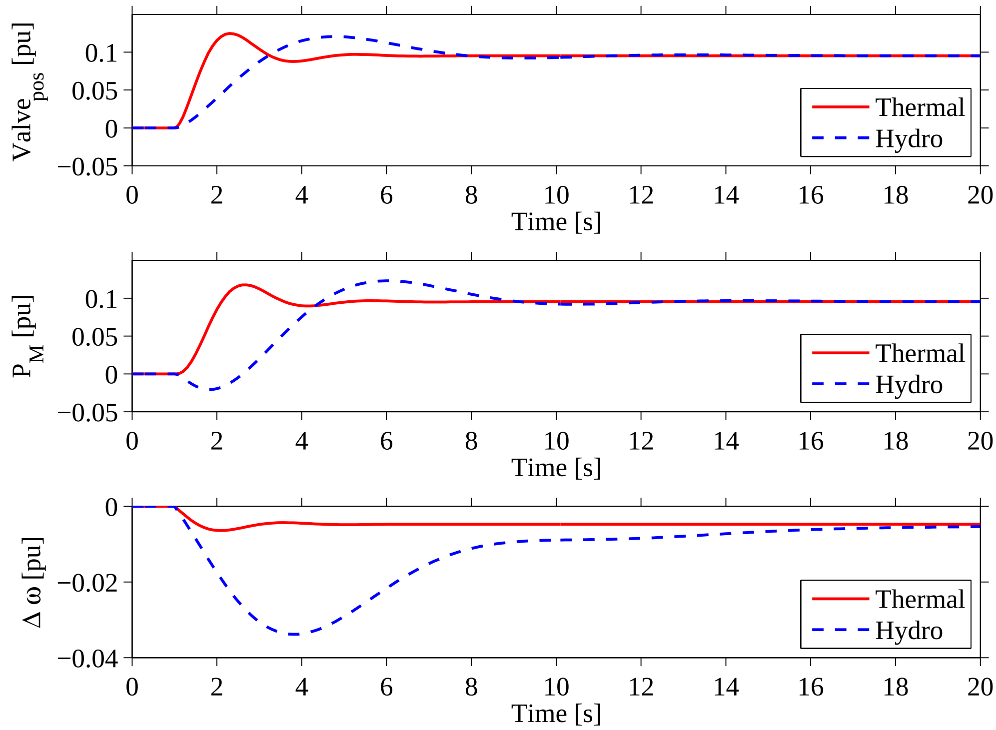


**Figure 2.13:** Responses of a hydro generator and a thermal generator to a 0.1 pu step increase in load, showing valve positions, mechanical powers and speed deviations [6].

The steady state deviations are the same for both types of power plants, even though the transient responses differs significantly. The initial mechanical power output $P_M$ of the hydro power plant is opposite to the gate position. This is because, when the gate valve is opened, the flow does not change simultaneously due to water inertia, but the pressure across the turbine is reduced which causes the power to decrease. The $T_W$ determines the response, the water flow accelerates and the power output reaches steady state when the water flow settles to a steady value. For this reason, the response of a hydro generator to a frequency change is slower than the thermal generator [6].

### 2.4.2 Icelandic Transmission System Model in PSS/E

Modelling of the Icelandic transmission system is carried out in a Siemens software called Power System Simulator for Engineering (PSS/E). The model is owned by Landsnet and updating and tuning is performed annually. The hydro generators of the system are modelled with the of the following two models [14]:

- **GENSAL** - 5th order salient pole generator model (quadratic saturation on d-axis).
- **GENSAE** - 5th order salient pole generator model (exponential saturation on both d and q-axis).

While all of the geothermal generators are modelled with:

- **GENROE** - 6th order round rotor generator model (exponential saturation).

The governor models used for the geothermal power plants are following [14]:

- **IEESGO** - IEEE standard model.
- **IEEEG1** - IEEE Type 1 Speed-Governing Model.
- **TGOV7** - User model designed for Landsnet.

The user model TGOV7 includes both load limit control mode and governor control mode. The model switches from load limit mode to governor mode at specified rotor speed deviation. The deadbands in the model, seen in Figure 2.14, determine at which speed deviation the switch occurs. The TGOV7 model is used for Krafla in the PSS/E model, Table 2.2 lists the descriptions and values of its parameters. The IEEEG1 governor model is presented in Figure 2.15. The IEEEG1 is used for the units at Hellisheiðarvirkjun and the the parameters of the model can be found in Table 2.2.

**Table 2.1:** Descriptions and parameters of the TGOV7 governor model of the units at Krafla.

| | Description |
|---|---|
| $S_1$ | Integral for Load |
| $S_2$ | Integral for LP |
| $S_3$ | HP Pressure Dynamics |
| $S_4$ | HP Control Valve |
| $S_5$ | LP Pressure Dynamics |
| $S_6$ | LP Control Valve |

| Parameters | |
|---|---|
| $\frac{K_1}{T_1}$ | 0.1 |
| Deadband #1 | 99.0 |
| $K_2$ | 20.0 |
| $K_3$ | 20.0 |
| $\frac{K_4}{T_2}$ | 2.0 |
| Deadband #2 | 0.02 |
| $T_1$ | 0.447 |
| $T_0$ | 0.3 |
| $T_2$ | 0.564 |
| $T_q$ | 0.477 |
| $f_1$ | 0.917 |
| $f_3$ | 0.175 |
| $f_2$ | 0.092 |

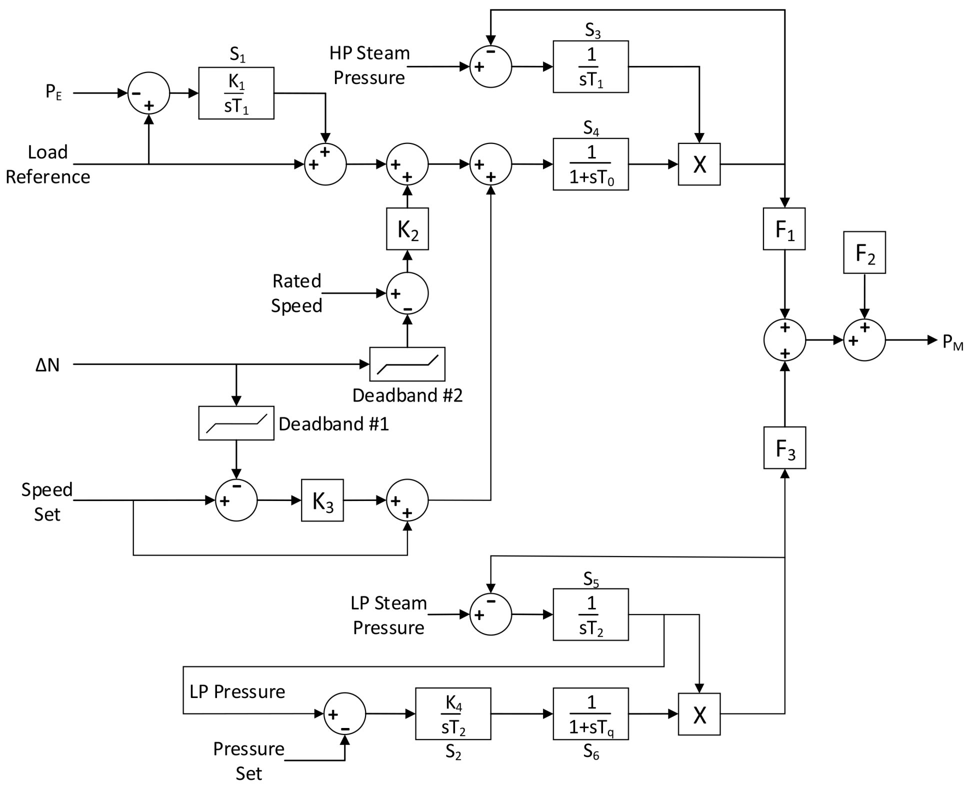


**Figure 2.14:** Block diagram of the TGOV7 governor model.

**Table 2.2:** Parameters of the IEEEG1 governor model of the units at Hellisheiðarvirkjun.

| Parameters | |
|---|---|
| K | 10.0 |
| T1 | 5.0 |
| T2 | 0.0 |
| T3 (>0) | 1.0 |
| $U_0$ | 1.0 |
| $U_c$ (<0) | -1.0 |
| $P_{max}$ | 1.0 |
| $P_{min}$ | 0.0 |
| $T_4$ | 1.0 |
| $F_1$ | 1.0 |
| $F_2$ | 0.0 |
| $T_5$ | 0.0 |
| $F_3$ | 0.0 |
| $F_4$ | 0.0 |
| $T_6$ | 0.0 |
| $F_5$ | 0.0 |
| $F_6$ | 0.0 |
| $T_7$ | 0.0 |
| $F_7$ | 0.0 |
| $F_8$ | 0.0 |

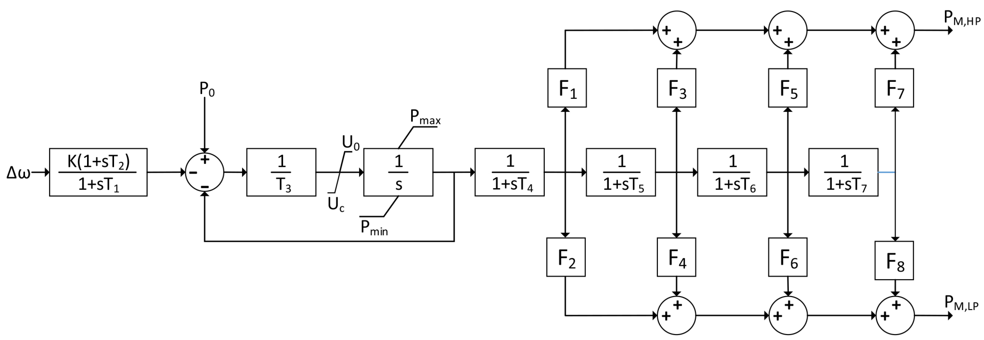


**Figure 2.15:** Block diagram of the IEEEG1 governor model[14].

## 2.5 Wide-Area Measurement Systems and Phasor Mesurement Units

Wide-area measurement systems (WAMS) are high resolution measurement system based on analogue and/or digital transmissions of GPS synchronized signals. The GPS give accuracy of 1 µs of the time reference compared to 1-10 ms for the SCADA monitoring system. This allows for much more detailed monitoring of the system dynamics [8]. Phasor measurement units (PMUs) are used in the measurement system, which allow measurements of voltage and current phasors, with resolution of 50 measuring points per second. WAMS allows for efficient real-time data management, archiving, visualisation and advanced applications including [15]:

- Voltage angle and magnitude monitoring
- System frequency monitoring
- Active and reactive power monitoring
- Transient monitoring
- Oscillatory stability monitoring
- Islanding recovery/resynchronisation

# 3

# Overview of the Icelandic Transmission System

An overview of the Icelandic system and the main operational problems will be presented in this chapter. First, the power regulation of the Icelandic system will be analysed with respect to the geothermal power plants. The power demand varies between an average summer load of 1850 MW to an average winter load of 2100 MW. Approximately 80% of the electricity is consumed by power intensive industries with fairly steady consumption all year round [3]. The Icelandic system is an islanded network and therefore the power demand has to be met with generation within the system, as there is no import or export of power. Secondly, frequency analysis of the Icelandic system will be performed and finally an overview of the Icelandic WAMS will be presented.

## 3.1 Main Operational Problems of the Icelandic System

The strongest part of the Icelandic transmission system is a 220 kV network located in the Southwest part of the country. Additionally, there is another 220 kV system in the Eastern part, which connects a large hydro power station to the largest aluminium smelter in Iceland. The two strong systems are coupled together with a fairly weak 132 kV interconnection, thus introducing challenges to the overall stability of the system. Figure 3.1 shows the two areas and the 132 kV ring connection. The main constraint in the Icelandic network is the ring connection, because it is heavily loaded and therefore it limits the power transfer between the West and East. Three congestion limits have been defined according to transient stability studies, which can be seen in Figure 3.2. The cut IV, which goes through transmission lines BL2 and SI4 is the most limiting of those three cuts [4].

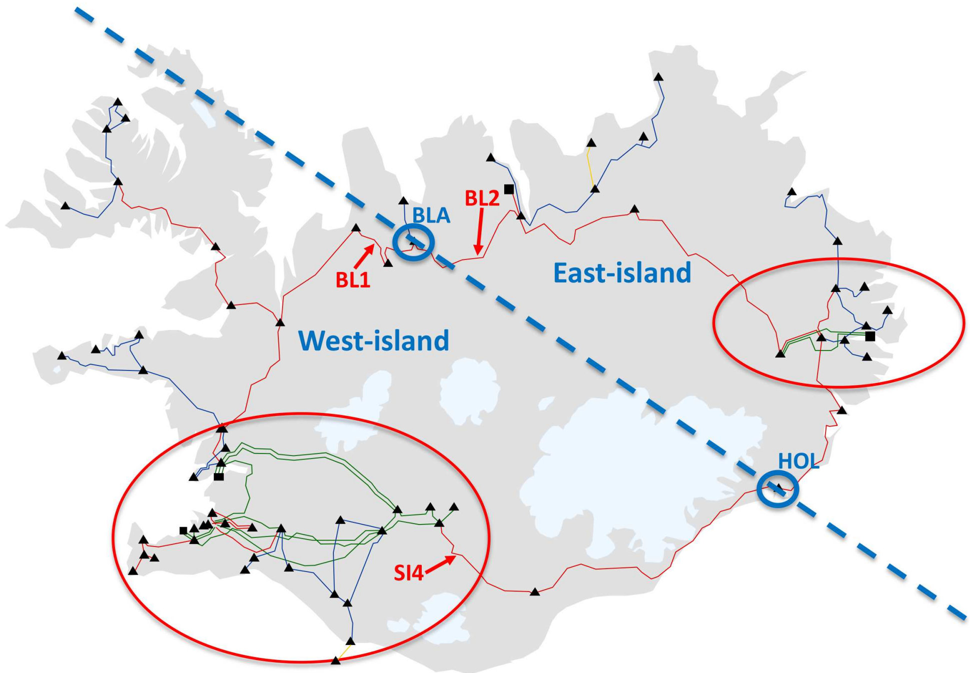


**Figure 3.1:** The most common system split and the two main consumption areas of the Icelandic transmission system.

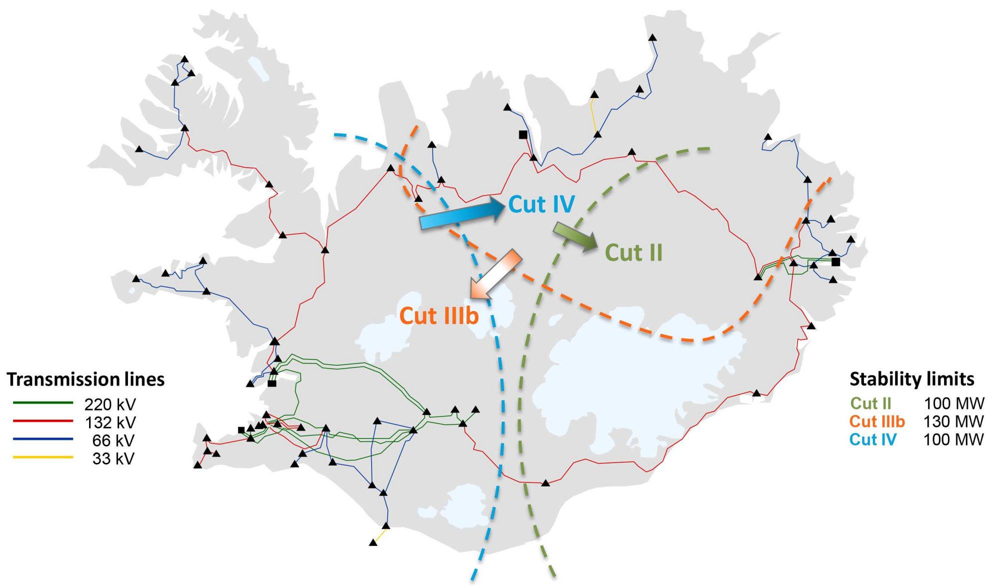


**Figure 3.2:** Defined congestion cuts in the Icelandic transmission system.

When the cuts are heavily loaded the system protections operate in order to secure stability of the system during faults and to avoid critical power oscillations on the ring connect. The bus coupler circuit-breaker of Blönduvirkjun (BLA) and the line breaker at Hólar (HOL) will trip if:

- Power-flow through transmission line BL1 exceeds 130 MW.
- Power-flow through transmission line BL2 exceeds 120 MW.
- Power-flow through transmission line SI4 exceeds 120 MW.

As a result, the network will split up into two islands, i.e. the West island and the East island. The split is illustrated in Figure 3.1. The islanding splitting is not favourable as it reduces the system inertia. Therefore it is important to keep the system attached, in order to increase the stability of the system. The stability limits in Figure 3.2 are a benchmark for guaranteed transient stability of the network. Occasionally the system is operated above these limits, therefore the BL1, BL2 and SI4 protection thresholds are kept higher than the stability limits.

The system is configured with under-frequency protection scheme to handle loss of generation. Most of the large industry users are equipped with automatic load shedding. The scheme is stepwise with different shed sizes and delay times, with activation range beginning at 48.7 Hz. The Icelandic network has relatively large units of energy-intensive loads, where the largest units are 100-500 MW. If these large units are tripped suddenly, the network will experience intense dynamics of power unbalance and the stability can become critical. Over-frequency events can trigger overspeed protections of the generators governor systems; as a result the generators will trip. Generally the geothermal power plants are more sensitive to over-frequency events than the hydro power plants. Over-speeding of the high speed synchronous generators causes mechanical resonances, therefore the geothermal units are more likely to be tripped in an over-frequency events than hydro power plants.

The current control strategy of the geothermal power plants is an extensive problem in today's operation. Geothermal power is 25% of the total capacity and does not contributes to the frequency regulation of the system. The governor controls have following functionality: if the system frequency is within $50 \pm 1$ Hz the plants are set to fixed generation given by a setpoint, i.e. load limit control mode. If the system frequency goes outside of $50 \pm 1$ Hz the generators will switch to primary frequency control, i.e. governor control mode. This control strategy can add extra stress on the power system during dynamics following a large system fault. Thus, increasing the risk of losing the system stability. An example of this behaviour is illustrated in Figure 3.3, in an idealized sequence of events after a 500 MW trip of a power intensive industry. Response results from one geothermal unit and one large hydro unit are presented in Figure 3.3, the idealized system is considered to include more power plants. The fault occurs at 5 s and the frequency immediately starts to increase after the fault, the hydro unit starts immediately to decrease its output due to the primary frequency regulation. After the frequency becomes more than 51 Hz the geothermal plant switches to the governor control and starts to decrease its output in order to restore the system frequency back to 50 Hz. At around 13 s the hydro generator reaches its minimum production, while other hydro generator in the system are still decreasing their production. When the frequency gets back below 51 Hz the geothermal power plant starts to return to its pre-fault generation by ramping up the generation again. This event will put extra stresses to the hydro generator because now it will be forced into reverse power (generators consuming power) to compensate for the increased geothermal generation. Note that no inertia response is taken into account in this idealized example.

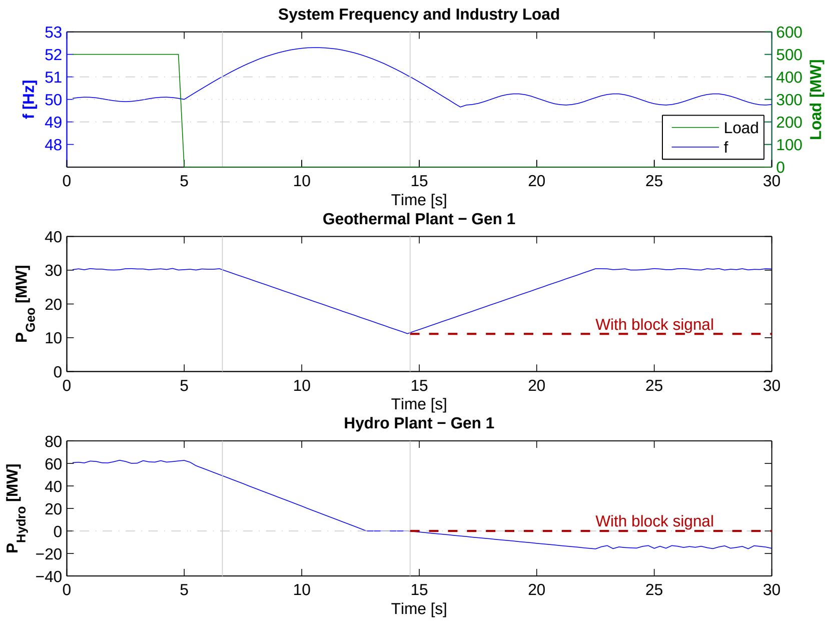


**Figure 3.3:** Idealized sequence of events following a trip of a power intensive load, showing the system frequency, the industry load, the mechanical power of a geothermal unit and the mechanical power of a hydro unit.

There are two main problems caused by this behaviour of the geothermal units that will be analysed in this thesis. The first problem is that this type of geothermal control increases the stress on the remaining hydro power plants, as they have to compensate for the immediate increase in geothermal production. During a low system load, for instance during the summertime, the geothermal is operated at its maximum capacity, while hydro power plants are operated at a low capacity. If a large industry fault would occur in such conditions some of the hydro power plants would be forced into reverse power. Most of the hydro power plants have Francis turbines which allow for momentary reverse power, but it should always be avoided. There are few of hydro power plants using Kaplan turbines which do not allow reverse power and will therefore be tripped in such scenarios. Those hydro power plants having Kaplan turbines do not have large capacities, therefore do not affect the overall performance in a great deal, but trips of generators should always be avoided. One option would be to improve the current control scheme for the geothermal power plants by blocking the ramp up of generation after they have regulated down following a fault. This could be achieved with a fast-acting setpoint change of the geothermal unit. The result can be seen on the red dashed lines in Figure 3.3. Such a control would reduce the regulation response on the hydro power plants during the dynamics following the fault.

The second problem is concerning the control of the geothermal power plant Krafla. A possible control option for that scenario is to block the governor at Krafla from switching to governor control mode. The benefits for such scenarios will be discussed further in Chapter 3.2.

## 3.2 Overview of the Geothermal Power Plants

Krafla (KRA) is a geothermal power plant located in Northeast Iceland, it will be the main focus for the primary frequency control studies in this thesis. The second geothermal power plant that will be investigated is Hellisheiðarvirkjun (HEL), located in the Southwest Iceland, as can be seen in Figure 1.1. The specifications for the plants is shown in Table 3.1.

**Table 3.1:** Specifications of the geothermal power plants Krafla and Hellisheiðarvirkjun[16].

| | Krafla | Hellisheiðarvirkjun |
|---|---|---|
| Installed capacity | 2 x 30 MW | 7 x 45 MW |
| Annual production | 500 GWh | 2660 GWh |
| Brought online | 1977 | 2006-2011 |
| Refurbished | 1997 | - |
| Pole pairs | 1 | 1 |
| Synchronous speed | 3000 rpm | 3000 rpm |
| Over speed protection | 3300 rpm | 3300 rpm |

Krafla is located at a week point of the 132 kV network. Despite its small capacity, it plays a vital role in the stability of the network. In some cases Krafla's control strategy can cause an islanding split of the system, as can be seen in Figure 3.1. For instance, when large load is tripped in Southwest of the country the frequency will start to rise and the power-flow from West to East will increase after the ring connection. When Krafla experiences over-frequency it will switch to governor control mode and rapidly starts to decrease its output. Consequently, the power-flow on the ring connection will increase further, until it might trigger the system protection and split the system. Another issue is that the PSS at Krafla is important for stabilizing the power oscillations on the ring connection. The problem is that the PSS is disabled at each generator at 15 MW output, therefore it is essential to avoid ramp downs at Krafla, because use of the PSS is crucial during fault events. The effects of changing the control strategy of Krafla will be investigated, to avoid events where the governor switches to governor mode.

The governor control settings for Krafla in today's system is as follows:

- Krafla operates in load limit control mode if the system frequency is within $50 \pm 1$ Hz.
- Generator unit 1 switches to governor control mode if the frequency is outside the $50 \pm 1$ Hz for more than 1 sec.
- Generator unit 2 switches to governor control mode if the frequency is outside the $50 \pm 1$ Hz for more than 3 sec.

The delays of the governor control are added to avoid an immediate switch to governor control mode for cases where the frequency briefly crosses the $50 \pm 1$ Hz threshold. The two generator units are configured with different delay times to avoid simultaneous response of the units. Another issue with the actual governor control of Krafla is that following a down regulation of the plant it is not capable of returning to its pre-fault production value immediately after the frequency has stabilized. This is due to the complexity of power plant, because it depends upon many mechanical systems with different pressure levels. It also depends on whether there is enough steam available from the boreholes at the moment the generation is ramped up. When the frequency returns within the $50 \pm 1$ Hz the power plant settles to a generation lower than the pre-fault value and the operators at the power plant have to manually trigger the ramp up of the plant, which is approximately 0.025 MW/s.

Hellisheiðarvirkjun is a much larger plant located in the Southwest 220 kV network. The concept for Hellisheiðarvirkjun is not to block the switch to governor mode like for Krafla, but rather to block the ramp up of the production following a down regulation due to a fault, like described in Chapter 3.1. Hellisheiðarvirkjun uses the following governor control settings for all of its generators:

- Hellisheiðarvirkjun operates in load limit control mode if the system frequency is within $50 \pm 1$ Hz.
- All generator units switch to governor control mode if the frequency is outside the $50 \pm 1$ Hz without any programmed delay.

If the plant does not trip during the disturbance, then it usually is capable of returning to its pre-fault production when the frequency has stabilized.

## 3.3 System Frequency Statistics

System frequency statistical analysis was performed in order to reflect the characteristics of the transmission system. The data used in this analysis is 10 second average values of the measured local frequency by the SCADA system. Empirical probability mass functions of the frequency for the past 5 years are presented in Figure 3.4. It can be seen that the frequency deviation from the nominal value has been increasing since the year 2009. It can also be confirmed with the standard deviation results presented in Table 3.2. This trend can be the result of multiple factors, e.g. the electric demand has been increasing while there has been very little reinforcements of the power system. Consequently the power system is being stressed closer to its limits. Weather conditions differ from year to year, where it effects the number of severe fault events and the water levels at the hydro power plants reservoirs.

**Table 3.2:** Frequency mean and standard deviation results for the years 2009-2013 in Iceland.

| Year | Mean [Hz] | Standard deviation [Hz] |
|---|---|---|
| 2009 | 49.9955 | 0.0419 |
| 2010 | 49.9957 | 0.0457 |
| 2011 | 49.9900 | 0.0467 |
| 2012 | 50.0003 | 0.0532 |
| 2013 | 50.0004 | 0.0501 |

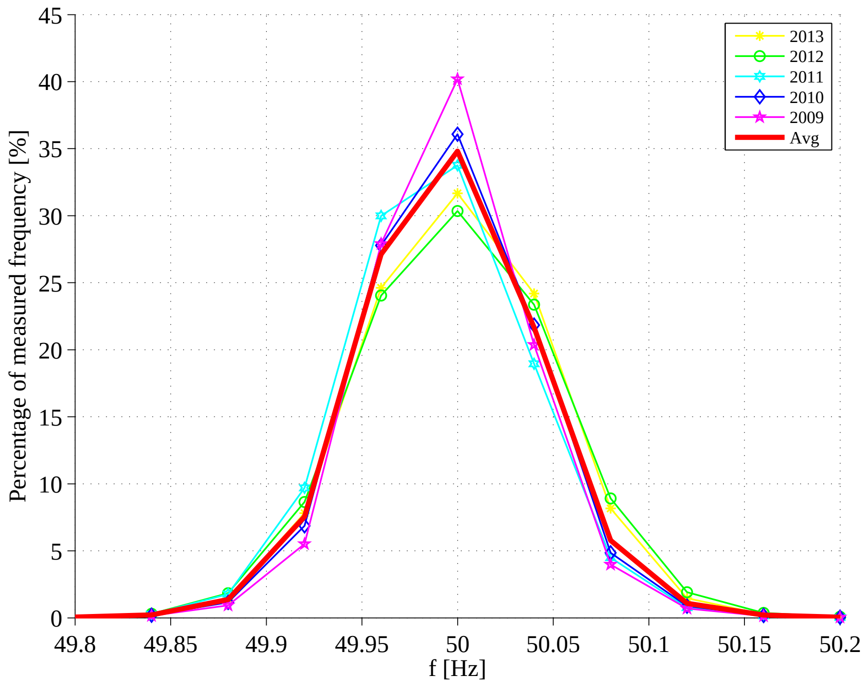


**Figure 3.4:** Empirical probability mass functions of the frequency for the years 2009-2013 in Iceland.

Landsnet has the objective to fulfil certain frequency standard regarding the quality of the system frequency. The standard is as follows:

- 99.5% of measured frequency should be within $50 \pm 0.2$ Hz (10 sec average values).

The percentage that the frequency was within the limits for the last 5 year can be seen in Table 3.3.

**Table 3.3:** Frequency standard results for the years 2009-2013 in Iceland.

| Year | Percentage within $50 \pm 0.2$ Hz |
|---|---|
| 2009 | 99.82% |
| 2010 | 99.73% |
| 2011 | 99.83% |
| 2012 | 99.83% |
| 2013 | 99.87% |

To investigate whether over- or under-frequency events is more frequent in the Icelandic system the same data is analysed for different frequency deviations. Table 3.4 shows the comparison between over- and under-frequency for the events with different frequency deviations.

**Table 3.4:** Frequency deviation statistics for the years 2009-2013 in Iceland.

| Frequency deviation | Number of measurements | Under-frequency | Over-frequency |
|---|---|---|---|
| $\geq 0.04$ Hz | $11.6 \cdot 10^6$ | 55.76% | 44.24% |
| $\geq 0.48$ Hz | 1339 | 22.18% | 77.82% |
| $\geq 1.00$ Hz | 288 | 6.60% | 93.40% |
| $\geq 1.48$ Hz | 149 | 1.34% | 98.66% |
| $\geq 2.00$ Hz | 30 | 3.33% | 96.67% |

Over-frequency events are more frequent and severe than under-frequency events in the Icelandic transmission system, i.e. large industry load trips are more common than trips of generation units. This thesis work will therefore only focus on over-frequency events. It can be noted that the rate of change of frequency (RoCoF) is not an issue in the Icelandic system. There are no transmission level load shedding schemes which are triggered by the RoCoF.

## 3.4 Overview of the Icelandic WAMS

Since 2007 Landsnet has been using WAMS application called PhasorPoint, owned and developed by Psymetrix (Alstom). PMU units have been installed at all of the power intensive industry customers and all the main power plants in the system. Monitoring with PhasorPoint system has been implemented into the real-time operation in the centralized control room, where it has improved islanding detection, resynchronisation and overall system condition monitoring. PhasorPoint has also improved testing and tuning of devices in the power system, e.g. governors and PSSs. Finally, the archived data from the PhasorPoint has greatly improved the system and disturbance analysis.

In the year 2011 Landsnet along with Psymetrix began developing control schemes by utilizing the control option of the PhasorPoint system. The goal was to improve the stability of the system and to drive the system harder with monitoring and control. There are many different control projects in progress, including this thesis work. An example of another project is the Icelandic wide-area defence scheme (WADS), project that will use an angular separation between the South and East centers of inertia, to trigger either generation shedding or fast ramp down of generators in south when necessary to maintain angular stability. The first implementation of a control scheme using the PhasorPoint application was tested and put into operation early 2014. The control scheme triggers sheddings of a controllable loads in East Iceland when certain power-flow thresholds are exceeded.

# 4

# Simulation of a Primary Frequency Control with a Simplified Model

This chapter will study different control strategies of geothermal power plants in a simple single bus system. The purpose is to investigate different primary frequency control strategies by studying dynamic responses of a system that experiences sudden load reduction. The geothermal energy is a renewable energy resource with a high availability. For this reason, the geothermal power plants are always operated at maximum capacity and more water can be stored in hydro reservoirs. Geothermal power plants normally do not have available reserve power, therefore a load reduction is more appropriate than a load increase.

## 4.1 Modelling of a Single Bus Power System

The models introduced in Chapter 2.4.1 are used to simulate single bus power system in MATLAB/Simulink. The primary frequency control considers an elaborated performance of all synchronised generators in the system. Theoretically, every generator unit should swing based on its own power balance between the mechanical power input and electrical power output, according to (2.13). However, a coherent response of all generators is assumed for the simulations and all the generator are aggregated together [6].

Figure 4.1 shows how a block diagram of different generator models can be combined, using coherent inertia. The simulation model used in this chapter includes one hydro unit, along with two identical geothermal units. The models are in per unit and the inertia and droops have to be expressed according to the power bases of each generator unit. The equivalent inertia is calculated as a weighted sum

$$H_{eq} = \frac{H_{hy}S_{b,hy} + H_{geo1}S_{b,geo1} + H_{geo2}S_{b,geo2}}{S_{total}} \tag{4.1}$$

where $H_{hy}$, $H_{geo1}$, $H_{geo2}$ are the inertia constants of each of the generator units, $S_{b,hy}$, $S_{b,geo1}$, $S_{b,geo2}$ are the apparent power bases of each of the generator units and $S_{total}$ is the total apparent power base of the system. The droops are calculated as

$$R_{hy} = \frac{R_{pu,hy}}{S_{b,hy}} \qquad R_{geo} = \frac{R_{pu,geo}}{S_{b,geo}} \tag{4.2}$$

where $R_{pu,hy}$ and $R_{pu,geo}$ are the droops on per unit base for each of the generator units. The droops of both the geothermal units are identical for this simulation [6].

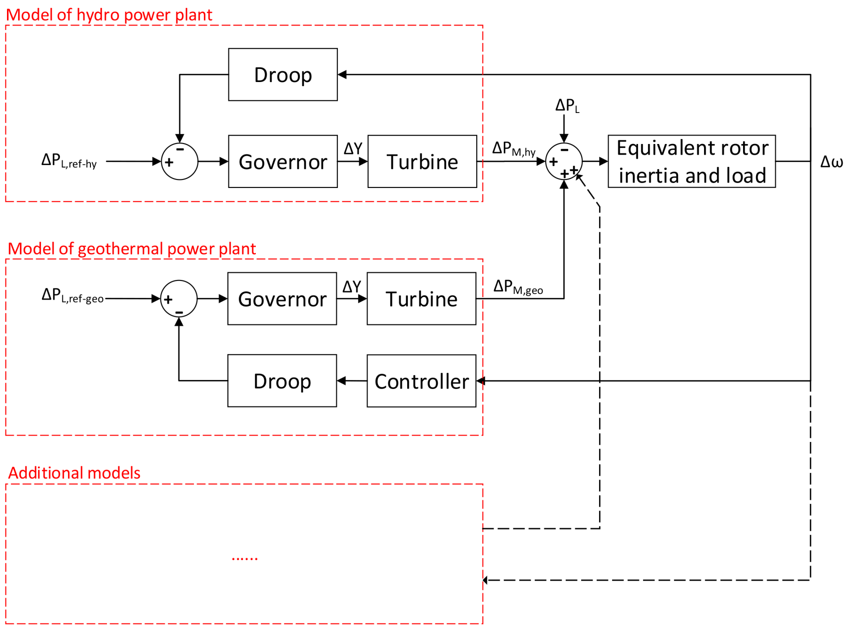


**Figure 4.1:** Block diagram of a single bus system with multiple generator units.

The geothermal power plants have logic controllers, in order to simulate the switch between load limit control mode and governor control mode. The controllers have the following settings:

1. *Governor control* #1: The logic controller is deactivated and the frequency signal is continuously feed to the governor, i.e. the geothermal power plants operate in governor control mode at all times.

2. *Governor control* #2: The geothermal power plants operates in load limit mode in normal conditions. If the frequency deviation goes outside defined band for longer than the specified delay, the feedback through the droop is activated, i.e. governor control mode. When the frequency returns inside the band for more than the specified delay, the feedback signal is shut off (directly to zero).

3. *Governor control* #3: Identical to governor control #1, except when the frequency returns within the band, longer than the defined delay, the actual frequency deviation signal through the droop will be reduced linearly by ramping it down to zero.

Diagram of the simulations model and block diagram of the governor logic controller constructed in MATLAB/Simulink can be found in Appendix A.1. The parameters used for each generator model and equivalent parameters of the simulation are presented in Table 4.1. Krafla's parameters are used for the geothermal power plant models for this simulation, while conventional hydro power plant parameters are used for the hydro power plant model.

**Table 4.1:** Specification for the hydro and geothermal generator models [6].

| Hydro power plant model | |
|---|---|
| $\tau_W$ | 1.0 s |
| $\tau_R$ | 5.0 s |
| $\tau_G$ | 0.2 s |
| $R_T$ | 0.38 |
| $R_p$ | 0.05 |
| $H$ | 3.0 s |
| $D$ | 1.5 |
| $S_{b,hy}$ | 0.70 pu |

| Geothermal power plant model | |
|---|---|
| $\tau_{CH}$ | 0.5 s |
| $\tau_G$ | 0.2 s |
| $R$ | 0.04 |
| $H$ | 6.58 s |
| $D$ | 1.5 |
| $S_{b,geo}$ | 0.15 pu |

| Equivalent parameters | |
|---|---|
| $H_{eq}$ | 4.07 s |
| $D_{eq}$ | 1.5 |
| $R_{hy}$ | 0.07 |
| $R_{geo}$ | 0.27 |
| $S_{total}$ | 1.0 pu |

The load, generation reference setpoints and size of disturbance for the simulations are presented in Table 4.2.

**Table 4.2:** Simulations parameters.

| $P_L$ | $P_{L,ref-hy}$ | $P_{L,ref-geo1}$ | $P_{L,ref-geo2}$ | $P_{disturbance}$ |
|---|---|---|---|---|
| 1.0 pu | 0.7 pu | 0.15 pu | 0.15 pu | -0.15 pu |

## 4.2 Simulations with Krafla's Governor Control Settings

The simulations in this chapter show the responses of the different control strategies using Krafla's actual governor control settings. The simulations only consider primary frequency control, therefore there will always be steady state frequency deviation, because there is no secondary frequency control to compensate for the load reduction. Simulations using governor control #1, where both the hydro and geothermal units are used in governor control are presented in Figure 4.2. As a result, both of the plants will respond instantaneously to a change in load. Note that the settling time $T_{settling}$ for each simulation is defined as the measured time from the start of the load disturbance until the frequency has settled to its steady state value. Additionally, the peak frequency deviation and the steady state frequency deviation are presented for each simulation.

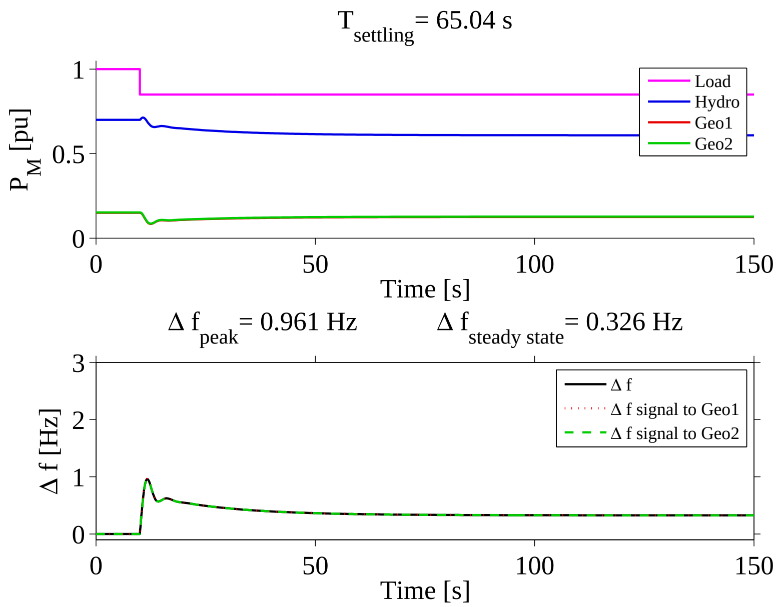


**Figure 4.2:** Simulation results for the governor control #1.

Simulation results of the load change, the mechanical power response of each generator unit, the frequency deviation and the applied geothermal governor signals are presented in Figure 4.2. The geothermal units are operated continuously in governor control mode, which can be seen from the applied frequency signals to the geothermal governors. The applied signals are always equal to the system frequency deviation, which confirms the functionality of control #1.

Figure 4.3 shows the results for the governor control #2. The geothermal unit 1 reacts to the disturbance one second after the frequency deviation becomes greater than 1 Hz, by applying the frequency signal to the governor. One second after the frequency deviation returns within 1 Hz the controller shuts off the governor signal. The same control logic applies to geothermal unit 2, except for a delay setting of three seconds instead of one second. The problem with this control is the resulting power oscillations between the hydro unit and the geothermal units. The hydro unit is not able to compensate in time, for the fast response of the geothermal units. Resulting in another frequency increase, leading to repeated response action of the geothermal units. The response of the geothermal power plants using control #2 resembles the response of Hellisheiðarvirkjun rather than the response of Krafla.

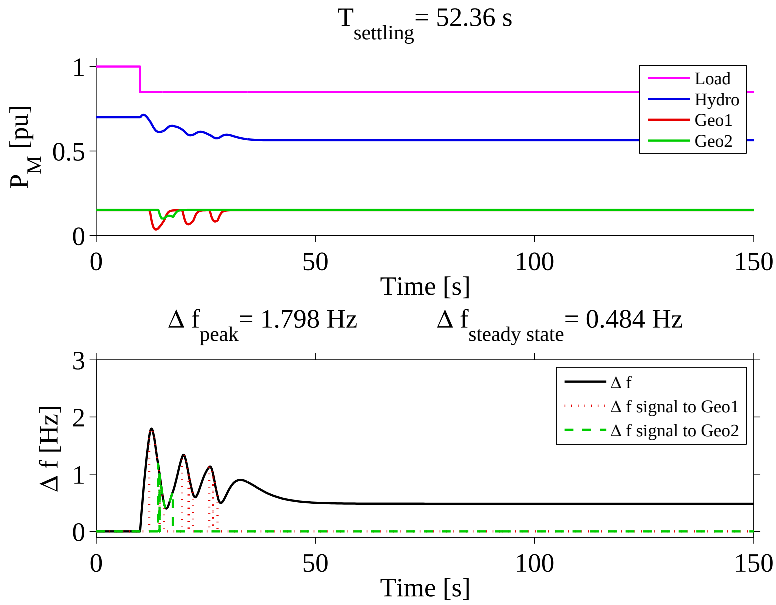


**Figure 4.3:** Simulation results for the governor control #2.

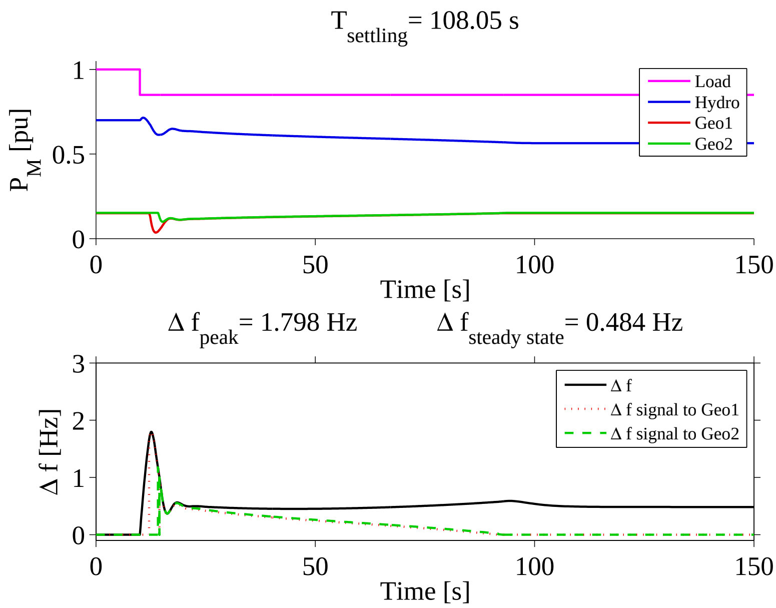


**Figure 4.4:** Simulation results for the governor control #3.

The governor control #3 is supposed to replicate the functionality of Krafla's actual governor system, described in Chapter 3.2. Figure 4.4 shows the simulation results for the governor control #3. It can be seen that when the frequency deviation returns within 1 Hz after the fault, the mechanical outputs of the geothermal power plants settles to production lower than the pre-fault value before it begins to slowly ramp up to its pre-fault value. This is achieved in the model controller by linearly decaying the frequency signal applied to the governors of the geothermal units, which can be seen in Figure 4.4.

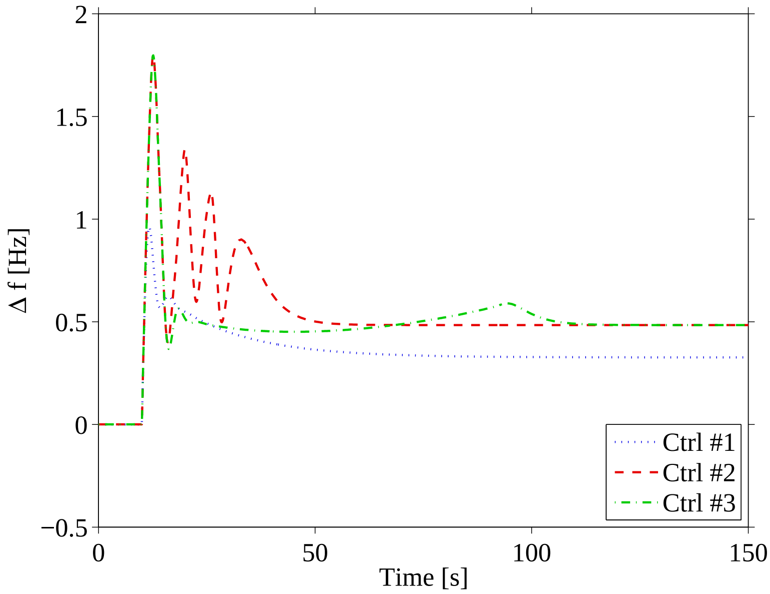


**Figure 4.5:** Comparison of the frequency deviations for the governor controls #1-3 using Krafla's governor control parameters.

Figure 4.5 shows the comparison of the frequency deviation for the different governor controls. Theoretically the control #1 gives the best response, where the peak frequency deviation is only 0.961 Hz. Moreover, the steady state frequency deviation is the lowest due to the shared generation reduction of all the units, determined by the droop settings. In conclusion, the control #1 is only useful for theoretical studies because it is not feasible in practice, due to the operational constraints of the geothermal power plants. The power plant owner requires steady operation of the plants in normal operation, because of the plant's mechanical complexities and to minimize a recurrent and costly maintenance.

Governor controls #2 and #3 both have the same peak frequency deviation of 1.8 Hz and the same steady state frequency deviation of 0.484 Hz. Both controls work exactly the same until the frequency returns back inside ±1 Hz and the steady state frequency deviation is only determined by the hydro power plant in both cases. The difference between those two controls is only in the dynamic response, where control #2 results in more fluctuation with a less settling time, while control #3 has a smooth response with longer settling time.

## 4.3 Simulations with Different Delay Settings

The model response is analysed for different delay settings, where the delay settings of geothermal unit 1 is varied from 0-3 seconds, while the delay of unit 2 is always set two seconds behind the unit 1. The frequency deviation pickup amplitude is kept constant at value of ±1 Hz. The frequency responses for governor controls #2 and #3 are presented in Figures 4.6-4.7. The complete simulation result for this parameter study can be found in Appendix A.2.

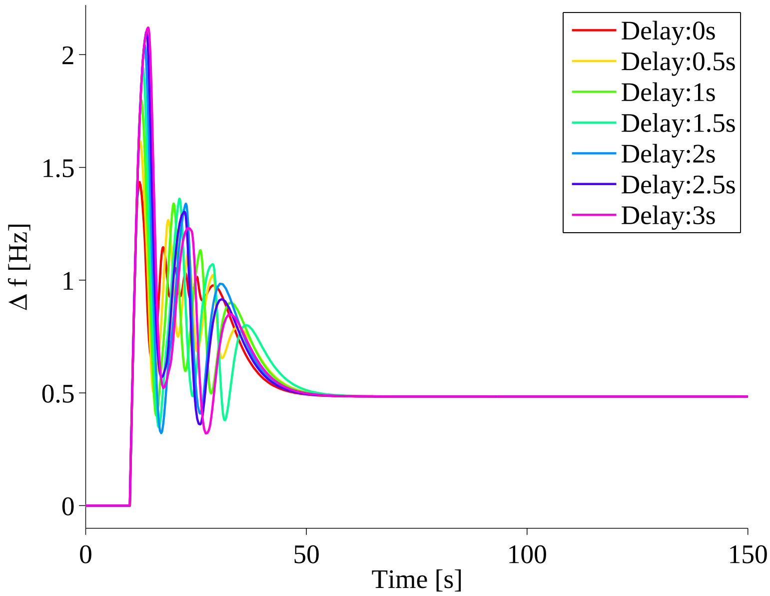


**Figure 4.6:** Comparison of the frequency response for the control #2 and for different delay settings.

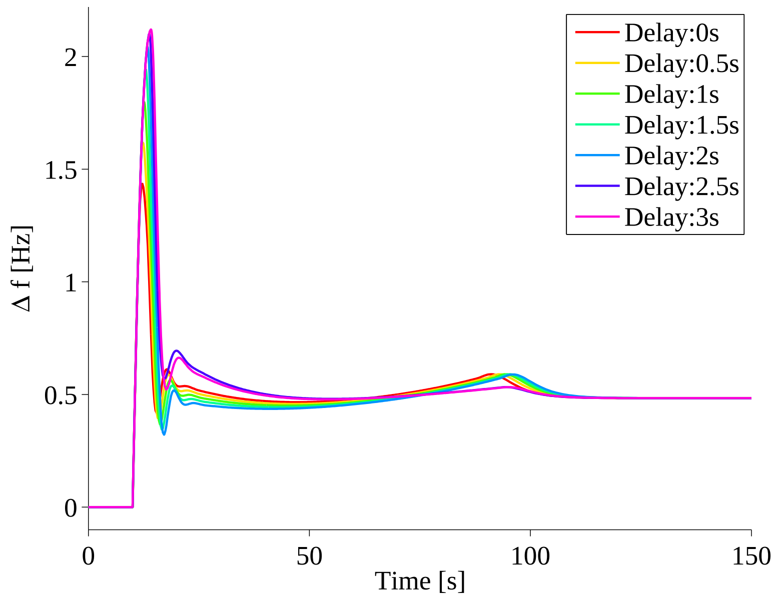


1

**Figure 4.7:** Comparison of the frequency response for the control #3 for different delay settings.

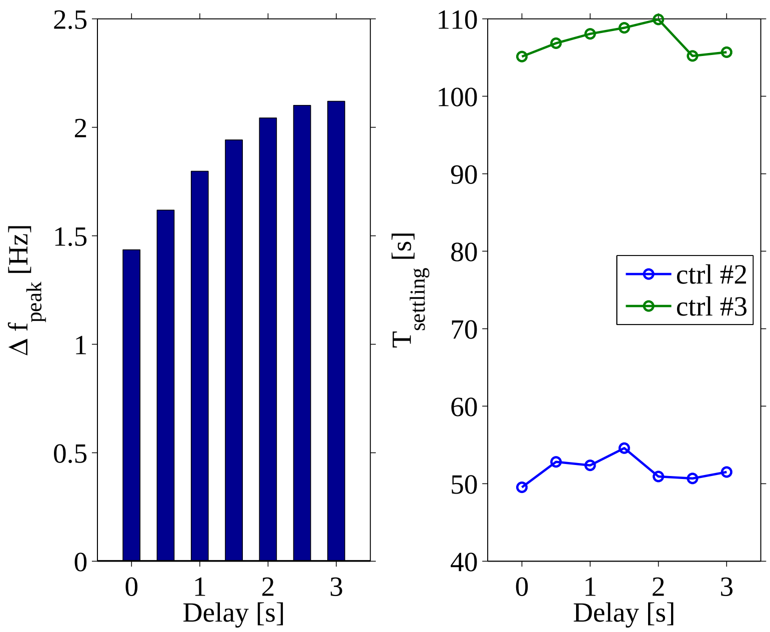


**Figure 4.8:** Summary of the peak frequency and the settling time for different delay settings of the governor controller.

The summary of the peak frequency deviations and the settling times $T_{settling}$ for the different delay settings is shown in Figure 4.8. The first frequency swing is the same for both controls. Increased delay time of the response of the geothermal unit will increase the initial swing of frequency, until it stabilizes at the delay of 3 seconds. The hydro unit manages to compensate for the frequency rise by that time, without requiring regulation contribution of the geothermal units. The settling times for each control varies with in a range of five seconds around the average settling times of 51.8 seconds for the control #2 and 107.1 seconds for the control #3. The differences in settling times for individual control, depends on the number of geothermal units needed to react to the fault. The difference in settling time between the control #2 and the control #3 is only dependant on the ramp up time in the control #3.

## 4.4 Simulations with Different Frequency Amplitude Settings

The model response is analysed for different frequency amplitude settings, where the frequency deviation pickup amplitudes for both of the geothermal units is varied from 0.5-2.5 Hz, while the delays are kept at default values of one second for geothermal unit 1 and three seconds for unit 2. The frequency responses for governor controls #2 and #3 are presented in Figures 4.9-4.10. The complete simulation result for this parameter study can be found in Appendix A.3.

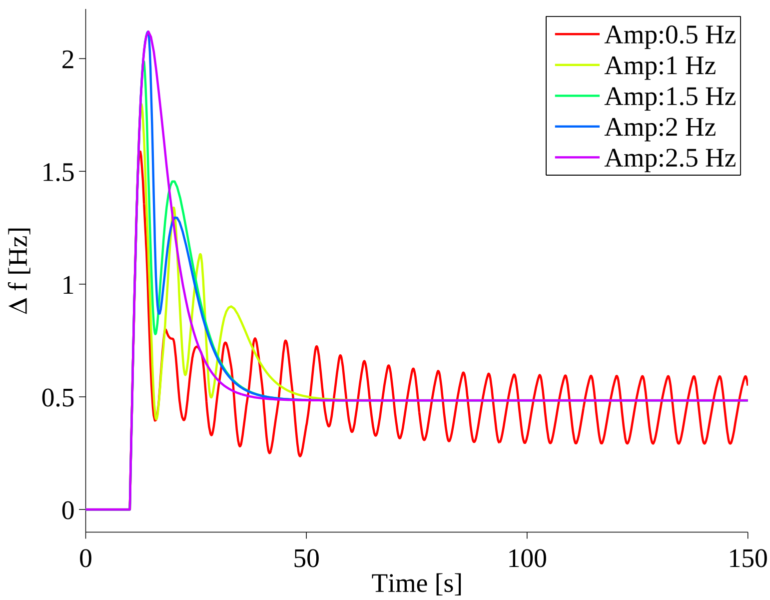


**Figure 4.9:** Comparison of the frequency response for the control #2 and for different frequency amplitude settings.

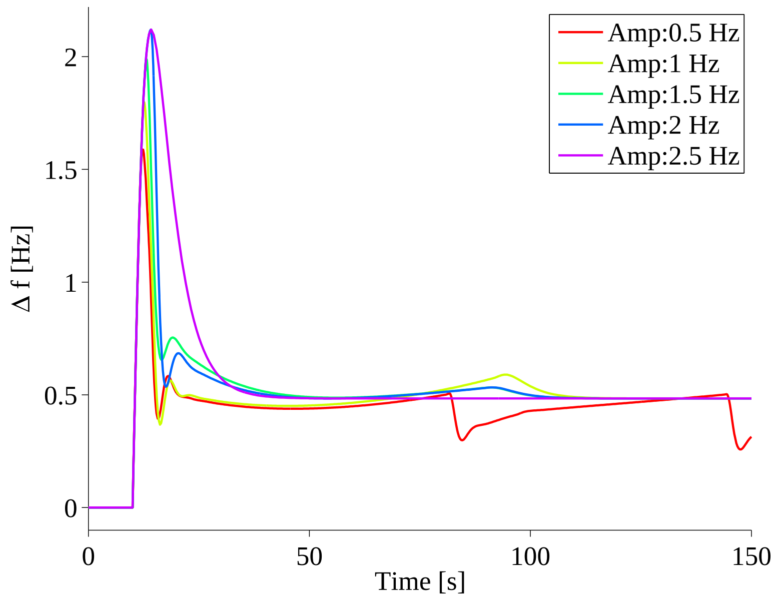


1

**Figure 4.10:** Comparison of the frequency response for the control #3 and for different frequency amplitude settings.

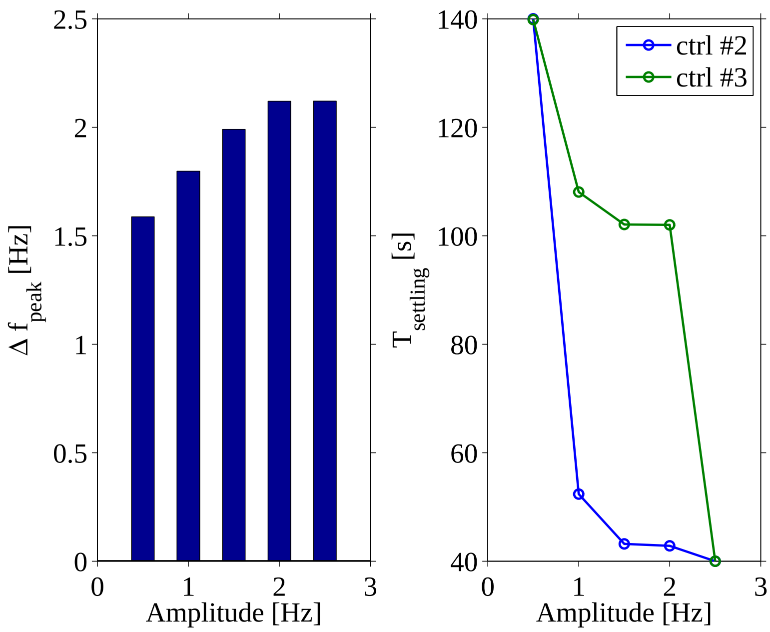


**Figure 4.11:** Summary of the peak frequency and the settling time for different frequency amplitude settings of the governor controller.

The peak frequency deviations and settling times $T_{settling}$ for the different frequency amplitude settings is summarized in Figure 4.11. As before, the first swing of the frequency is the same for both controls. The peak frequency deviation of the simulations rises with increased pickup amplitude of the controller, until the amplitude of 2.5 Hz. Then the pickup amplitude becomes too high for the geothermal to react to the fault and the hydro manages to regulate the system without reaction of the geothermal units. The peak frequency deviation settles to value of 2.12 Hz for any amplitudes higher than 2.5 Hz. This result can also be seen in the settling time, both controls #2 and #3 result in the same settling time, because the geothermal units do not respond to the fault. On the other hand, if the pickup amplitude is to low, i.e. 0.5 Hz, then the governor controls are not capable of stabilizing the system on their own. A secondary frequency control is needed to stabilize the system. This result can be seen in Figures 4.9-4.10 for amplitude of 0.5 Hz. For those cases the settling times become 140 seconds, that is only because of the simulations timeframe. The 140 seconds corresponds to infinity, because the system is unstable.

## 4.5 Simulation of Fast-Acting Setpoint Change of Generators

The effect of fast-acting setpoint change of the geothermal units, introduced in Chapter 3.1 will be examined in these simulations. The purpose of the new applied setpoint is to block the geothermal units to return to their pre-fault values, immediately after the frequency returns within $50 \pm 1$ Hz. The simulation setup consists of one hydro unit and one geothermal unit, the parameters are presented in Table 4.3.

**Table 4.3:** Parameters used in simulations for fast-acting setpoint change of geothermal generators.

| $P_L$ | $P_{L,ref-hy}$ | $P_{L,ref-geo}$ | $P_{disturbance}$ |
|---|---|---|---|
| 1.0 pu | 0.7 pu | 0.3 pu | -0.15 pu |

Krafla's governor control settings are used. The simulation results for the governor controls #2 and #3 can be found in Figures 4.12-4.13. The principles of this control strategy is to change the generator setpoint when a fault is detected. The new setpoint will not effect the response of the plant while it operates in the governor control mode. When the plant switches back to the load limit control mode the governor will regulate the plant according to the new setpoint. The new setpoint used for this simulation is the power output of the geothermal plant at the moment the frequency returns within $50 \pm 1$ Hz.

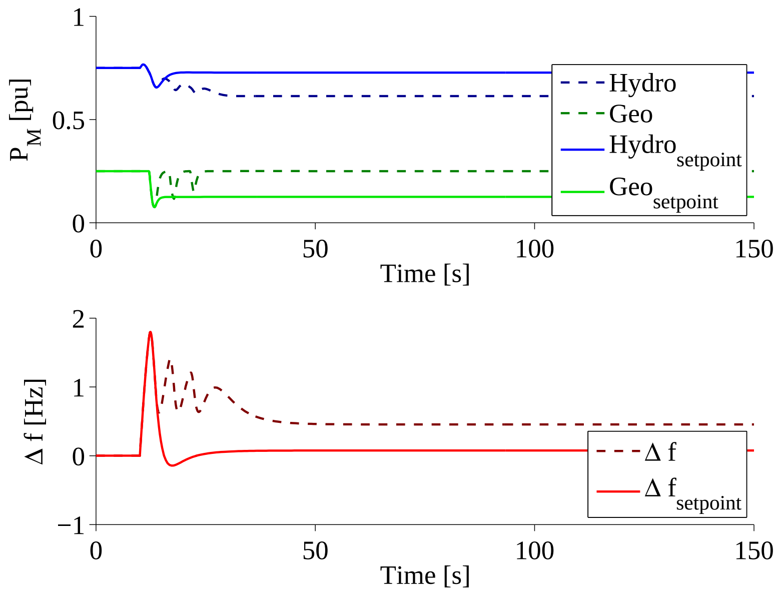


**Figure 4.12:** Simulations for the control #2 with and without setpoint change of the geothermal generators.

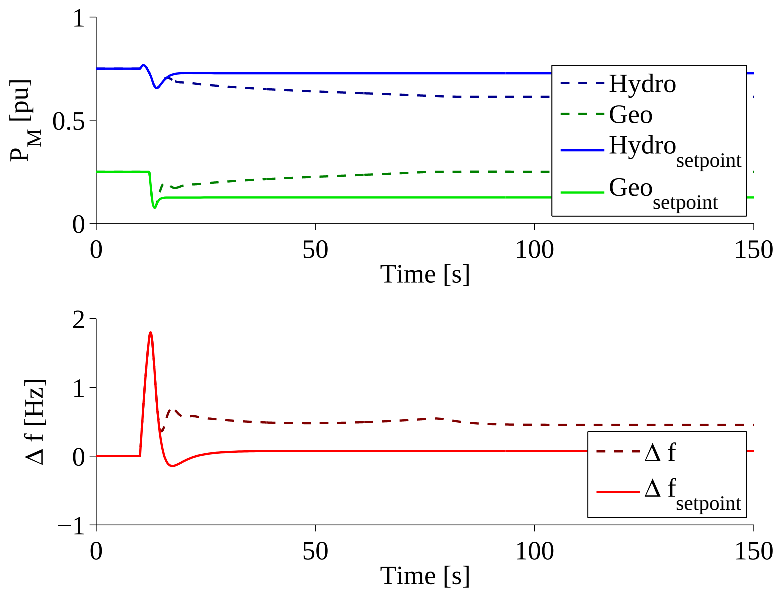


**Figure 4.13:** Simulations for the control #3 with and without setpoint change of the geothermal generators.

These results from Figures 4.12-4.13 clearly show the impacts and benefit of using the fast-acting setpoint change of the geothermal units. The setpoint change leads to less power oscillations following a fault and the system frequency is therefore restored much quicker with a less steady state frequency deviation. The frequency quality is improved but the maximum frequency is still the same. Possible real-time implementations of such a control scheme which can lower the peak of the frequency will be analysed in Chapter 6.2.2. These MATLAB simulation results are not significant for such a simple system, nevertheless it gives a indication of possible improvements that can be made for real power systems. If this control scheme could be implemented in a real system, it would allow the systems to stabilize quicker and with less power oscillation following large faults. After the system has become stable following the system dynamics, the system operators could manually ramp up the geothermal generation again, while monitoring the regulation of the remaining hydro generators in a more secure way.

# 5

# Simulation of Primary Frequency Control with the Icelandic PSS/E Model

In this chapter the system simulations of the Icelandic transmission system will be conducted in PSS/E. At first, both the MATLAB model and the PSS/E model will be compared with real-time measurements in order to verify the models. Next, the PSS/E model will be used for dynamic studies for various system conditions. The objective will be to suggest a control logic for Krafla's governor blocking signal. Finally, the effect of fast-acting setpoint change of Hellisheiðarvirkjun will be investigated.

## 5.1 Krafla's Simulation Models Verification

The simulation models of Krafla are compared with real-time measurements for an event, when a 325 MW power intensive industry load tripped in the Southwest of Iceland. Governors of both Krafla and Hellisheiðarvirkjun reacted to the fault and it did not cause an islanding separation of the system.

### 5.1.1 Verification of Krafla's PSS/E Governor Model

Krafla's governor model in PSS/E was compared with measured data from the Phasor-Point system. Unfortunately there is no PMU measurements for individual generator at Krafla. However, the power-flow is measured to and from the plant; those measurements were summed up to estimate the total generator response. The comparison between PSS/E simulation of the event and the combined generator response measurements of Krafla can be found in Figure 5.1.

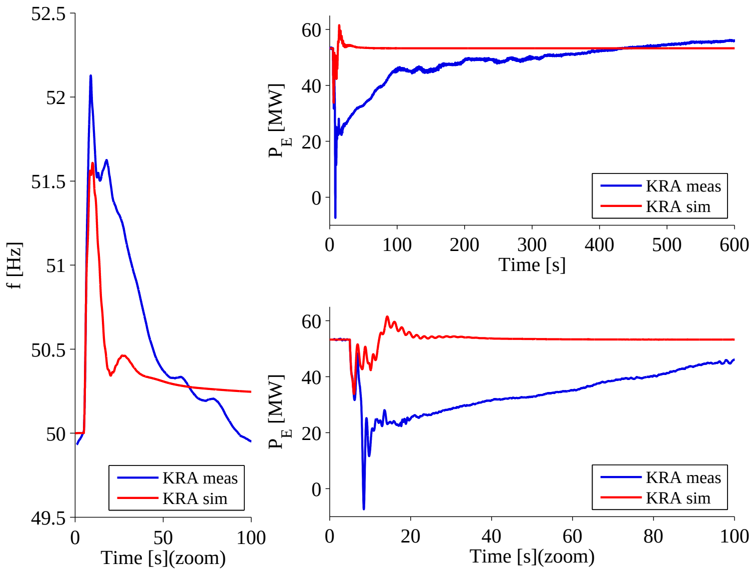


**Figure 5.1:** PSS/E simulation results compared to measured PhasorPoint data for the total power output and the frequency of Krafla for the event, note the time-scale on two of the subfigures.

Measurements for each generator are logged in the SCADA system, it indicates that only generator unit 1 switches to governor control mode, as can be seen in Figure 5.2.

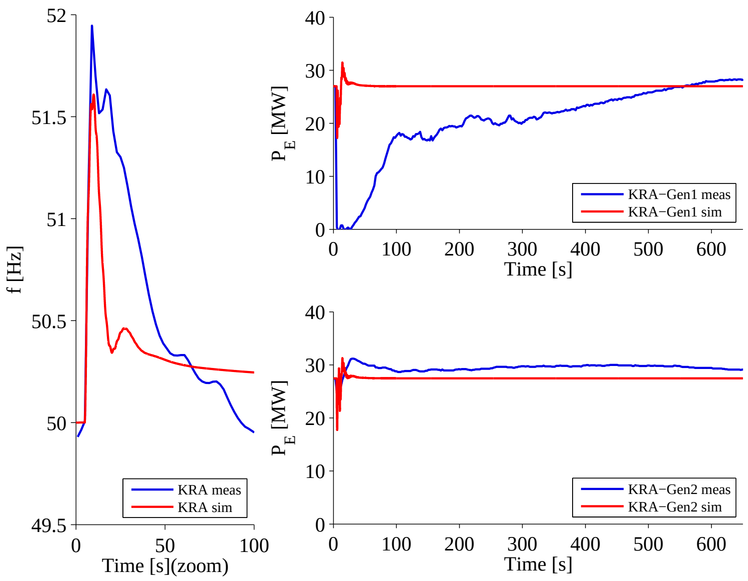


**Figure 5.2:** PSS/E simulation results compared to measured SCADA data for both the generator 1 and 2 at Krafla for the event, note the time-scale on the subfigure of the frequency.

The comparisons in Figures 5.1-5.2 clearly shows the difference between actual response and the simulated response. There is a potential for improvements of the Icelandic PSS/E model. The simulated frequency stabilizes much quicker than in the real system, because the governor models have shorter response time. Figure 5.2 shows that the governor of unit 2 does not switch to governor mode even though the frequency is greater than 51 Hz for more than three seconds. Possible reason for such malfunction is saturation in measuring transductors of each governor system, during large power oscillations. The functionality of the governor is to switch to manual mode when the transductors become saturated and therefore there will be no action taken by that generator.

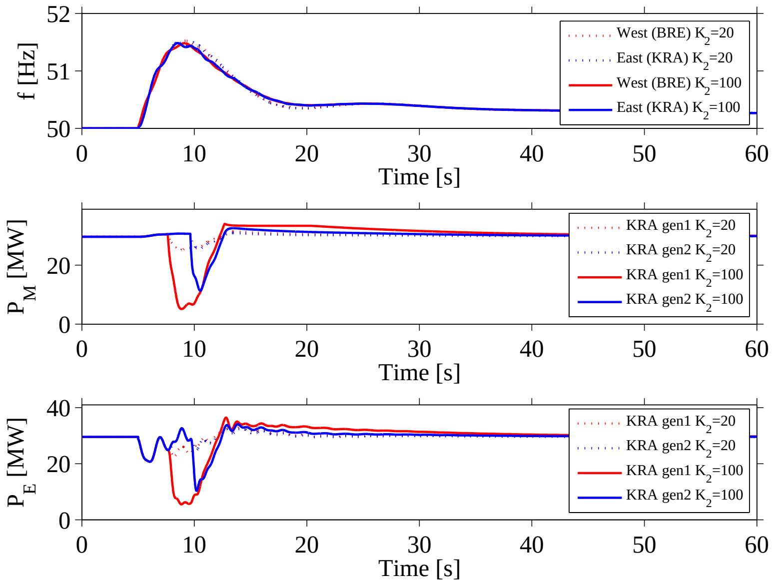


**Figure 5.3:** PSS/E simulation comparison for different values of $K_2$ in Krafla's TGOV7 governor model.

Another interesting result detected in Figures 5.1-5.2 is how small the down regulation of Krafla is in the simulations compared to the measurements. The TGOV7 user model for Krafla's governor is capable of switching between the load limit control mode and governor mode according to the frequency deviation. The delays can be manually configured in the simulation setup but the ramp up characteristics of Krafla (described in Chapter 3.2), cannot be simulated with the TGOV7 model.

The sensitivity of the governor control mode of TGOV7 can be tuned with the gain $K_2$, seen in the model block diagram in Figure 2.14. Comparison of Krafla's response for two different values of $K_2$, i.e. the default value of $K_2 = 20$ and a tuned value of $K_2 = 100$ are presented in Figure 5.3. The results clearly shows the opportunities for improved performance of the model by increasing the $K_2$ gain to boost the sensitivity of the governor control mode.

### 5.1.2 Verification of the MATLAB/Simulink Model with Measured Frequency Signal

The MATLAB model of the geothermal power plant described in Chapter 4, where the geothermal power plant was assumed to be a conventional thermal plant without reheat, was verified with real measured data from the event. The MATLAB/Simulink model was modified in order to use the measured frequency signal as an input. The simulated electric power is compared with Krafla's measured electrical power in Figure 5.4

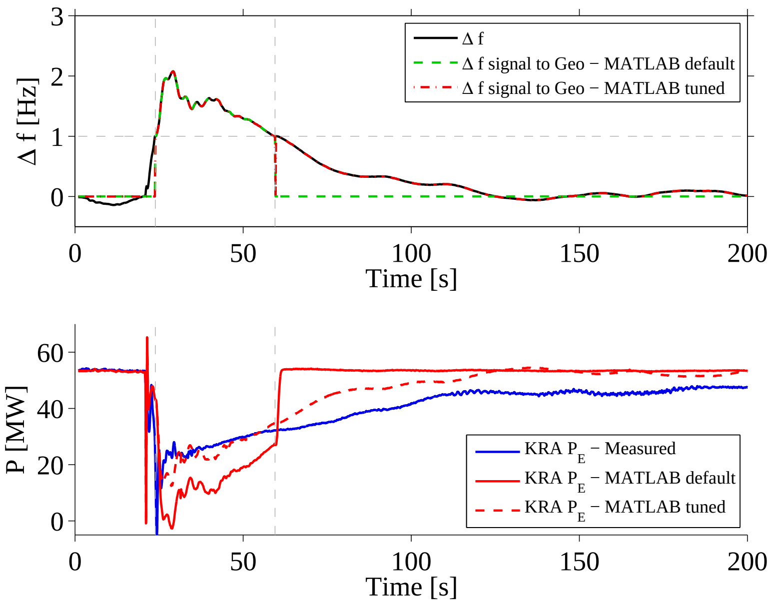


**Figure 5.4:** MATLAB/Simulink simulation response of the frequency and electric power of Krafla compared with measured PhasorPoint data for the event.

Governor control #2 with the default governor control parameters of Krafla was used to verify the MATLAB model as shown in Figure 5.4. The response of the model was considered sufficient for the primary frequency control studies in Chapter 4. The simulated down regulation is greater than the measured data for the given parameters of the geothermal power plant. The model parameters can be tuned in order to simulate the event in a better way. By increasing the droop settings of the governor system from 4% to 5% and by keeping the plant in governor control mode after the frequency returns within 51 Hz, the result with the dotted line in Figure 5.4 was obtained.

### 5.1.3 Simulation Model Verification Results

The response of the MATLAB model was similar to the real-time measurements and the model was considered a reliable base for the studies conducted in Chapter 4. The fine tuning of the PSS/E model is outside the scope of this thesis, therefore the 2014 version of the Icelandic PSS/E model with default parameters, will be used without the suggested modification of the governor parameters, i.e. $K_2$ of TGOV7. The suggestions for improvements of the model will be delivered to the persons responsible for the tuning and updating of the Icelandic PSS/E model.

## 5.2 Dynamic Studies in PSS/E for Various System Conditions

The complete Icelandic PSS/E model was used to simulate dynamic responses for different system conditions, when subjected to a large load trip. The objective was to determine a control logic which blocks the switch between control modes of Krafla's governor. A typical high winter load was used as a base case for the study and the information about the case can be found in Table 5.1.

**Table 5.1:** Information about simulation case used in the PSS/E simulations.

| | |
|---|---|
| Total Generation | 2223.7 MW |
| Total Load | 2161.9 MW |
| System Losses | 61.8 MW |
| Hydro Generation | 73.1% |
| Geothermal Generation | 26.9% |

Only large industry faults in Southwest of Iceland will be considered for the simulations. Large industry faults in East Iceland do not have serious impact on the 132 kV ring connection. In such events, the system protections split the Eastern 220 kV system from the rest of the network and the power imbalance is usually not critical for the rest of the system. The simulations are conducted for different magnitudes of faults and with different power-flows between West and East Iceland, i.e. power-flow through the Cut IV, seen in Figure 3.2.

### 5.2.1 Summary of Dynamic Simulations

A series of dynamic simulations was conducted and the result summary can be found in Table 5.2. The simulations were performed for two common magnitudes of severe faults and for different power exchange between West and East Iceland. Pre-fault-, post fault- and peak power-flows of CutIV, BL1, BL2 and SI4 are documented for each simulation. Peak power-flows which triggers islanding split are marked with a bold red font in Table 5.2. The peak frequencies in East and West islands, along with relative peak rotor angle difference between East and West, i.e. measured at Brennimelur (BRE) and Krafla (KRA), are also documented. It can be noted that if the angle difference becomes more or less than $[-180° \ 180°]$, it is an indication of loss of synchronism between the two areas.

**Table 5.2:** Summary of dynamic simulations with a large industry faults in the Southwest part of Iceland.

| **Simulation #** | **1** | **2** | **3** | **4** | **5** | **6** | **7** | **8** |
|---|---|---|---|---|---|---|---|---|
| System split | Yes | No | No | Yes | Yes | Yes | Yes | No |
| Load trip [MW] | 325.9 | 326.0 | 325.9 | 495.6 | 495.6 | 495.6 | 495.6 | 495.6 |
| **Power-flows [MW]** | | | | | | | | |
| $\text{CutIV}_{\text{Pre-fault}}$ | 90 | 80.5 | 29.5 | 29.5 | 10 | 0 | -9.9 | -19.5 |
| $\text{CutIV}_{\text{Post-fault}}$ | 98.8 | 142.4 | 95.7 | 84.6 | 79.7 | 77.1 | 74.5 | 85.4 |
| $\text{CutIV}_{\text{Peak}}$ | 236.6 | 228.1 | 191.3 | 254.9 | 250.4 | 246.2 | 239.4 | 229.6 |
| $\text{BL1}_{\text{Pre-fault}}$ | 73 | 75.1 | 92.8 | 92.8 | 98.9 | 102.3 | 105.7 | 108.9 |
| $\text{BL1}_{\text{Post-fault}}$ | 24.3 | 24.9 | 42 | 17.5 | 18.4 | 18.9 | 19.4 | 26.4 |
| $\text{BL1}_{\text{Peak}}$ | 73.1 | 75.1 | 92.8 | 92.8 | 99 | 102.3 | 105.7 | 108.9 |
| $\text{BL1}_{\text{Threshold}}$ | 130 | 130 | 130 | 130 | 130 | 130 | 130 | 130 |
| $\text{BL2}_{\text{Pre-fault}}$ | 56.9 | 54.9 | 37.2 | 37.2 | 31 | 27.6 | 24.3 | 21 |
| $\text{BL2}_{\text{Post-fault}}$ | 87.8 | 72.5 | 56.3 | 73.6 | 68.7 | 66.1 | 63.4 | 49.7 |
| $\text{BL2}_{\text{Peak}}$ | **123.6** | 110.3 | 96 | **134.5** | **131.4** | **128.5** | **124.2** | 111.1 |
| $\text{BL2}_{\text{Threshold}}$ | 120 | 120 | 120 | 120 | 120 | 120 | 120 | 120 |
| $\text{SI4}_{\text{Pre-fault}}$ | 33 | 25.6 | -7.7 | -7.7 | -21 | -27.7 | -34.2 | -40.5 |
| $\text{SI4}_{\text{Post-fault}}$ | 11 | 69.8 | 39.5 | 11 | 11 | 11 | 11 | 35.7 |
| $\text{SI4}_{\text{Peak}}$ | **124.3** | 117.9 | 95.3 | **134.3** | **131** | **128.3** | **123.7** | 118.5 |
| $\text{SI4}_{\text{Threshold}}$ | 120 | 120 | 120 | 120 | 120 | 120 | 120 | 120 |
| **Frequency [Hz]** | | | | | | | | |
| West $f_{\text{Peak}}$ | 51.9 | 51.5 | 51.5 | 52.8 | 52.7 | 52.6 | 52.6 | 52.5 |
| East $f_{\text{Peak}}$ | 50.6 | 51.5 | 51.5 | 51.5 | 51.9 | 52.1 | 52.3 | 52.5 |
| **Relative rotor angle difference [degrees]** | | | | | | | | |
| $\Delta Angle_{West-East.Peak}$ | 15240 | 45.2 | 49.3 | 13336.7 | 8897.9 | 6578.5 | 4304.5 | 75.5 |

Simulations #1 and #3 are studied and analysed in more details in Chapters 5.2.2 and 5.2.3. The remaining simulation results are found in Appendix B.

### 5.2.2 Simulation Results #1

For the first simulation case a fault was applied to a power intensive industry in the Southwest, where 325.6 MW was tripped instantaneously. The pre-fault power transfer from West to East was 90 MW. Figure 5.5 shows the simulation results of all the power intensive industry loads and the power-flows of the transmission lines monitored by the system split protections. It can seen that the fault causes minor fluctuation at other large frequency dependant loads. The trip will cause the excessive power to flow towards East, through the ring connection. In this case the power-flows in SI4 and BL2 will exceed the limits which results in a system split. The protection scheme splits the system at Hólar (HOL), therefore the power-flow of SI4 drops to a lower value, which is needed to support the remaining load at HOL. The other split occurs at the bus-tie of Blanda (BLA), where one generator is connected to the West bus and two generators are connected to the East bus. After the split the power-flow to West from BLA will decrease, while the Eastern power-flow from BLA increases to compensate for the loss of Eastern power-flow through HOL.

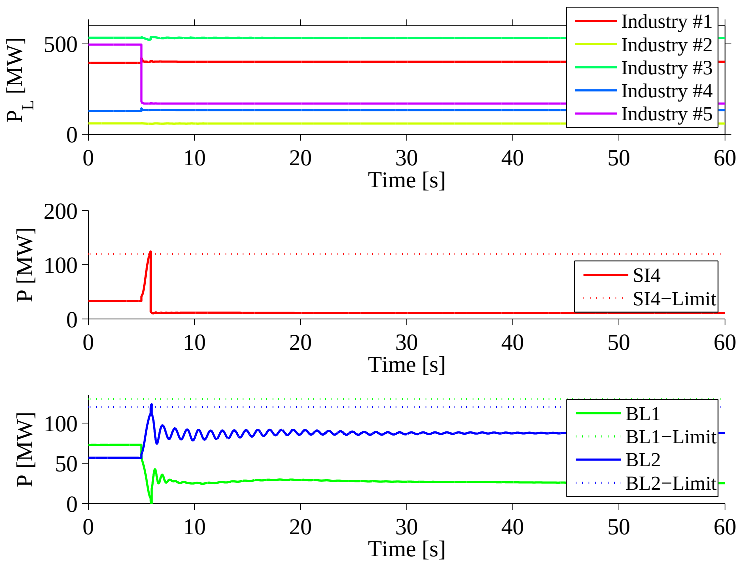


**Figure 5.5:** Simulation results of power intensive industry loads and transmission line power-flows.

Figure 5.6 shows the frequency in the West island, East island and the mechanical power outputs for the two generators at Krafla. The frequencies start to deviate from each other upon the loss of synchronism following the islanding split. It can be examined that the frequency in the East island does not exceed the frequency deviation of $\pm 1$ Hz and therefore there will be no regulation by Krafla in this case. The high frequency oscillations of the East frequency is because of a weaker system in the East island with less regulation capability.

The mechanical powers of the main geothermal power plants and hydro power plants are presented in Figure 5.7. Most of the geothermal units keep their production value following the fault, except Hellisheiðarvirkjun (HEL) and Svartsengi (SVA), both plants regulate down to compensate for the load loss. The governor models for those plants need to be investigated, because in reality they return to their pre-fault generation when the frequency returns within 51 Hz. All of the hydro units participate in the down regulation. The power plants in the East island, i.e. KAR and two generators of BLA, do not have to down regulate as much as the rest of the hydro power plants located in the West island.

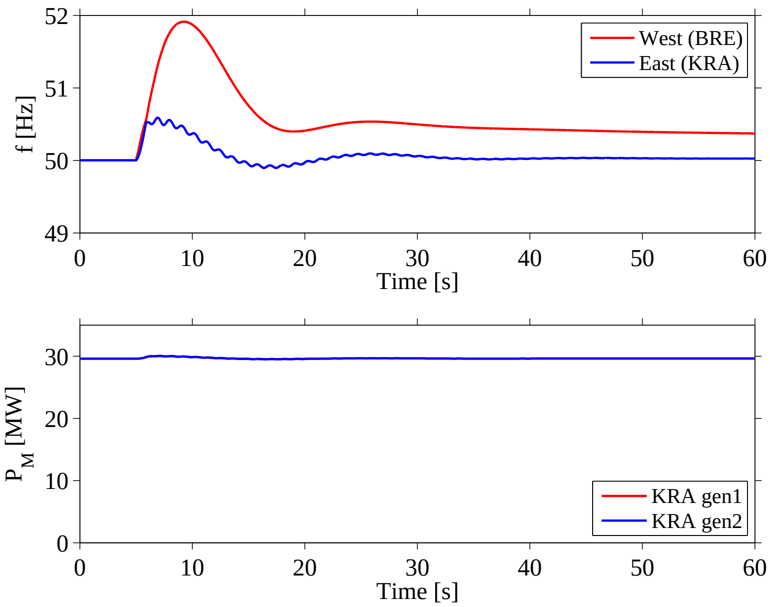


**Figure 5.6:** Simulation results of frequencies and mechanical power outputs of each generator at Krafla (KRA).

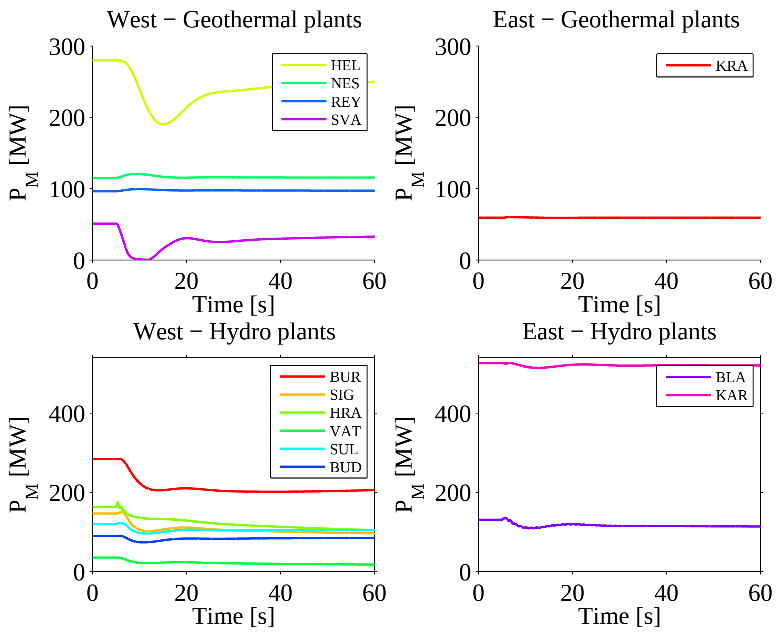


**Figure 5.7:** Simulation results of mechanical power responses of the hydro power plants and the geothermal power plants.

Figure 5.8 shows the power-flow through CutIV and the relative rotor angle difference between the West and East Iceland, i.e. measured at Brennimelur (BRE) where the load is located and at Krafla (KRA). The relative angle difference increases because of the loss of synchronism between the West and East.

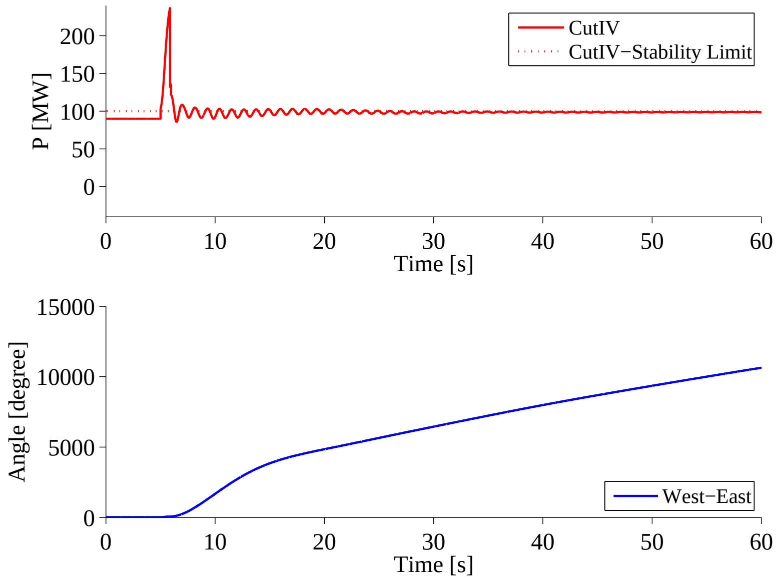


**Figure 5.8:** Simulation results of the CutIV power-flow and the relative rotor angle difference between West and East Iceland.

### 5.2.3 Simulation Results #3

In this simulation the same fault as in simulation #1 was applied, but the pre-fault power-flow from West to East was 30 MW instead of 90 MW. It can be seen from Figure 5.9, that the power-flows on the transmission lines following the fault do not exceed the triggering limits of the system protections. Accordingly, the system will stay intact and the frequency will be about the same in all of the system, it will peak at about 51.5 Hz. This event will cause the Krafla to switch over to governor control, see Figure 5.10. For this particular case it would be beneficial to block the switch at Krafla to avoid the events discussed in Chapter 3.2. Figure 5.11 shows the mechanical power outputs of the main power plants in the system, the main difference when compared to the simulation #1 is the regulation response of the plants in the East island, i.e. Krafla (KRA) and Kárahnúkavirkjun (KAR). With the system staying intact more regulation is required from the power plants in the East. A rotor angle jump of 49.3° between the West and East Iceland is detected after the fault as can be seen along with power-flow through CutIV in Figure 5.12.

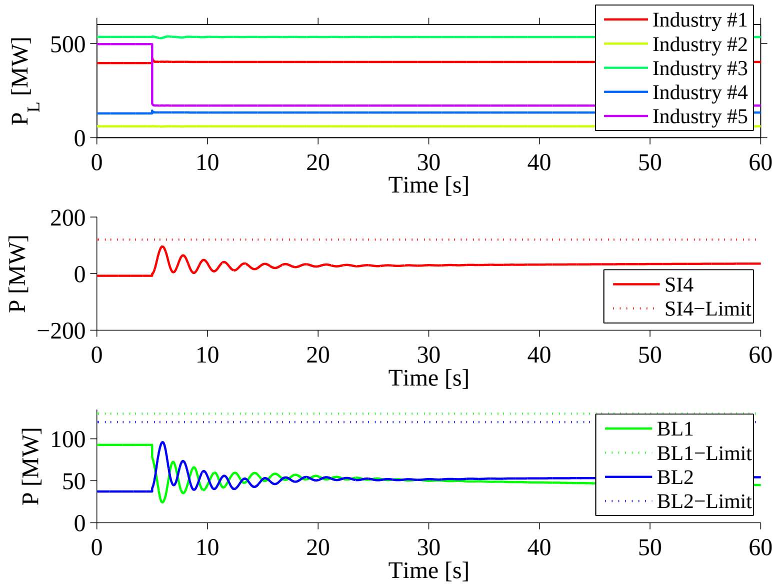


**Figure 5.9:** Simulation results of power intensive industry loads and transmission line power-flows.

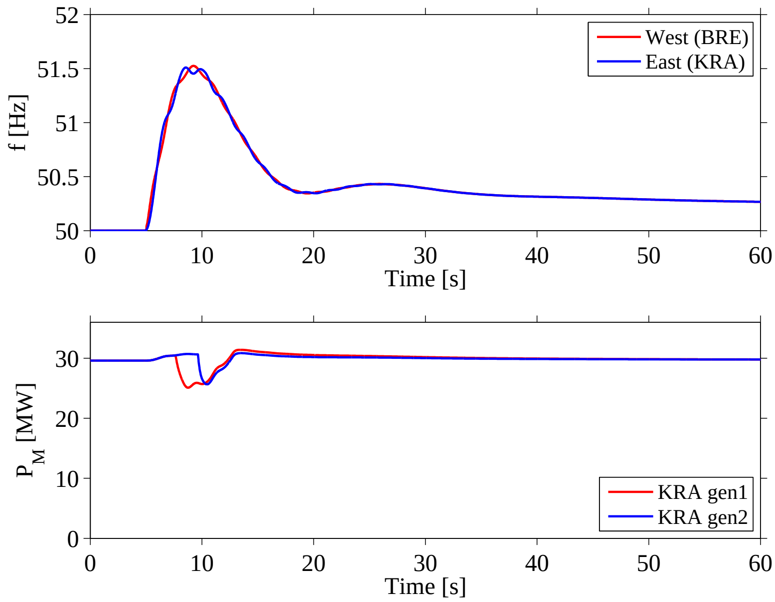


**Figure 5.10:** Simulation results of frequencies and mechanical power outputs of each generator at Krafla (KRA).

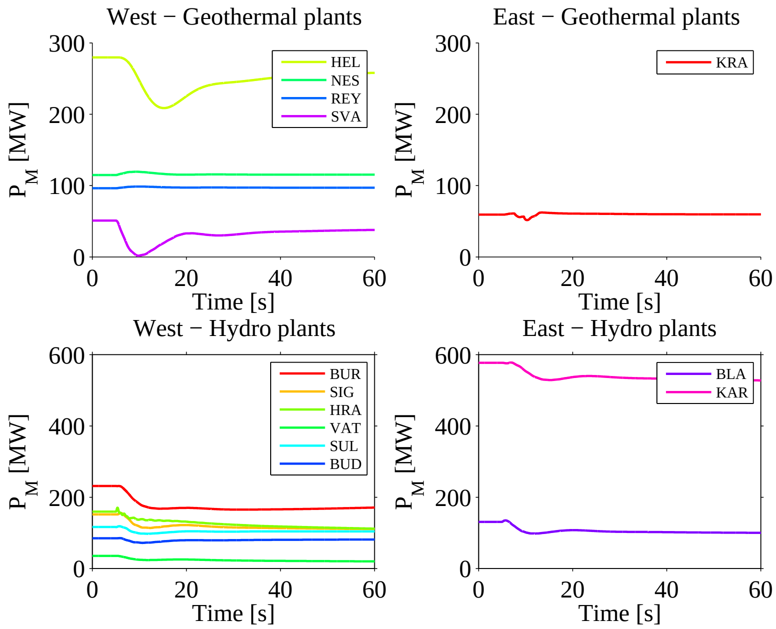


**Figure 5.11:** Simulation results of mechanical power responses of the hydro power plants and the geothermal power plants.

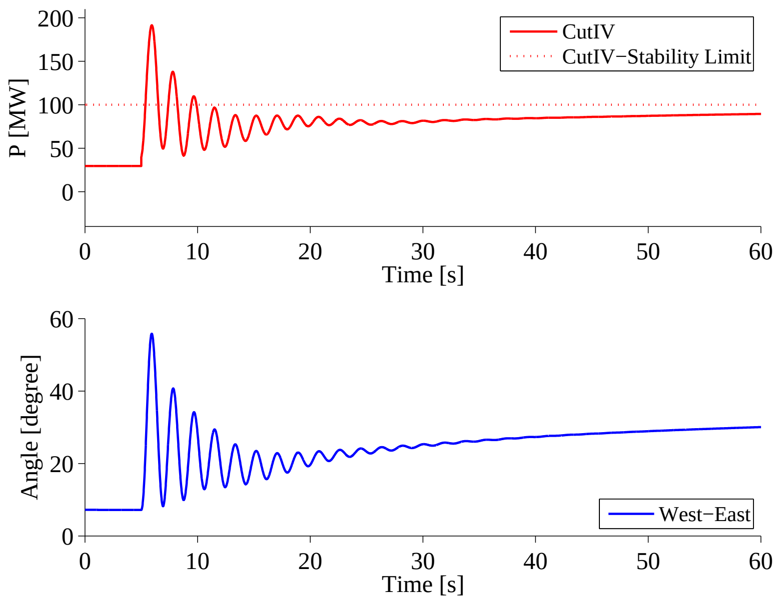


**Figure 5.12:** Simulation results of the CutIV power-flow and the relative rotor angle difference between West and East Iceland.

## 5.3 Control Logic Design for Krafla

The simulation results in Table 5.2 were useful for understanding and evaluating the dynamic behaviour of the system when subjected to a heavy industry fault. The objective was to design a simple but reliable control logic, which should block the governor control of Krafla when the system is intact and remove the block signal upon system split. The following logic suggestion was considered the most suitable solution.

$$\text{AND}\left\{\begin{array}{l}\text{Signals available}\\ \text{NOT (Island Alert/Alarm)}\end{array}\right\}\Rightarrow \text{Block signal} \tag{5.1}$$

The control blocking signal should be designed so it does not override manual commands by the local control center. All PMU signals used in the scheme need to be GPS-locked and validated, for the triggering of control logic. The scheme uses the built-in islanding detection of PhasorPoint. The detection uses algorithm based on angles and frequencies differences between different PMU measuring points. After a frequency disturbance the software application applies hysteresis to verify if the system is islanded. The algorithm takes about one second to identify an islanding condition. The main concern with this control logic design is the processing time of the built-in islanding detection. The detection and communications needs to be tested upon the implementation, to guarantee that the control manages to remove the block signal in time, without causing any additional problems.

An alternative solution is a more customized control logic, which would evaluate the system condition upon a system faultm in order to predict for a system split. The simulated results in Table 5.2 could be used for the criteria of the custom design. A draft of the customized control logic based on the dynamic simulation results is suggested as

$$\text{AND}\left\{\begin{array}{l}\text{Signals available}\\ \text{NOT (Island Alert/Alarm)}\\ \text{Fault location in Southwest Iceland}\\ \text{OR}\left\{\begin{array}{l}|\text{Fault}| > 330\text{ MW}\left\{\begin{array}{l}\text{Powerflow is from West to East}\\ \text{Pre-fault CutIV Powerflow} < \text{-40 MW}\\ \text{Post-fault }\Delta\text{Angle}_{\text{West-East}} < 85^\circ\end{array}\right\}\\ |\text{Fault}| < 330\text{ MW}\left\{\begin{array}{l}\text{Powerflow is from West to East}\\ \text{Pre-fault CutIV Powerflow} < \ \text{50 MW}\\ \text{Post-fault }\Delta\text{Angle}_{\text{West-East}} < 60^\circ\end{array}\right\}\end{array}\right\}\end{array}\right\}\Rightarrow \text{Block signal.} \tag{5.2}$$

The condition for fault magnitude larger than 330 MW uses the simulation result #8 with addition safety margin of 20 MW for the West to East flow and 10° in the angle jump. The fault magnitude with less than 330 MW uses the simulation result #3 with the same safety margin as before. The software uses the post-fault angle difference in the island detection algorithm to determine if there is a loss of synchronism between the areas. Such a control logic increases the level of complexity and it would need further investigation before implementation. The more simple design (5.1) is expected to be more robust and reliable.

## 5.4 Dynamic Simulations of Hellisheiðarvirkjun

The dynamic response of Hellisheiðarvirkjun is examined for the same event as in Chapter 5.1.1. The PhasorPoint measurements for all of the generators can be found in Figure 5.13, where it can be verified that the governor control works according to the specification described in Chapter 3.2. The generators are able to return to its pre-fault generation values immediately after the frequency has returned within 51 Hz. Generator units 5 and 6 are the latest addition to the power plant and they are the most active of all the generators in the down regulation.

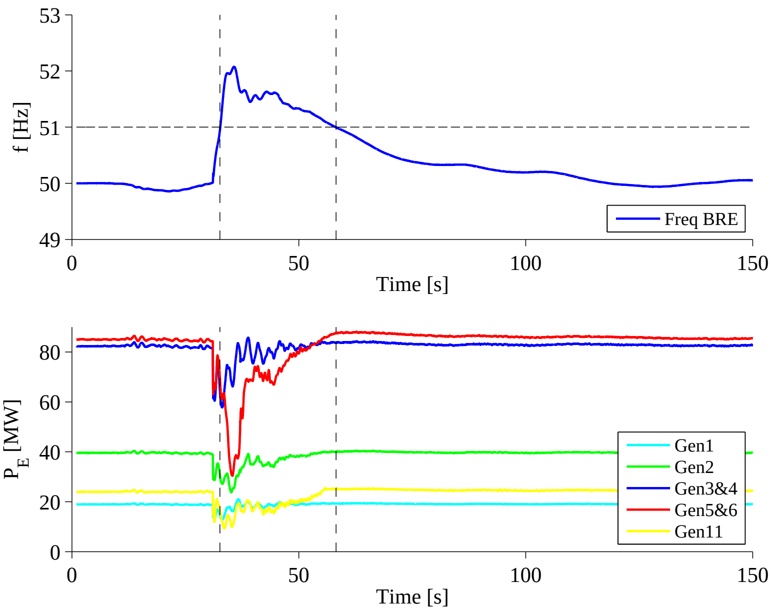


**Figure 5.13:** Measured PhasorPoint data of the generators responses at Hellisheiðarvirkjun for the event.

The PSS/E governor model for Hellisheiðarvirkjun is verified with the measured result for the same event. The default governor model used for Heilisheiðarvirkjun is the IEEEG1 model. The comparison between the simulated event and the measured event is presented in Figure 5.14. The response comparison reveals that there are opportunities for further enhancements, both in the dynamics and in the steady state of the model. The generation steady state values in the simulation is lower than the pre-fault generation due to the functionality of the IEEEG1 model.

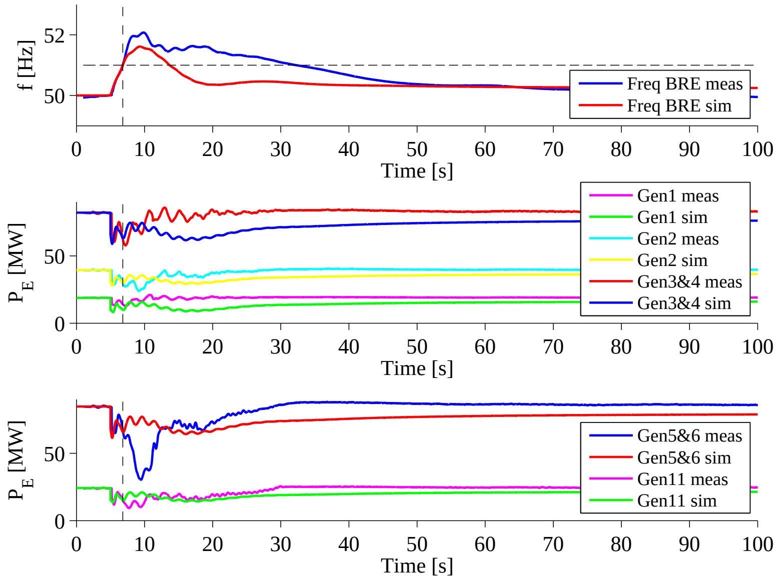


**Figure 5.14:** Measured PhasorPoint data of the generators responses at Hellisheiðarvirkjun compared with PSS/E simulation results using the IEEEG1 governor model for the event.

The specification of the Hellisheiðarvirkjun governor control is equivalent to the functionality of the TGOV7 governor model. Therefore the event was simulated again with an untuned TGOV7 model instead of the IEEEG1 model, i.e. $K_2 = 20$ was used in the TGOV7. The simulation results can be found in Figure 5.15.

The results in Figure 5.15 shows that by using the TGOV7 model the steady state production returns to the pre-fault values, as the measurements indicated. The dynamics of the simulation can be improved further by adjusting the $K_2$ gain in the TGOV7 model, as described in Chapter 5.1.1.

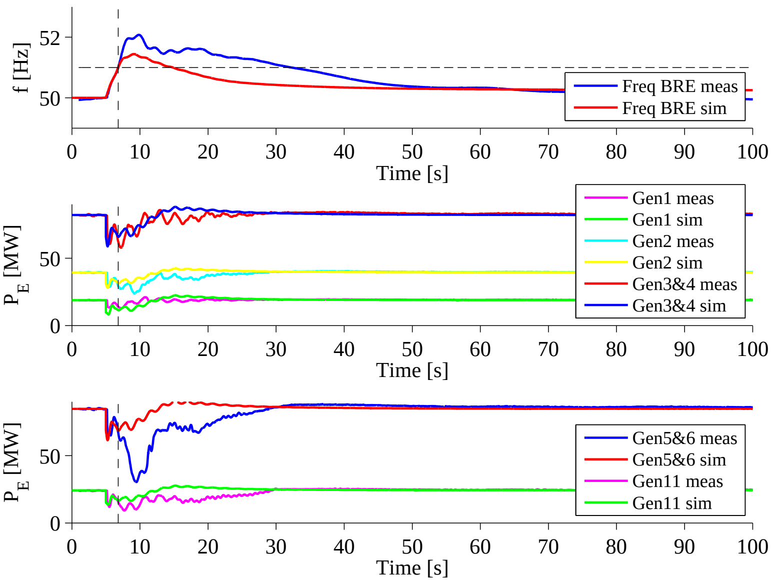


**Figure 5.15:** Measured PhasorPoint data of the generators responses at Hellisheiðarvirkjun compared with simulations using the TGOV7 governor model for the event.

## 5.5 Control Logic Design for Hellisheiðarvirkjun

The different responses of the simulations in Figures 5.14-5.15, can be used to demonstrate the effect of fast-acting setpoint change, similar to the study carried out in Chapter 4.5 using the MATLAB/Simulink model. The comparison between the simulated frequency response for the two different governor models can be found in Figure 5.16.
The reduction in the geothermal generation outputs following a fault, i.e. by using the IEEEG1 model, will cause a faster stabilization of the frequency and decrease the regulation of the remaining hydro power plants. The simulations with the TGOV7, results in a lower peak value of the frequency and a longer stabilizing time of the frequency. That is because the units at Hellisheiðarvirkjun are returning to their pre-fault generations, while the hydro power plants have to compensate for it. A new control strategy, i.e. the fast-acting setpoint change, would utilize the advantages of both controls. Normally the governor would operate like the TGOV7, with a fast regulation action, which would lower the peak value of the frequency rise. The controller would then apply new setpoints to the units before the plant is able to return to its pre-fault production again, which would make the frequency stabilize faster due to increased regulation capacity from the geothermal units. Such a control strategy would always be preferred, especially during

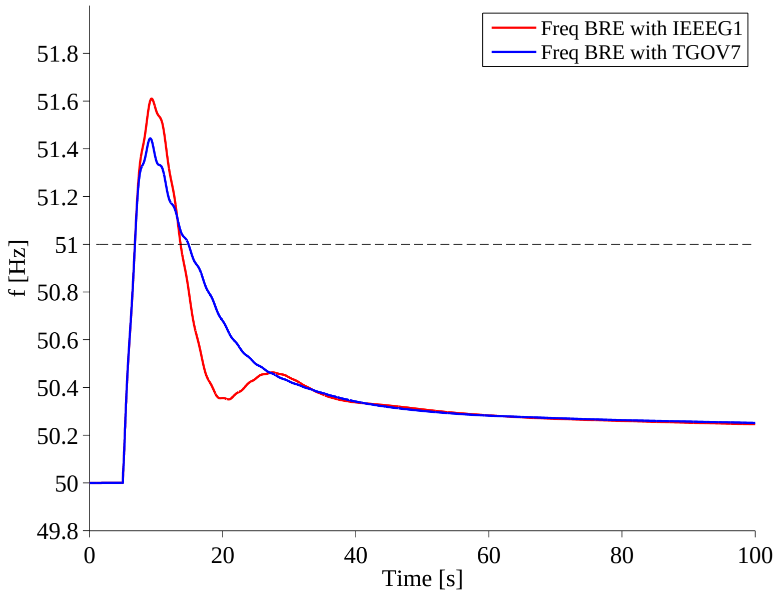


**Figure 5.16:** Frequency comparison between simulations with different governor models for the event.

summer time when the total load demand is low. For such scenarios the geothermal units are at maximum production while hydro units are at low production. If a large industry fault would take place in such conditions many of the hydro power plants would be forced in reverse power, i.e. the generators would consume power. For this reason, it would be preferred that the control scheme would automatically assign new setpoints to the geothermal power plants.

A design suggestion of a control logic for triggering of such a control scheme, involving fast-acting change of generators setpoints is presented in (5.3).

$$\text{AND}\left\{\begin{array}{l}\text{Signals available}\\ \text{Load trip in Southwest Iceland}\\ f_{local} > 50.35\,\text{Hz}\\ \frac{df_{local}}{dt} > 0.1\,\text{Hz}\end{array}\right\} \Rightarrow \left\{\ \text{Algorithm}\ \right\} \Rightarrow \text{New Setpoints} \tag{5.3}$$

The scheme is triggered if a heavy industry load trip is detected in Southwest of Iceland. The trip is verified by checking the conditions of the local frequency and the rate of change of frequency. The chosen frequency thresholds are based on research from the Icelandic WADS project, carried out by Psymetrix and Landsnet [17]. Once the scheme is triggered, an algorithm starts to process the new setpoint. In principle the algorithm would work as a fast-acting emergency AGC. The available setpoint changes would be discretized in a lookup table, dependent on regulation capabilities of each geothermal unit. The possible setpoint changes of each unit would need to be carefully designed in cooperation with the power plant owners. When the algorithm is triggered the needed regulation capacity would be calculated based on the location and the magnitude of the fault. Finally, the algorithm would optimise the available setpoint changes from the lookup table according to the needed regulation capacity and transmit the new setpoints to the selected power plants.

# 6

# Utilization of PMU to Improve Control Schemes

In this chapter implementations and configurations of improved frequency control schemes will be laid out. The configuration of different application will be studied and the most promising suggestions will be presented. Finally, an addition to Landsnet's requirements for new construction projects will be recommended.

## 6.1 Implementations of Control Schemes Based on PMU

The process from PMU measurements to an output control signal can be designed in many different ways. The design prerequisites include communications, delays, response times, networking/broadcasting, application interfacing, etc. The different applications considered for this evaluation are PhasorPoint, PMU, SCADA, PhasorPoint substation system, PhasorPoint control unit, National Instrument (NI) control unit and the local power station control system, e.g. governors.

### 6.1.1 Combined PhasorPoint and SCADA Configuration

The first configuration examined is the utilization of the PhasorPoint measurements and the SCADA system. Landsnet would need to develop a new software that would use the PMUs real-time data streams to the centralized PhasorPoint data server. The software would execute the control logic and export the output signals to the SCADA system. The configuration of SCADA system would need to be altered, in order for the output signals to bypass the AGC and be transmitted over the SCADA communication channels to the D20 substation controllers. Schematic of the process is shown in Figure 6.1. Bypassing the AGC is necessary because of its slow response time, like seen for the secondary frequency control in Figure 2.7. The benefits of this configuration is that it does not require any additional hardware and Landsnet has experience with similar kind of configurations for other systems.

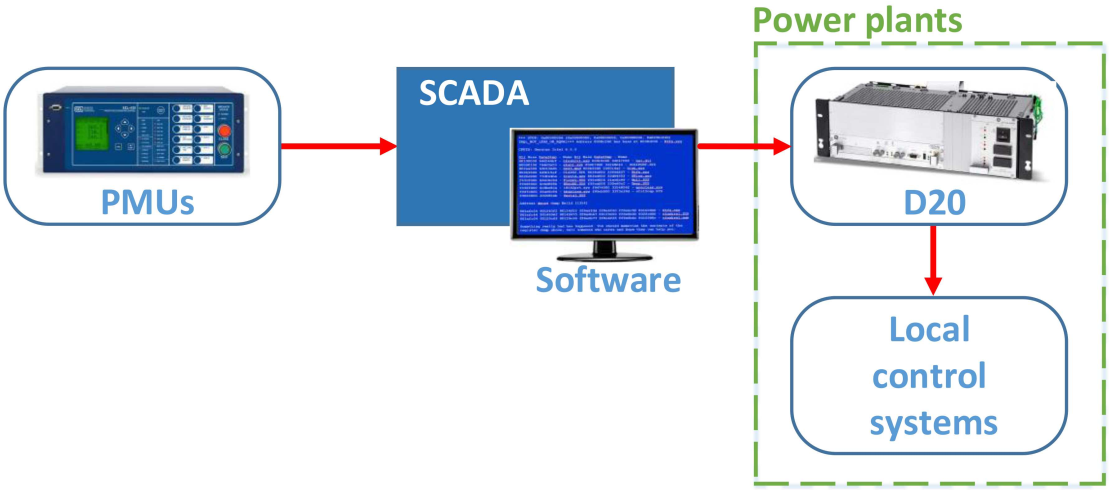


**Figure 6.1:** Process of the combined PhasorPoint and SCADA configuration.

The disadvantage is the overall response time of the control action. This configuration might introduce too much communication and processing delays, which might affect the performance of the control scheme compared to using faster communication channel and priority processing. The baud rates of SCADA communication channel is only 9600 Baud and the D20 substation controllers use queued processing, which further increase the response time of the control scheme. In addition, the AGC has operational issues during severe faults. Firstly, it can only manage regulation of one system, therefore it can only regulate the West island if the system gets separated. Secondly, the AGC will go into suspend if the frequency deviation exceeds 2.5 Hz. As a result the operators have to manually give setpoints to generator units to regulate the system. Table 6.1 shows a rough estimate of the response time of the configuration.

**Table 6.1:** Rough estimates of the response time of the combined PhasorPoint and SCADA configuration.

| | |
|---|---|
| Measurement detection time | 100 ms |
| Transmission time to centralized server | 100 ms |
| Software processing time | 150-500 ms |
| SCADA transmission time | 1500-2000 ms |
| D20 controller response time | 50-500 ms |
| Total response time | 1900-3200 ms |

### 6.1.2 PhasorPoint Based Configuration

Psymetrix is developing a complete monitoring and control system based on PhasorPoint. Currently there is only a prototype of a simple control scheme available, comprising:

- PMUs.
- Central PhasorPoint system.
- Substation phasor data concentrator (S-PDC) for aggregating streams and managing data routing.
- PhasorPoint substation systems for producing the output control signalling.

The substation system is a third party industrial PC platform with limiting control output capability, no defined response time and frequent hardware reliability problems. Psymetrix is developing a new product called PhasorPoint control unit, which is an embedded real-time control platform, specially designed for wide-area control and protection applications. The specifications for the device include [18]:

- PMU data stream inputs and other status inputs, e.g. IEC 61850 GOOSE.
- Triggering outputs in standard forms to implement fast response including IEC 61850 GOOSE and hardwire relay.
- Defined response time of 16 ms.
- Ability to provide digital and continuous analogue sampled signals to other local controllers.
- Flexible logic to implement a variety of control designs.
- Implementation of specific functions required to implement control designs.

The intention is to develop a common control platform that is compatible to the wide variety of control systems and communication systems used in the operation of power systems. The process of the control configuration can be found in Figure 6.2. This structure improves the networking by broadcasting PMU data streams, which allows direct communication between control units and PMU without going through the data server located in Southwest Iceland. The controller configuration is managed through the PhasorPoint system. Table 6.2 shows a rough estimate of the response time of the configuration.

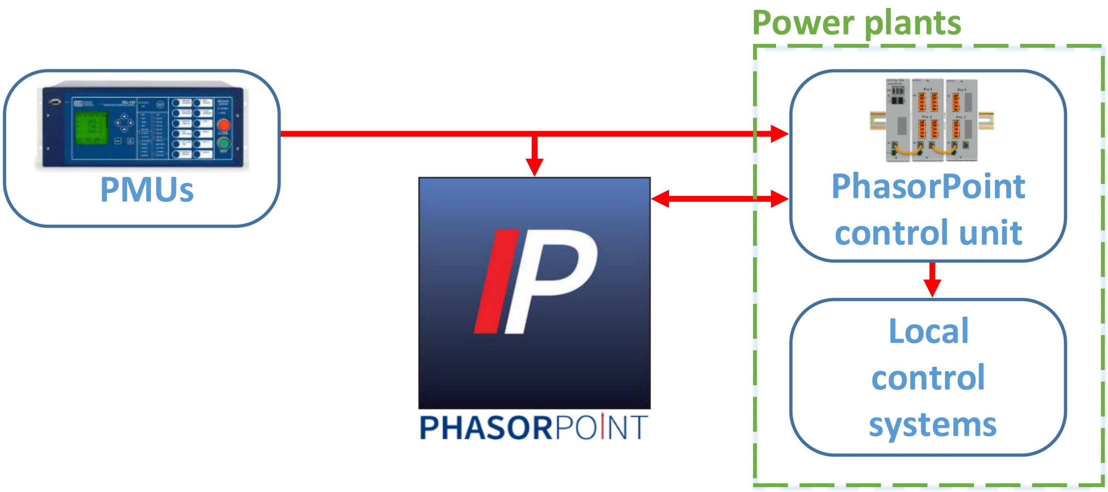


**Figure 6.2:** Process of the PhasorPoint based configuration.

**Table 6.2:** Rough estimates of the response time of the combined PhasorPoint and NI based configuration.

| | |
|---|---|
| Measurement detection time | 100 ms |
| Transmission time to centralized server | 100 ms |
| Software processing time | 150-1000 ms |
| Transmission time to substation | 100 ms |
| Local controller response time | 16 ms |
| Total response time | 416-1316 ms |

### 6.1.3 Combined PhasorPoint and NI Configuration

The last configuration examined is the combined utilization of PhasorPoint and a PXI platform, developed by National Instrument. PXI is an industry standard modular platform that can be used as a substation control unit [19]. The process of the configuration can be seen in Figure 6.3. This configuration is similar to the process in Figure 6.1, where a software developed by Landsnet will process the control logic with data streams from the PhasorPoint server. The control outputs will then be sent by new and faster communication channel to the PXI control units instead of using the SCADA communications system. An alternative is to use NI hardware for the measurements instead of PMU measurements, then software integration problems between all the different systems could be avoided. Table 6.3 shows a rough estimate of the response time of the configuration.

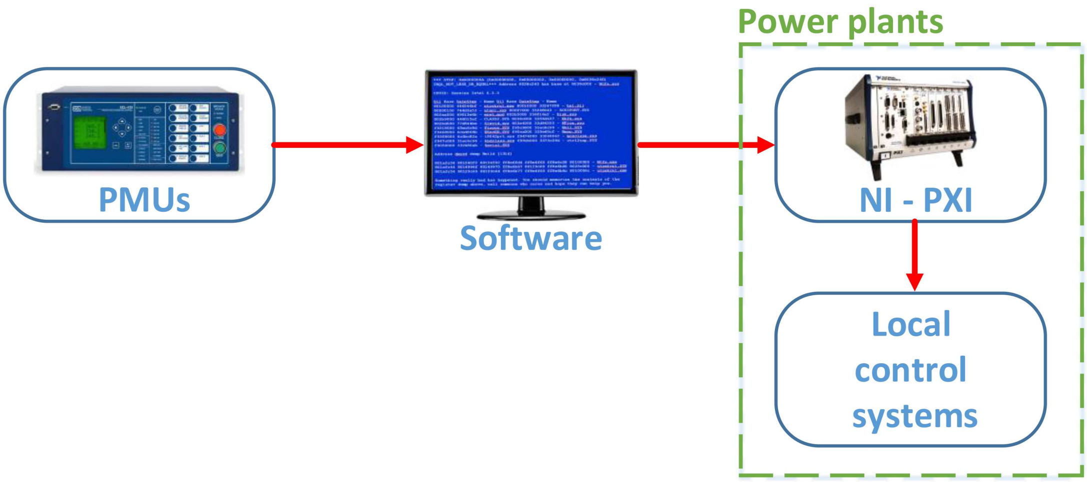


**Figure 6.3:** Process of the combined PhasorPoint and NI based configuration.

**Table 6.3:** Rough estimates of the response time of the combined PhasorPoint and NI based configuration.

| | |
|---|---|
| Measurement detection time | 100-200 ms |
| Transmission time to centralized server | 100 ms |
| Software processing time | 150-700 ms |
| Transmission time to substation | 100 ms |
| Local controller response time | 50-100 ms |
| Total response time | 500-1200 ms |

## 6.2 Suggestion for Implementation of Improved Frequency Control Strategies

The most promising implementations of frequency control strategy associated with the geothermal power plants will be discussed in this subchapter, beginning with the blocking of governor response at Krafla. Second, the fast-acting setpoint change of generators, i.e. to block Hellisheiðarvirkjun to return to its pre-fault generation setpoint following a large fault.

### 6.2.1 Blocking Signals of Governor Controls

The governor blocking of Krafla is a time-critical scheme, therefore using the SCADA system is not a feasible option. The PhasorPoint based configuration in Chapter 6.1.2 is recommended for this scheme, since the control logic will be depending on built-in functions of PhasorPoint for detection of a loss of synchronism between different areas. The configuration in Chapter 6.1.3 is not recommended, because the algorithm for the synchronism detection would need to be designed from scratch. The control output signal needed is only an on/off signal, which is supported by the prototype substation system. The new PhasorPoint control unit is highly recommended to ensure as quick response as possible. The prototype can be used for testing until the new controller will be available. The prototype has already been implemented for non-time-critical load shedding scheme, where terrestrial trunked radio (TETRA) modem is used for the communications. The testing of the Krafla's governor blocking scheme with the prototype controller can be connected with fiber optic communications to minimize communication delay.

### 6.2.2 Fast-Acting Setpoint Change of Generators

The control scheme that comprises fast-acting setpoint change requires digital signal output from the controller unit for the transmission of the new setpoint value. The scheme would use the PMU load and frequency measurements to detect a trip of the power intensive industries in much faster way than the frequency based AGC system. The PhasorPoint prototype is not capable of generating such outputs, it could only send digital signals to the power station control system which could trigger pre-defined generation reduction. The new PhasorPoint control unit would be ideal for such a control scheme, until the controller will be available for operation it is recommended to use other implementations for testing. The SCADA implementation in Chapter 6.1.1 is an option for the testing regarding Hellisheiðarvirkjun. However, the many disadvantages of SCADA/AGC system can introduce problems in the performance of the control scheme. In order to guarantee reliability of the system the AGC implementation needs to be revised. The control scheme in Chapter 6.1.3 is the most probable implementation for the testing of this control scheme. It allows for better response time and can be fully designed and implemented by Landsnet. This implementation can also be used for testing of other projects, such as the fast-ramping of hydro units.

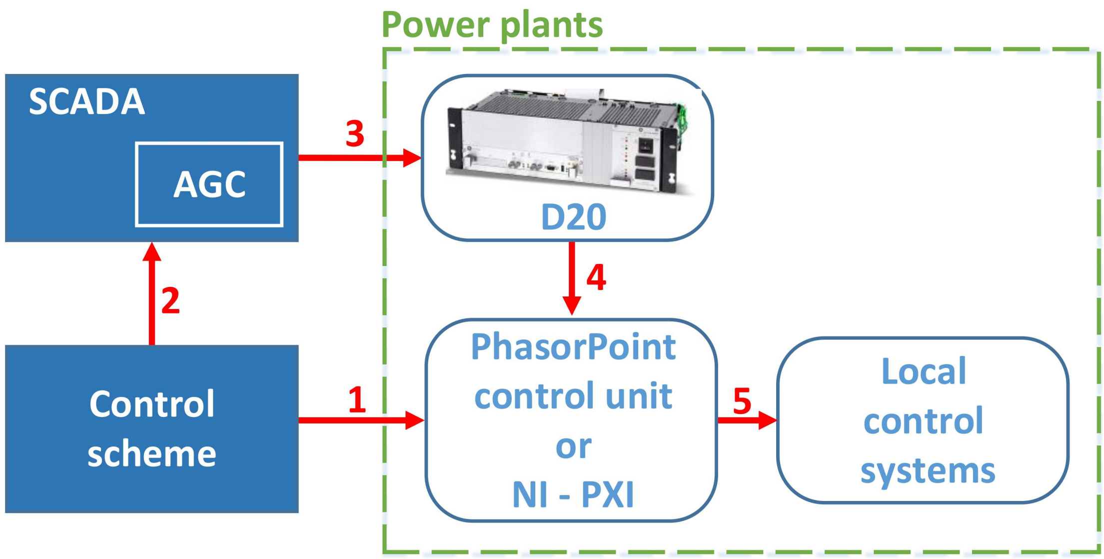


**Figure 6.4:** Diagram of how local control unit prioritizes the inputs from the AGC and the control scheme.

Control systems which apply new setpoints to generator units by bypassing the SCADA/AGC need to ensure that the new setpoints are not overwritten immediately by the AGC. Figure 6.4 shows a diagram of how local control unit prioritizes the input signals applied from the AGC and the control scheme. In normal conditions the control scheme is not active and no setpoint signals are applied, i.e. in arrows 1 & 2. The AGC regulates the system by sending new setpoints to the local control through arrows 3,4 & 5. If the control scheme is triggered it sends out new setpoints through arrow 1. The control unit has higher priority on inputs from the control scheme and therefore it blocks the channel from AGC. The control scheme also sends the setpoint reference to the AGC, which processes the information and transmits the new setpoint to the power plant. The communication takes much longer time for the SCADA channel compared to the direct link between the control scheme and the control unit. When the AGC has reached the same setpoint as the control scheme the control unit switches back to the AGC input.

## 6.3 Requirements for New Construction Projects

With increased demands for secure and reliable system operation it is essential to expand Landsnet's standards for monitoring and control for all new construction projects. Recommendations for Landsnet's requirements in tender documents for new power plants are as follows:

- PMU measurements for each installed generator unit.
- PMU measurements for all connected transmission lines.
- PMU mesasurements of governor valves/wicket-gate position.
- PhasorPoint control units.

It is revised that tender documents for new heavy industry should include:

- PMU measurements of the load.
- PhasorPoint control units.

# 7

# Conclusions and Future work

## 7.1 Conclusions

Investigation of the primary frequency control of the geothermal power plants in the Icelandic transmission system has been in the main focus in this thesis report. At first a MATLAB/Simulink model was built to simulate the fundamental behaviour of both hydro and geothermal power plants. Next, a complete model of the Icelandic power system was simulated in PSS/E and the results were used to suggest a control logic for improved frequency control strategies of the geothermal power plants. Finally, different implementations of the control schemes utilizing PMU measurements were examined and the most promising results were presented.

### 7.1.1 Simulations with a Simple MATLAB/Simulink Model

The simple single bus power system simulated in MATLAB/Simulink is helpful in the study of responses and characteristics of different type generator units. Moreover, the model is useful to analyse the effect of different control strategies. Obviously, the model is too simple to generalize about an actual response of the Icelandic power system. The simulation results indicate that if no utilization of a block signals would be implemented in the control scheme, it would be beneficial to increase the frequency amplitude and/or the delay settings of current governor controller at Krafla. By increasing Krafla's thresholds of frequency amplitude and delay the plant would be less sensitive to governor switch into governor control mode, recommended settings would be a delay of 1.5-2 seconds or a frequency amplitude of 1.5 Hz. On the other hand the proposed setting changes would not be beneficial when a system split occurs, as it would increase the regulation stress in the East island. Wide-area control scheme is considered a more profitable solution for the improvements of the geothermal regulation response. The simulation results of the fast-acting setpoint change of generators units following a fault indicate that the regulation response of the system can be improved with such a control strategy.

### 7.1.2 Simulations with a Complete PSS/E Model

The Icelandic PSS/E model was used to simulate the system conditions that would lead to islanding between West and East Iceland following a large industry fault in the Southwest part. The simulation gave sufficient results for use in the design of control logic for the wide-area control scheme. The control scheme regarding fast-acting setpoint change of generator units in Hellisheiðarvirkjun was simulated by using different governor models. The outcome supports the MATLAB simulation results found in Chapter 4.5.

Verification of the model consisted of detailed comparison from one event between PMU measurements and PSS/E simulations. Further installations of PMU in the system, especially PMU of generator unit outputs will allow for better tuning of the Icelandic PSS/E dynamic model. The verifications showed that dynamic simulations of the system can be improved by revising and retuning of the governor models. Following modifications are recommended:

- Krafla's governor $K_2$ gain should be tuned to a value around 100.
- The governor models for Hellisheiðarvirkjun should be changed to TGOV7 and tuned with gain $K_2$ for each generator unit.
- Perform a comparison study for all of the power plants with available PMU measurements of generator units.

### 7.1.3 Control Logic Design for Improved Control Strategies

The challenge of the system increases in both generation and load and with little reinforcement of the system by building new transmission lines will require further need for resource management. Wide-area control is essential to operate and control the system under such conditions. The design of control logic for the blocking of Krafla's governor mode switch was conducted in Chapter 5.3. The control logic design was kept as simple as possible, the only concern with the design is the response time of the PhasorPoint built-in islanding detection. Testing of the implemented control scheme will clarify if the response time is sufficient. An alternative solution is to design a more customized control logic based on the results in Table 5.2. The control logic for the scheme of fast-acting setpoint change of generators, needs to be designed in cooperation with power plant owners, in order to determine the possible regulation range and response performance of each unit, both of geothermal and hydro generators.

Advances in system control and enhanced system stability can be achieved with Landsnet's wide-area control projects. Along with those improvements it is recommended that existing system protections, which trigger the islanding separation seen in Figure 3.1, will be revised. The current protections are sensitive and often it is only the first power oscillation swing that causes the split of the system, like seen in Chapter 5.2. It would be beneficial to increase the thresholds or add delays to the triggering, in order to minimize the risk of system split.

### 7.1.4 Suggested Implementation of Improved Control Strategies

PhasorPoint is operational approved for real-time monitoring, disturbance analysis and system testing. The control capabilities of the PhasorPoint system have not been utilized yet. For the implementations of Landsnet's wide-area control projects it is recommended that the complete control system should be based on PhasorPoint application, i.e. measurements, processing and control units. It guarantees uniformity for the operation and all the applications. Until the PhasorPoint control unit will be available, expected in 2-3 year timeframe, the development and testing of control schemes should be continued with other configurations.

With future plans of increased installation of geothermal and wind power in the system it is recommended that Landsnet raises its standards when it comes to control and monitoring of power plants. Further installation of non-controllable power plants will further increase the regulation stress of the hydro units and the system stability will be compromised. Additional PMU measurement requirements will enhance the analysis of the control scheme performance, e.g. GPS time synchronised measurement of wicket-gate position will allow for better analysis of achievable improvements in generator responses.

## 7.2 Future Work

Suggested future work regarding the improved frequency control strategies for geothermal power plant is as follows:

- Install PMU measurements for the two generator units at Krafla.
- Test and validate the suggested control scheme for Krafla, with the PhasorPoint substation system prototype.
- Establish cooperation with power plant owners to evaluate and test the control scheme of fast-acting setpoint change of both geothermal power plants and hydro power plants, with a focus on a testing at Hellisheiðarvirkjun.
- Adjust the generators responses of the PSS/E dynamical model with suggested improvements. Use the method of comparing model results with real-time PMU measurements to improve generator models for the rest of the system.
- Continue developing the wide-area control schemes for the Icelandic transmission system.

# Bibliography


[1] Landsnet, Annual report (Ársskýrsla) (2012).

[2] Orkustofnun, The energy agency - electrical energy (orkumál-raforka) (2012).

[3] Orkustofnun, Energy statistics in iceland (orkutölur) (2012).

[4] Landsnet, Network development plan for 2013-2017 (Kerfisáætlun Fimm ára áætlun), Landsnet, 2013.

[5] B. S. Einar Eliasson, Sverrir Thorhallsson, Geothermal power plants, short course on geothermal drilling, resource development and power plants (2011).

[6] P. Kundur, Power System Stability And Control, EPRI power system engineering series, McGraw-Hill Education (India) Pvt Limited, 1994.

[7] L. Mitsubishi heavy industry, Mitsubishi mechanical drive steam turbines @ONLINE (Jan. 2014).
URL `https://www.mhicompressor.com/en/technology/catalog/pdf/turbine.pdf`

[8] J. R. B. Jan Machowski, Janusz W. Bialek, Power System Dynamics and Stability, John Wiley & Sons, 2008.

[9] M. E. corporation, Mitsubishi electric power system stabilizers (pss) @ONLINE (Jun. 2014).
URL `http://www.meppi.com/Products/GeneratorExcitationProducts/Static%20Excitation%20System/Power%20System%20Stabilizer.pdf`

[10] H. Saadat, Power Systems Analysis, McGraw-Hill series in electrical and computer engineering, McGraw-Hill Primis Custom, 2002.

[11] ENTSOE, Continental europe operation handbook. (2004).

[12] M.Bollen, Transmission and distribution course compendium (Mar. 2003).

[13] P. Pourbeik, Dynamic models for turbine-governors in power system studies, Tech. rep., IEEE Power and Energy Society (2013).

[14] S. PTI, PSSE 32.0.5 Online Documentation, Siemens, 2010.

[15] Psymetrix, Wide-area solutions @ONLINE (May 2014).
URL `http://www.psymetrix.com/home.html`

[16] Landsvirkjun, Krafla power station @ONLINE (Mar. 2014).
URL `http://www.landsvirkjun.com/company/powerstations/`

[17] D. Wilson, D. Wang, Landsnet Wide Area Defence Scheme Design Document, Psymetrix, 2012.

[18] D. Wilson, Proposal for Landsnet Wide Area Control Project, Psymetrix, 2014.

[19] N. Instrument, Pxi platform @ONLINE (May 2014).
URL `http://www.ni.com/pxi/`

# A

# MATLAB/Simulink Models

This appendix contains models developed in MATLAB/Simulink for simulations of a single bus system, including one hydro power plant and two geothermal power plant.

## A.1 Simulink Model of a Single Bus System

Figure A.1 contains the block diagram of the simulation model built in MATLAB/Simulink. The block diagram of the governor control logic used in the simulation model is presented in Figure A.2

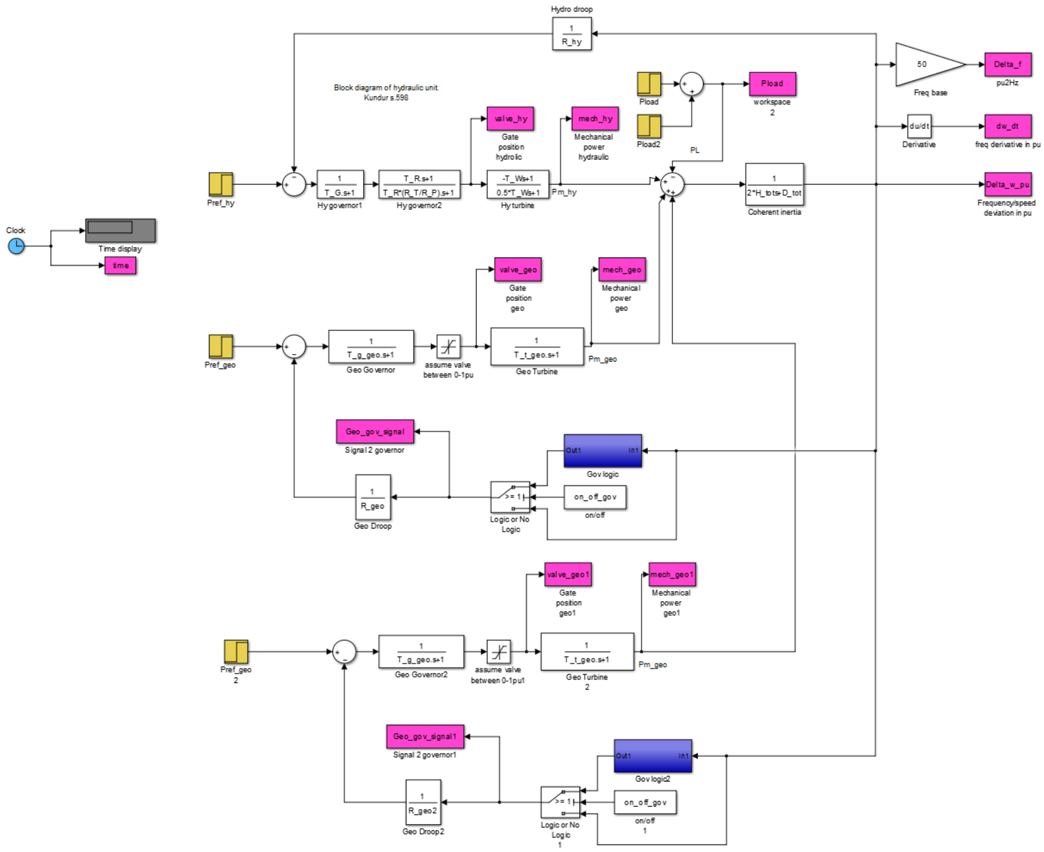


**Figure A.1:** Simulink model used in Chapter 4.

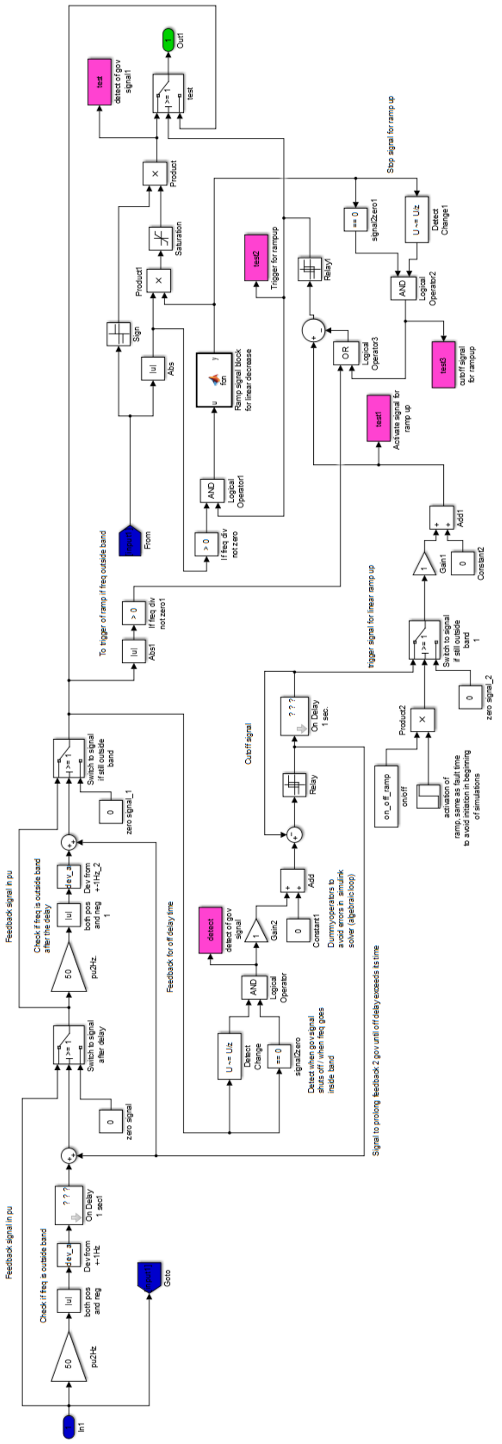

**Figure A.2:** Governor control logic block of the Simulink model used in Chapter 4.

## A.2 Simulations for Different Delay Settings

Summary of the simulation result conducted in Chapter 4.3, for different delay settings is presented in this chapter. Figure A.3 shows the results for governor control #2 and Figure A.4 shows the results for governor control #3.

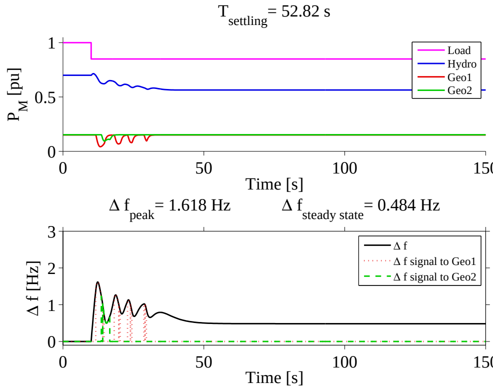


**(a)** Delay of 0.5 s

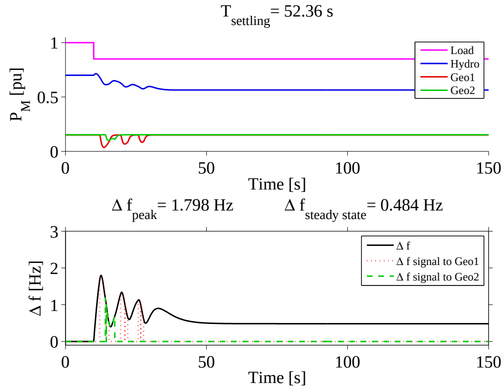


**(b)** Delay of 1.0 s

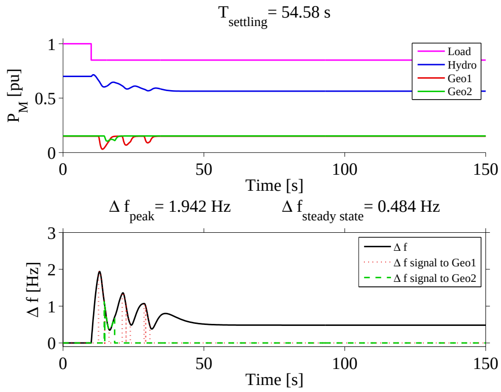


**(c)** Delay of 1.5 s

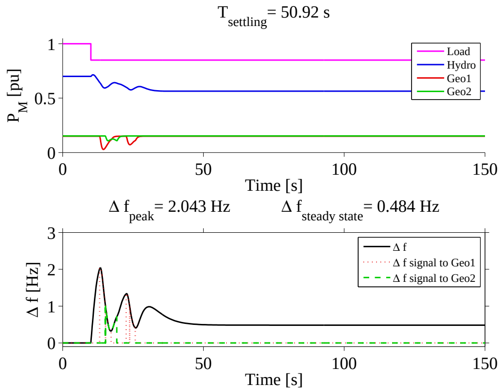


**(d)** Delay of 2.0 s

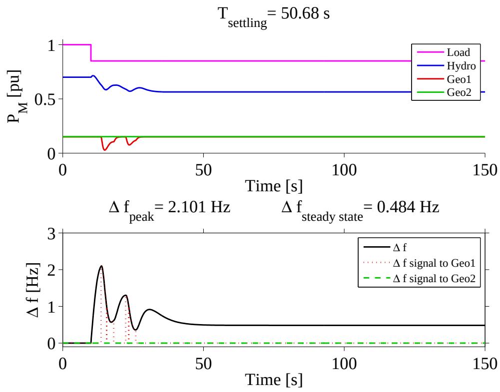


**(e)** Delay of 2.5 s

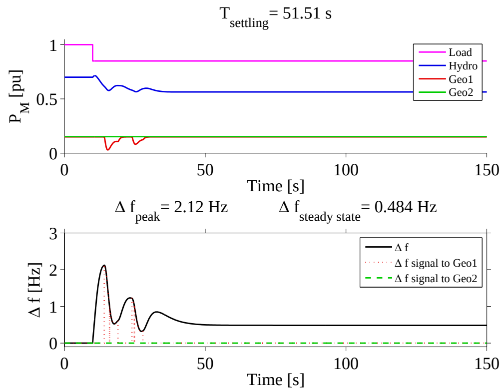


**(f)** Delay of 3.0 s

**Figure A.3:** Simulation results with the governor control #2 and different delay settings.

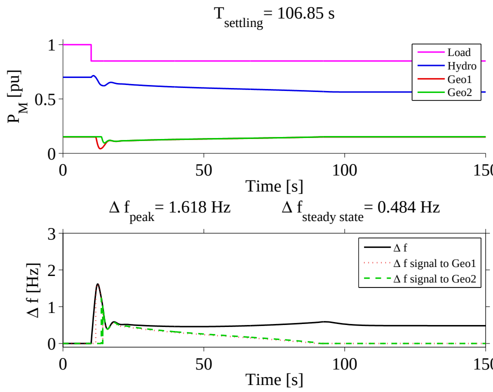


**(a)** Delay of 0.5 s

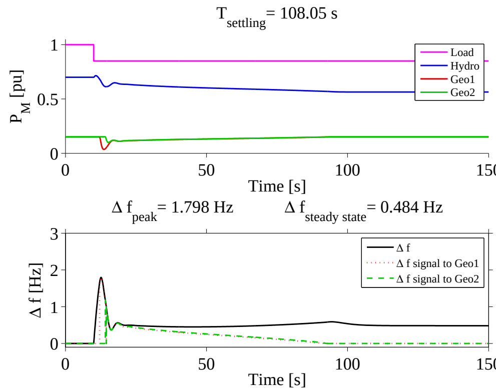


**(b)** Delay of 1.0 s

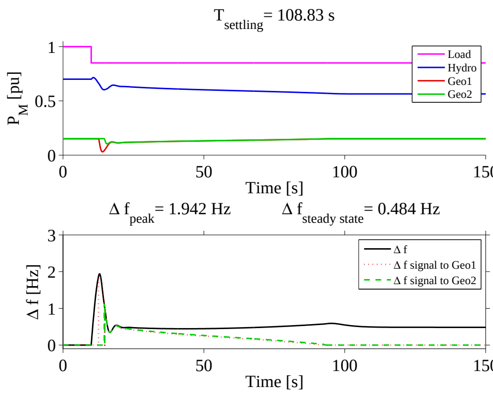


**(c)** Delay of 1.5 s

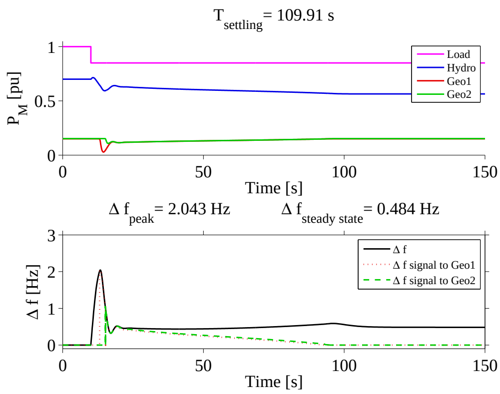


**(d)** Delay of 2.0 s

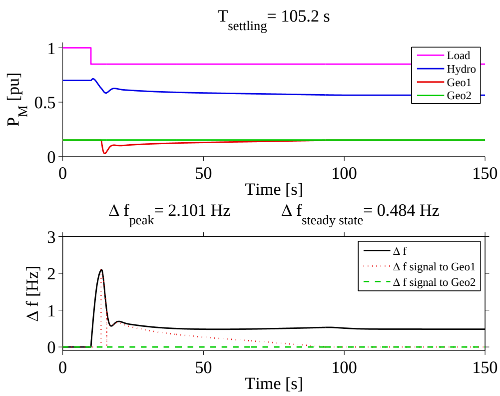


**(e)** Delay of 2.5 s

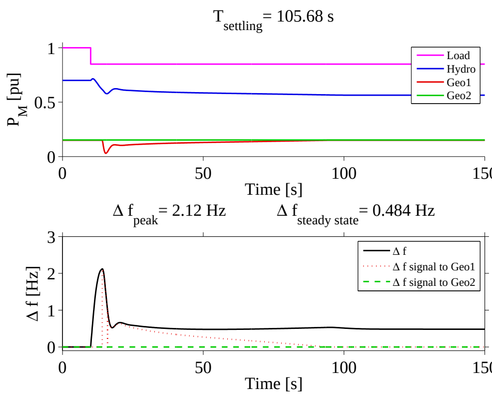


**(f)** Delay of 3.0 s

**Figure A.4:** Simulation results with the governor control #3 and different delay settings.

## A.3 Simulations for Different Frequency Amplitude Settings

Summary of the simulation result conducted in Chapter 4.4, for different frequency amplitude settings is presented in this chapter. Figure A.5 shows the results for governor control #2 and Figure A.6 shows the results for governor control #3.

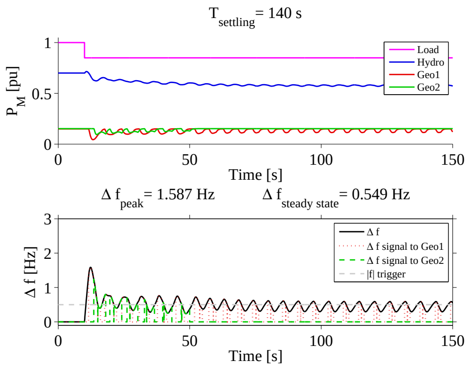


**(a)** Amplitude of 0.5 Hz

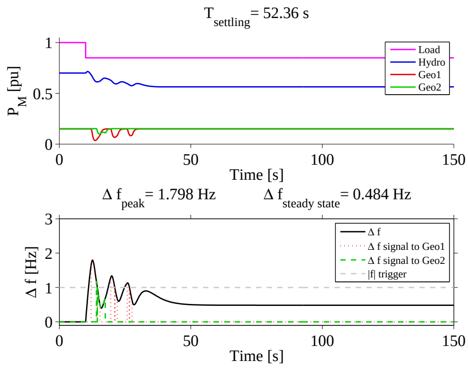


**(b)** Amplitude of 1.0 Hz

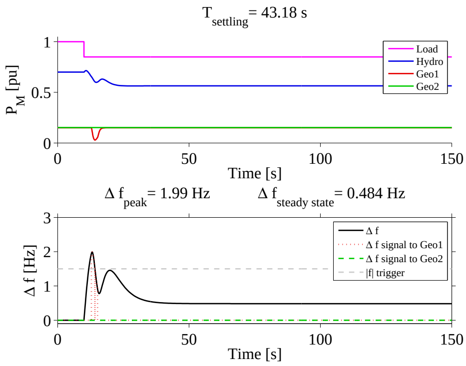


**(c)** Amplitude of 1.5 Hz

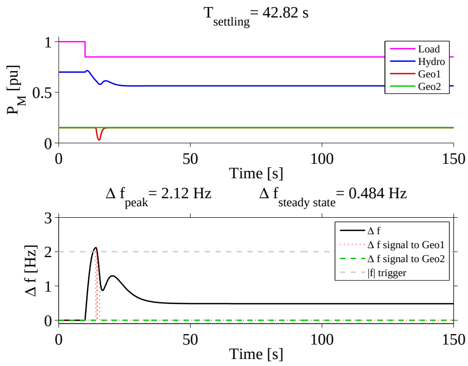


**(d)** Amplitude of 2.0 Hz

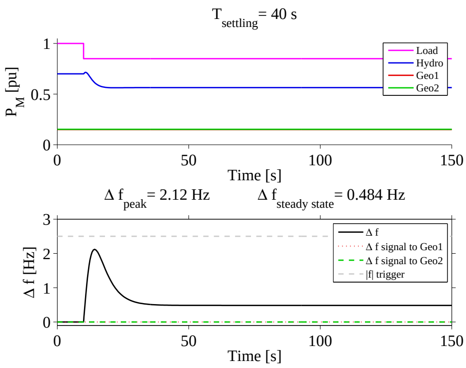


**(e)** Amplitude of 2.5 Hz

**Figure A.5:** Simulation results with the governor control #2 and different frequency amplitude settings.

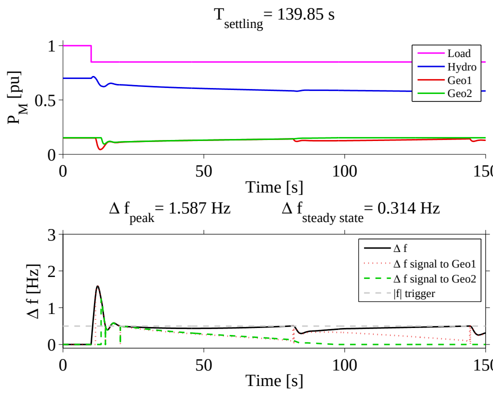


**(a)** Amplitude of 0.5 Hz

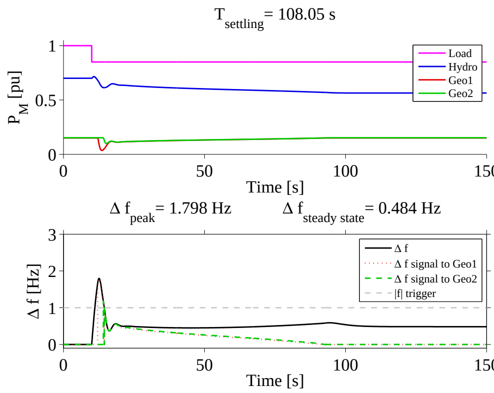


**(b)** Amplitude of 1.0 Hz

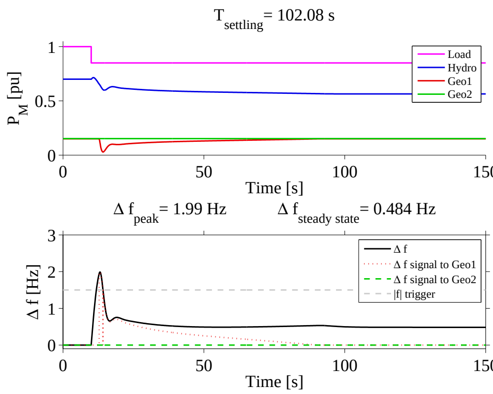


**(c)** Amplitude of 1.5 Hz

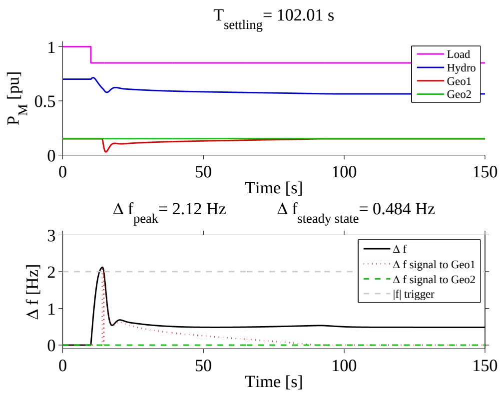


**(d)** Amplitude of 2.0 Hz

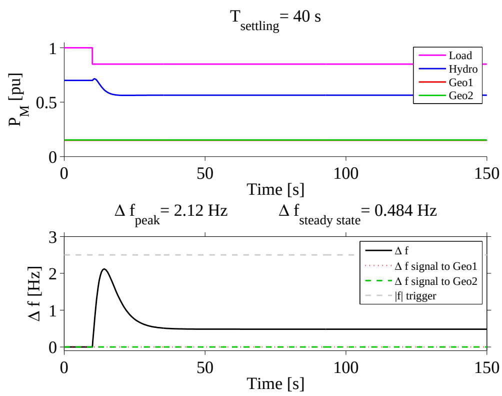


**(e)** Amplitude of 2.5 Hz

**Figure A.6:** Simulation results with the governor control #3 and different frequency amplitude settings.

# B

# PSS/E simulation results

This appendix contains simulation results conducted in PSS/E in Chapter 5.2. The PSS/E simulation results for simulation #2 and #4-8 are presented in Figures B.1-B.6. Simulations results #1 and #3 are presented and analysed in Chapter 5.2.2-5.2.3.

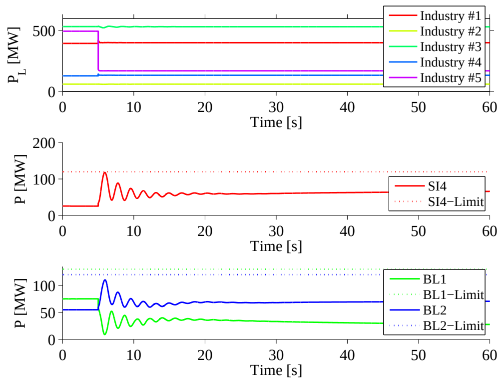


**(a)** Industry loads and transmission line power-flows.

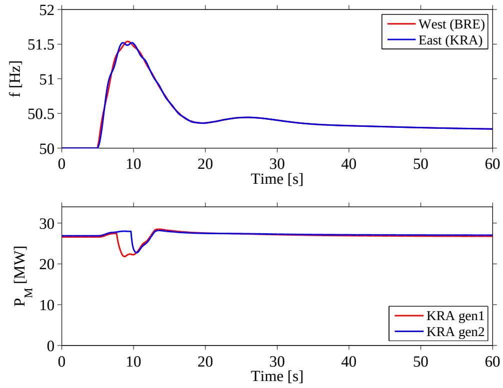


**(b)** Frequencies and mechanical power outputs of each generator at Krafla.

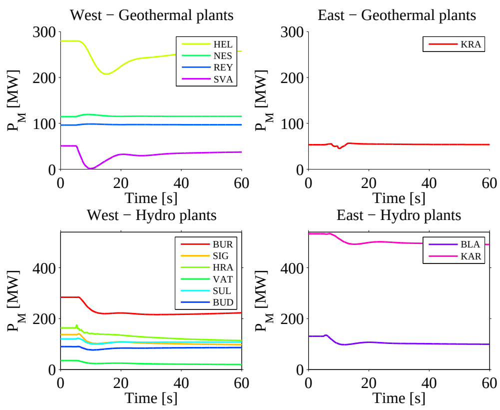


**(c)** Mechanical power responses of the hydro power plants and the geothermal power plants.

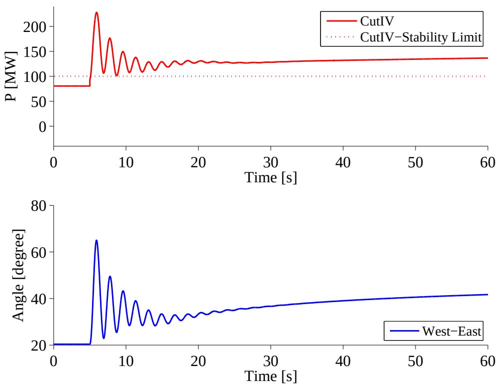


**(d)** CutIV power-flow and the relative rotor angle difference between West and East Iceland.

**Figure B.1:** PSS/E simulation results #2 from Chapter 5.2.

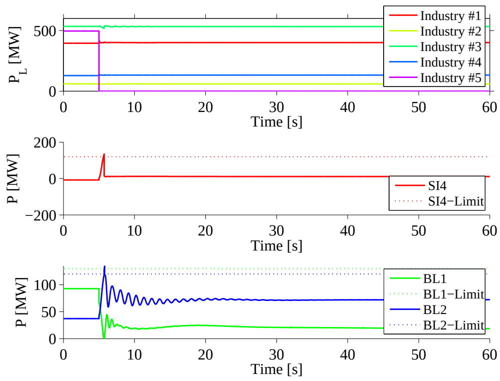


**(a)** Industry loads and transmission line power-flows.

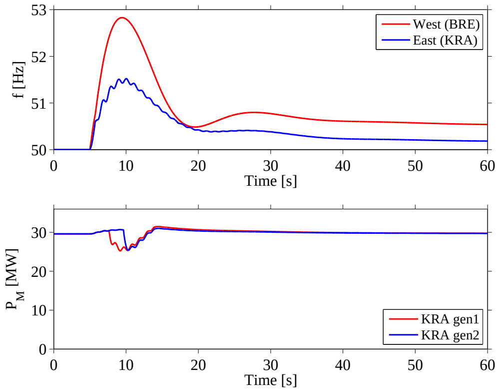


**(b)** Frequencies and mechanical power outputs of each generator at Krafla.

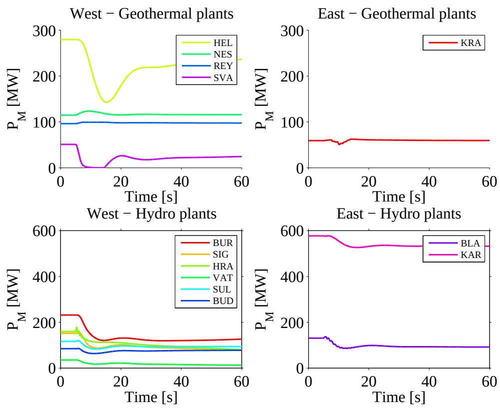


**(c)** Mechanical power responses of the hydro power plants and the geothermal power plants.

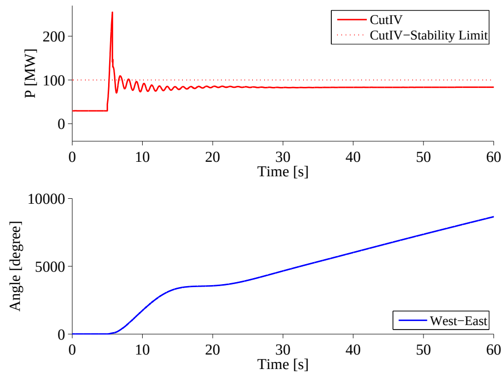


**(d)** CutIV power-flow and the relative rotor angle difference between West and East Iceland.

**Figure B.2:** PSS/E simulation results #4 from Chapter 5.2.

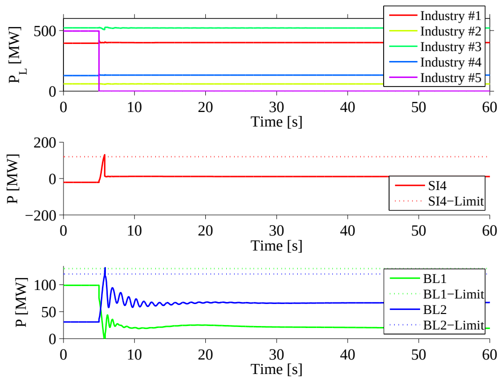


**(a)** Industry loads and transmission line power-flows.

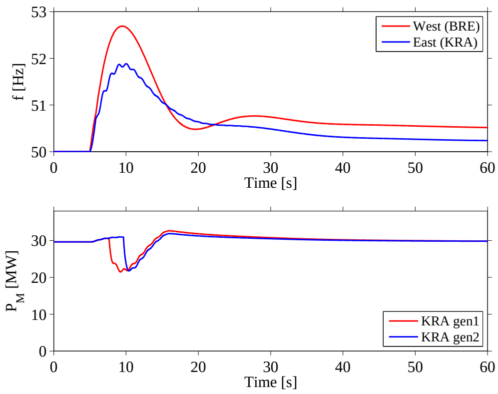


**(b)** Frequencies and mechanical power outputs of each generator at Krafla.

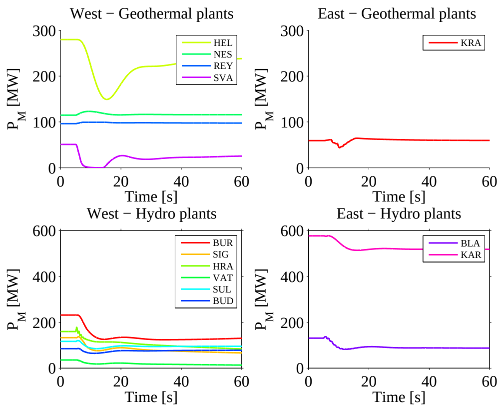


**(c)** Mechanical power responses of the hydro power plants and the geothermal power plants.

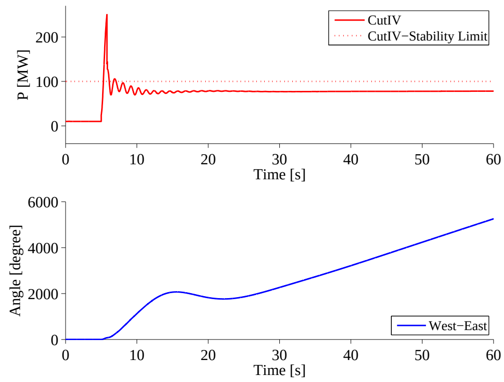


**(d)** CutIV power-flow and the relative rotor angle difference between West and East Iceland.

**Figure B.3:** PSS/E simulation results #5 from Chapter 5.2.

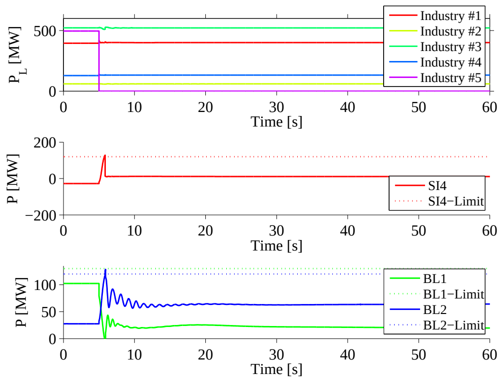


**(a)** Industry loads and transmission line power-flows.

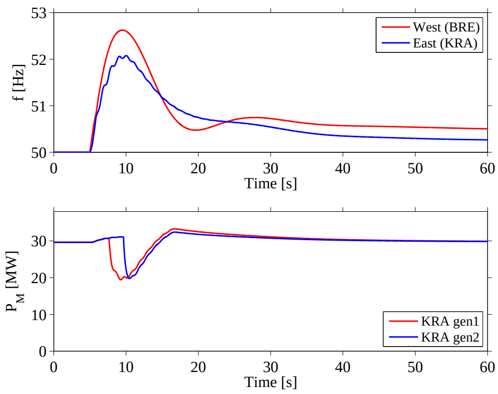


**(b)** Frequencies and mechanical power outputs of each generator at Krafla.

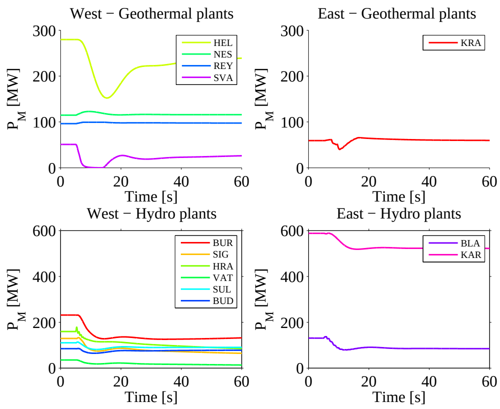


**(c)** Mechanical power responses of the hydro power plants and the geothermal power plants.

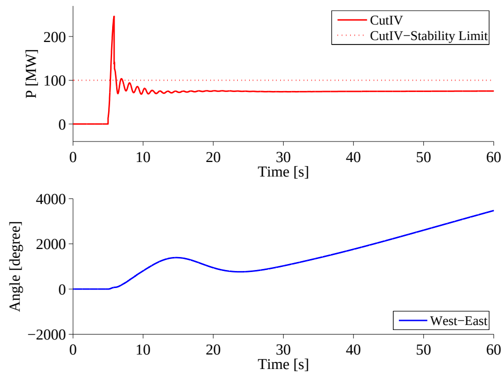


**(d)** CutIV power-flow and the relative rotor angle difference between West and East Iceland.

**Figure B.4:** PSS/E simulation results #6 from Chapter 5.2.

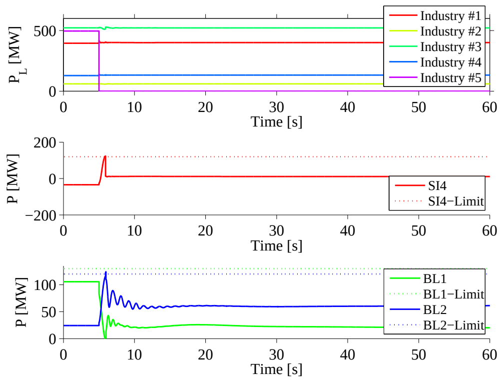


**(a)** Industry loads and transmission line power-flows.

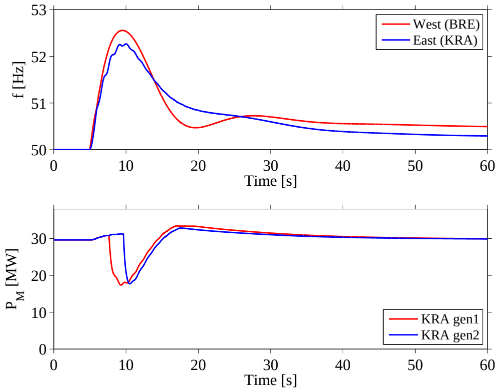


**(b)** Frequencies and mechanical power outputs of each generator at Krafla.

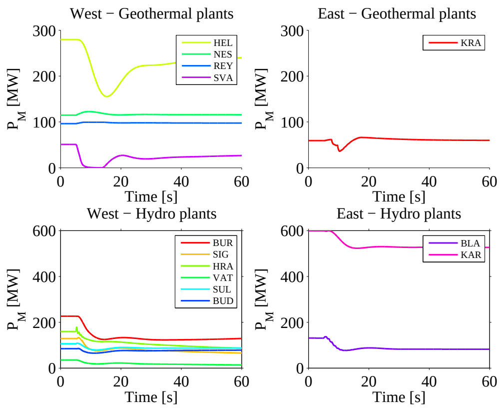


**(c)** Mechanical power responses of the hydro power plants and the geothermal power plants.

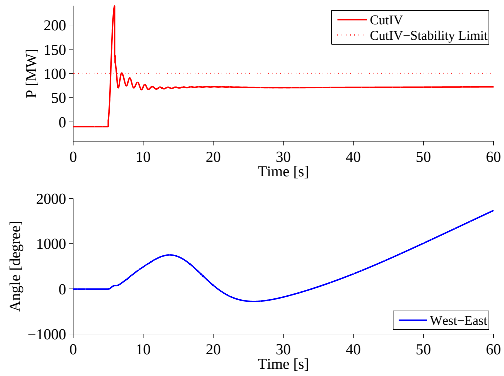


**(d)** CutIV power-flow and the relative rotor angle difference between West and East Iceland.

**Figure B.5:** PSS/E simulation results #7 from Chapter 5.2.

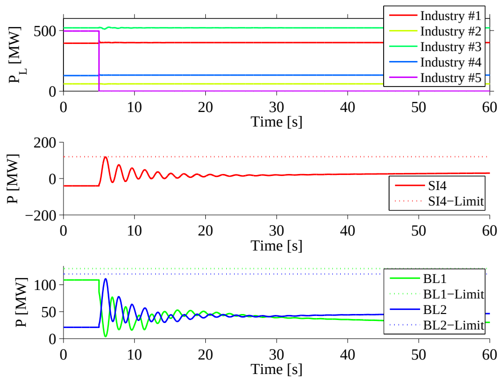


**(a)** Industry loads and transmission line power-flows.

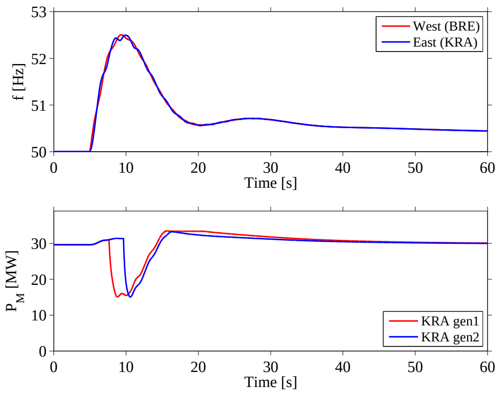


**(b)** Frequencies and mechanical power outputs of each generator at Krafla.

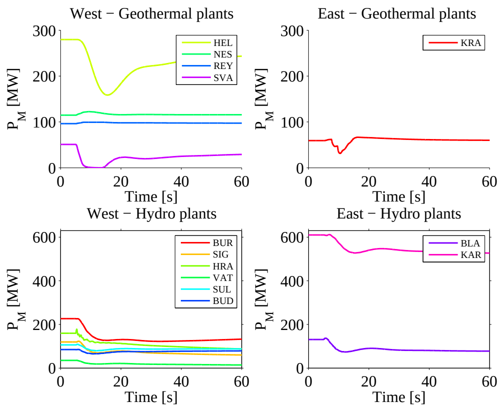


**(c)** Mechanical power responses of the hydro power plants and the geothermal power plants.

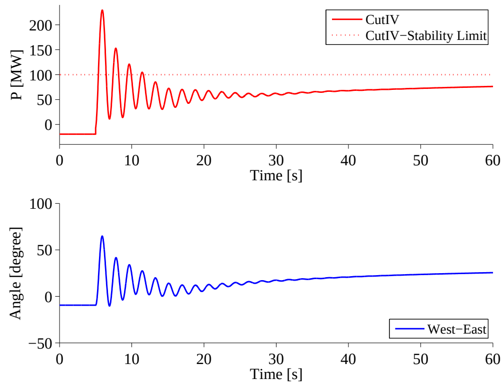


**(d)** CutIV power-flow and the relative rotor angle difference between West and East Iceland.

**Figure B.6:** PSS/E simulation results #8 from Chapter 5.2.